The influence of thermal gradients in steel columns due to pool fires

W. Boon

Delft University of Technology

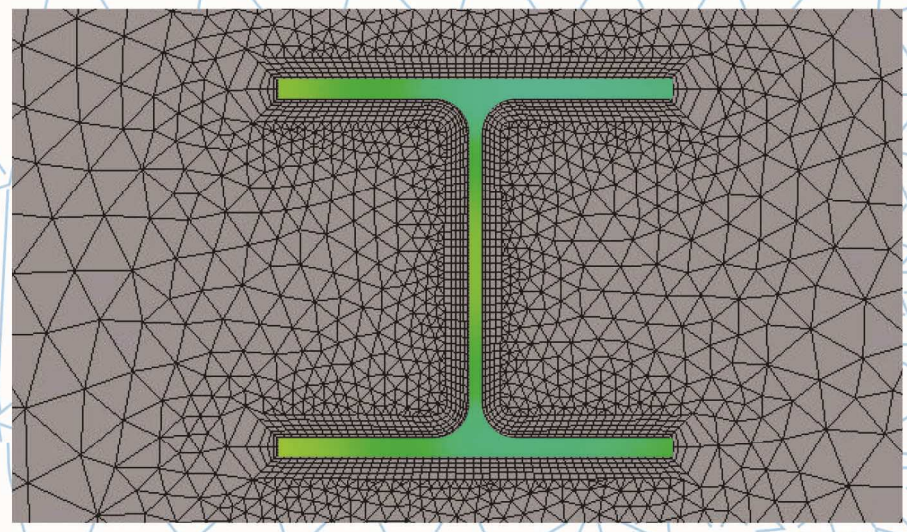

TU Delft Delft University of Technology

Challenge the future

The influence of thermal gradients in steel columns due to pool fires

By

W.Boon

in partial fulfilment of the requirements for the degree of

Master of Science
in Civil Engineering

at the Delft University of Technology,
to be defended publicly on Thursday September 25th, 2014.

Student number:	4128303	
Thesis committee:	Prof. Ir. F.S.K. Bijlaard,	TU Delft
	Ir. R. Abspoel,	TU Delft
	Dr. Ir. M.A.N. Hendriks,	TU Delft
	Ir. L.J.M. Houben,	TU Delft
	Ir. C. Tang,	Tebodin
	Prof. Dr. Ir. J. Maljaars	TNO

An electronic version of this thesis is available at http://repository.tudelft.nl/.

Preface

Steel structures are often used in industrial practice. This also applies for structures which are used in the chemical industry. In this industry liquids which are flammable are regularly used and it could occur that a liquid ignites due to some reason inside the steel structure. Because of the energy that is released by the burning liquid the structural elements will be heated. In the case that the structure is made of steel this heating could result in severe unfavourable effects. Due to the rising of the steel temperature the strength and stiffness properties of the steel decrease rapidly. At a steel temperature of 550°C the yield stress of the steel is only 60% of the yield strength at ambient temperature. Due to the higher temperatures of the steel the yield strength will decrease. When the yield strength becomes lower than the stresses in the structural element the element will fail on strength. At raised temperature the Young's modulus also decreases causing stability to be an issue as well. The steel temperature at which an element fails is called the critical steel temperature. When studying a column the stiffness is an important property which needs to be kept in mind. As the stiffness of the steel reduces with higher temperatures buckling could be an important subject. From previous research a hydro-carbon pool fire around the base of a column the temperature of the steel section could increase in such a fast manner that the column will fail within a few minutes.

W.Boon
Delft, September 2014

Contents

1

Start note

1.1. Problem

When a flammable liquid is spilled and for some reason ignites we call this a pool fire. A pool fire therefore is described by the volume of the flammable liquid, which is ignited. When a pool fire is present around the base of a column a thermal gradient will be along the height of the column. In case the pool fire is at a certain distance from the column a thermal gradient will be over the cross section of the column and over the height of the column. The size of this thermal gradient depends on multiple factors, the burning time of the fire and the volume of the pool fire for example. As one side of the section heats up and the other side heats up less an eccentricity will develop which results in a lower buckling force.

The goal of this thesis is to gain more knowledge in the effects of thermal gradients in steel columns due to pool fires. During this research different scenarios shall be investigated. A compartment from an ongoing project at Tebodin will be used and the fire location will vary inside the compartment. Using two fire locations the influence of the thermal gradient can be investigated for both the strong and the weak axis of the column. Using the fire safety engineering approach a fire curve will be chosen such that it represents an actual hydrocarbon fire.

1.2. Research methodology

During this thesis different models and setups will be elaborated. The location of a fire with respect to the column has a large influence on the thermal gradient. Different locations result in different thermal gradients in the column. This means that the column does not have a uniform temperature in the cross section. As the column does not have a uniform temperature distribution it could occur that the column is fire resistant longer than has previously been thought. Due to the heating from one side an eccentricity will occur as that side of the column expands more than the other side. This will have a negative effect on the buckling force. What is the effect of a thermal gradient on the buckling force of a column?

Software which has been used during this thesis:

- OZone
- Brawesta
- ANSYS workbench
- ANSYS CFX
- ANSYS CFD Post
- ArcelorMittal – CTICM Columns Calculator

The input data for the software will have to be from a representative model. The simplest case is a simply supported column which is axially compressed. The downside of this model is that in practise it is rarely used. Columns are often continuous and reach through multiple storeys resulting in a different model than a

simply supported column. As the model increases and gets more complex, the calculation will become more complex and extensive as well.

Perhaps it is possible to perform a test in which a pool fire is near a column. Using the data of such tests the thermal gradient can be obtained and compared with the software calculations and hand calculations.

1.3. Composition of the graduation committee

Committee chairman:	Prof. Ir. F.S.K. Bijlaard
Committee member TUDelft:	Ir. R. Abspoel
Committee member TUDelft:	Dr. Ir. M.A.N. Hendriks
Committee member TUDelft:	Ir. L.J.M. Houben
Committee member Tebodin:	Ir. C. Tang
Committee member TNO:	Prof. Dr. Ir. J. Maljaars

2

Literature review

2.1. Summary

This literature review is related to the thesis subject “influences of thermal gradients in steel columns due to pool fires”. This review has been set up to gain more information in the effects of fires on steel and steel columns in particular. The effects of temperature on the material properties of steel have been investigated and noted. Different other parameters which appear to be important in fire safety design have also extensively been described. These include the section factor and the critical temperature as well as the fire scenario used. In this review different fire scenarios have been shown and discussed but during this thesis the fire curve will be closely related to the fire engineering approach.

The effects of temperature on a steel column include a reduction in strength and stiffness. Due to a reduction in strength the column can fail while the load stays the same but the temperature increases. Another important item is the section factor. This is used to determine the heating rate of a profile. A very slender section will heat up a lot faster than a fat stocky section due to the thickness of the material.

The situation in this thesis will be a compartment with two columns supporting the roof structure. The focus of this thesis is on these columns and not the rest of the compartment structure. To find out what the influence is of a thermal gradient in the column this must first be created. To create a thermal gradient in a column the column must be affected by the fire from one direction. In the case where the fire is surrounding the column only a temperature difference over the height of the column will be seen. As we want to investigate a thermal gradient over the cross section of the column the fire must be situated at a certain distance from the column. This thesis is to investigate the influence of a pool fire on a steel column. This will be a certain hydrocarbon liquid which has been spilled at a distance from the column. Usually a floor will have a certain slope so liquids will never stay close to a column. In this thesis we will make the assumption that the floor has no slope. This way a pool can be formed and the effect of the pool fire can be investigated. Due to the thermal gradient which has been created the column will bow. This effect could result in a lower buckling load because of the eccentricity created in the column.

There are multiple fire scenarios which can be incorporated in the calculations for fire safety. The current Eurocode and other guidelines show a curve named the standard fire curve (ISO). This is a standardized curve for the temperature in a compartment during a fire. A drawback of this fire curve is that it is not a realistic curve. The standard fire curve is a logarithmic curve which as time goes to infinity the temperature will remain high. Fire Safety engineering is the study of describing a fire more accurately by studying the type of materials in the compartment and the total amount of energy which could be released. This way a more realistic fire curve can be obtained showing a growth phase, a fully developed fire phase and a decay phase. This type of fire curve will then give a more realistic result with respect to the reaction of the steel column. The temperatures obtained will be more accurate than the standard fire curve or the hydrocarbon fire curve. The production of smoke and the evacuation of people is also an important aspect of fire safety engineering. During this thesis the effects of smoke and the evacuation of people will not be discussed.

All materials which are subjected to fire will have some reaction to the heat which is produced. Some materials will behave better than others in this situation. Steel is less fire resistant than concrete for example as the properties of steel decrease rapidly as it heats up and concrete remains intact up till very high temperatures. In steel structures many times fire proofing materials will be used. Even though this thesis is about unprotected steel sections, it is still important to realise that there are different methods of fire protection and will be discussed in this literature review.

There are different types of calculation methods ranging from simple hand calculations to complex Computation Fluid Dynamics models. The Eurocode describes a method to calculate the fire safety of a column. This calculation however only complies with the standard fire curve and a uniform temperature distribution in the cross section and over the height of the column. In this thesis we want to investigate the influence of an actual thermal gradient in a column. The results obtained cannot be directly compared to the Eurocode because this will be just one scenario. This scenario is based on multiple assumptions and will not result in a confirmed conclusion to say that the Eurocode might be overestimating the temperatures, which is in fact the reason to be investigating the thermal gradient. With the help of Fire Safety Engineering a more realistic fire scenario will be set up to test a column. Using calculation methods and a CFD or a finite element model the thermal gradient can be investigated. After the thermal gradient is known we can expand the study to failure load and temperature of the column. Using the reduced material properties the effect of the thermal gradient on the buckling load of the column can be investigated.

2.2. Introduction

Structural steel is a construction material which is widely used in practise and is also used extensively in the chemical industry. In this industry where chemicals are transported or produced many types of accidents could occur including spilling or leaking of a liquid. [20]. The most important subject related to flammable liquids is fire safety. In 41% of the incidents occurring in this industry a fire was involved and that pool fires are the most frequent [22]. A pool fire is a pool of a flammable liquid which is by any means ignited. Pool fires are a big concern as they burn very fast and violently. Because of this there are many rules and regulations which need to be kept in mind for safety reasons. The effects of a pool fire must be accurately known to be able to calculate the influence on the steel structure. Using a hydrocarbon fire curve it is stated that a pool fire close to a steel column could result in failure of the column in a matter of minutes. As steel heats up its material properties change, the strength and the stiffness of the material will decrease. The fact that the stiffness decreases in time will result in a different failure load with respect to the failure mechanism buckling. Pool fires surrounding a column in a compartment will result in a thermal gradient over the height of the column. In the case of a pool fire which is situated at a distance from the column it will result in a thermal gradient over the cross-section of the column. In this case one side of the steel column is heated more than the other side. This means that the heated side will expand more and bending of the column will occur. As Eurocode 3 [2] at present only looks at prescribed standard curves and the assumption that the cross-section of a column has a uniform distributed temperature, the effect of an acting gradient is not taken into account.

The goal of this study is to determine the effect of this thermal gradient in a steel column caused by a fire curve which is closely related to an actual fire. With this natural fire curve and the resulting thermal gradient it will be possible to calculate the fire resistance of the column and see if it is more than described by Eurocode 3 [2].

During this literature review the influences of different parameters will be discussed related to pool fires and heating of steel columns. Also background information will be discussed related to the topic of fire safety of steel columns. First the steel properties of steel at elevated temperatures will be explained and the section factor which is an important parameter for fire resistance of structural members. The various heat transfer mechanisms will be discussed and the influence and differences of fire curves used in literature. Even though

in this study an unprotected steel column will be investigated it is still important to realise there are different types of fire protection which will be discussed as well. The behaviour of the structural elements will be explained as well as the behaviour of a system. There are quite a number of mathematical calculations for calculating the temperature in a column. Some of these numerical methods will be discussed as they are described in literature. Fire Safety Engineering has become an extensively growing branch of engineering which has shown to be helpful in designing more efficiently. Finally some different methods of testing will be discussed involving programs and software.

2.3. Steel properties

2.3.1. Introduction

When steel is exposed to a source of heat the steel will gradually be heated up. As steel has a relatively high thermal conductivity coefficient it will heat up more quickly than materials with a low conductivity coefficient which will be elaborated on in the chapter on material properties. This causes unfavourable effects in the steel as both the strength and the stiffness will decrease. As the strength of the steel decreases with increasing temperature the yield strength will decrease as well.

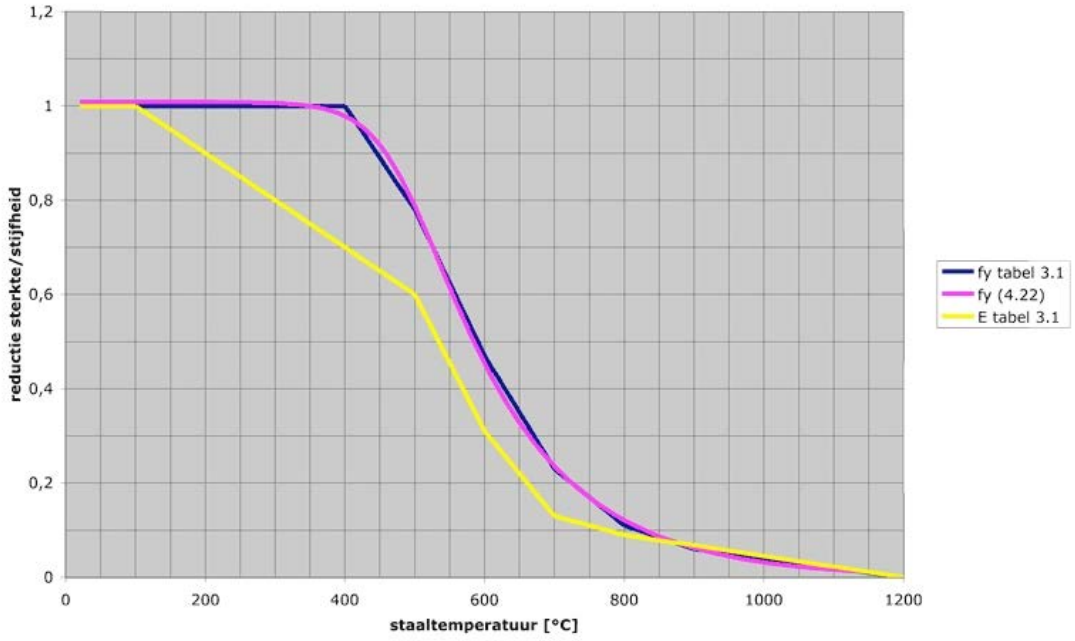

Figure 2.3.1-1: Reduction of strength and stiffness as temperature increases. [2]

2.3.2. Strength and stiffness

Eurocode 3 part 1-2 shows the reduction factor which has to be taken into account for strength and stiffness for steel for every 100°C of temperature raise. These reduction factors for strength and stiffness are given in tables which have been incorporated in a graph as shown above. For all intermediate points linear interpolation may be used to find the reduction factor. In figure 1 it can be clearly seen that when steel reaches 400°C the strength of the material will start to decrease. The yellow line presents the Young's modulus of steel and already starts to decrease after 100°C. Due to the fact that the Young's modulus decreases sooner than the strength it can cause stability problems before strength problems are encountered. [35].

From previous research and testing it has been found that when the cross-section of the profile has not been heated to 500°C it should still be able to withstand the acting forces without deformation of the steel. It could be that the section resists far higher temperatures, for example a composite beam consisting of a steel beam with a concrete deck. This type of section is heated from three sides, meaning the top flange will heat much slower causing a thermal gradient. As the bottom flange surpasses 550°C and becomes plastic the cooler, still elastic, regions will take over the load. Eventually when the entire cross-section of the steel becomes plastic the beam will fail [10]. Test results show that this occurs when the bottom flange reaches 620°C [8].

When steel has cooled down after it has experienced temperatures caused by a fire it can recover its original yield strength under circumstances. As long as the steel has not passed 600°C there will be no permanent loss in the yield strength of the steel depending on the steel grade [5].

2.3.3. Ratio of utilization (η)

The ratio of utilization is the ratio between the acting loads during the exceptional load combination fires and the resistance of a steel element at room temperature. Safety factors used in this exceptional load case is set to unity. The resistance of the steel element at normal temperature still has the normal safety factors. The ratio of utilization has a direct link to the critical temperature. These safety factors can be found in the national annex of Eurocode 0. The Dutch national annex states that the safety factor for permanent loads must be γG = 1.2 and γQ = 1.5. For centrically loaded columns with n floors and a braced structure the following upper boundary for the ratio of utilization can be found at room temperature [37].

$$\eta_{fi} = \frac{nG_{rep} + n\psi_2 Q_{rep}}{n\gamma_G G_{rep} + \gamma_Q Q_{rep} + (n-1)\gamma_Q \psi_0 Q_{rep}} \geq \mu_0$$

In case of one floor this equation can be simplified to the following equation which is the same for beams:

$$\eta_{fi} = \frac{G_{rep} + \psi_2 Q_{rep}}{\gamma_G G_{rep} + \gamma_Q Q_{rep}} \geq \mu_0$$

The symbols used in the equations above will be explained below

N	amount of floors in the structure
G_{rep}	permanent load in on the structure
Qrep	live load on the structure
γG	safety factor for permanent loads
γQ	safety factor for live loads
Ψ0	0.5 for usual load combinations
Ψ2	0 in the special loadcase fire (for roof structures)

2.3.4. Critical steel temperature

When steel is heated the yield stress lowers. This means that heating a steel member could cause failure without changing the load on it. When the stresses due to a certain load are known the critical temperature at which the element will fail can be calculated. In case the yield strength becomes lower than the acting stresses (due to temperature raises) in the cross-section the column will fail. When temperatures increase in the column, buckling will have a more significant role. The temperature at which this occurs is called the critical steel temperature. Depending on the ratio of utilization the critical steel temperature can be calculated. An element which has been over-dimensioned and can easily carry a certain load will allow for a big decrease in yield stress before collapse resulting in a high critical temperature. In case of a steel member which can just carry a load only a small reduction in yield stress will result in failure of the member. This will happen at a rather low temperature [35][36].

When steel has been exposed to a fire load it is often the question if the steel still fulfils the requirements of the codes. A rule of thumb which is regularly applied is that when the steel has no significant deformations it will probably still be fit for use. Because of the fact that nearly no deformations can be seen it means that the steel probably has not been heated over 600°C and is probably still good. In many cases it is still advisable to test the hardness of the steel to check this assumption. Depending on the result it can be determined if a member is still fit for use.

2.3.5. High strength steel

High strength steel is commonly used where very high stresses can be observed. The main advantage of this steel grade is that we can use less material or allow higher stresses. High strength steel has the same Young's modulus as regular carbon steel but in a fire situation the higher yield strength of the steel can be an advantage. When instead of regular steel high strength steel is used with the same cross sectional area it will result in a lower ratio of utilization due to the higher yield stress allowed. As a result the critical steel temperature will increase and the fire resistance of the element will be longer in time. So by over dimensioning a steel element the fire resistance in time can be increased [4]. In case a structure is dimensioned and calculated in steel grade s235 but executed in s355 the structure will be able to cope with higher temperatures. A disadvantage to this is the fact that higher steel grades are more expensive but can still be advantageous to the cost of fireproofing a structure.

2.3.6. Microstructure

Aside from the fact that some steel properties decrease as a result of heating also the microscopic material structure will experience changes. At about 650°C the microscopic steel structure will change but this is higher than the 550°C at which it is assumed all steel will have failed [27].

2.3.7. Material properties

In this section relevant steel material properties will be treated as discussed in researched literature and the Eurocode. Some of these material properties are dependent on the temperature of the steel.

2.3.7.1. Density

The density of a material is a physical property. Qualitatively density can be defined as the heaviness of an object whilst the volume is constant. Usually density is denoted as "ρ" and the unit used is kg/m3 [17]. The Eurocode handles a constant value of 7850 kg/m3 for any temperature. [2]

2.3.7.2. Thermal conductivity

The thermal conductivity of a material is defined as the amount of heat flux passing through a material depending on the thermal gradient. Thermal conductivity plays a large role in heat and mass transport and is denoted by "λ_a". The unit used for thermal conductivity is W/mK [17]. Thermal conductivity of steel is temperature dependant and can be found in the Eurocode [2].

For $20°C \leq \Theta_a \leq 800°C$ $\lambda_a = 54 - 3.33*10^{-2} *\Theta_a$ W/mK
For $800°C \leq \Theta_a \leq 1200°C$ $\lambda_a = 27.3$ W/mK

2.3.7.3. Specific heat

The specific heat is a property which is independent of the mass of a material. The definition is: specific heat is the amount of heat flux needed to increase the temperature of one gram of material by 1°C. In the Eurocode specific heat of steel is denoted as "c_a" is temperature dependant [17][2].

For $20°C \leq \Theta_a \leq 600°C$ $\quad c_a = 425 + 7.73*10^{-1}\,\Theta_a - 1.69*10^{-3}\,\Theta_a 2 + 2.22*10^{-6}\,\Theta_a{}^3 J/kgK$
For $600°C \leq \Theta_a \leq 735°C$ $\quad c_a = 666 + 13002/(738 - \Theta_a)\ J/kgK$
For $735°C \leq \Theta_a \leq 900°C$ $\quad c_a = 545 + 17820/(\Theta_a - 731)\ J/kgK$
For $900°C \leq \Theta_a \leq 1200°C$ $\quad c_a = 650\ J/kgK$

Θ_a is the steel temperature

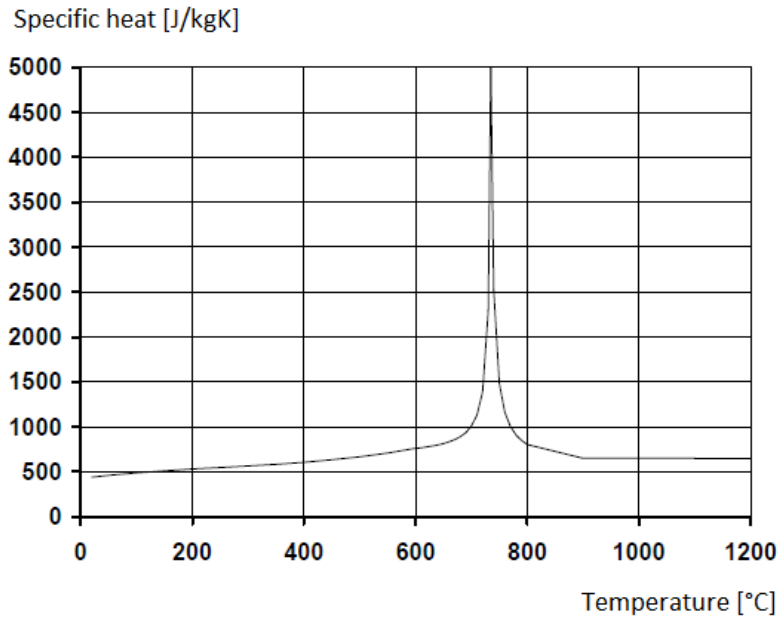

Figure 2.3.7.3-1: Specific heat of steel at elevated temperatures. [2]

2.3.7.4. Coefficient of thermal expansion

The effects of thermal expansion in a structure can cause very important deformations and even damage at low temperatures could occur. When steel is heated, just like any material, it will expand. This temperature raise could result in buckling or deformation of the structure if the element is clamped at both ends. Due to a relatively small temperature raise of 100°C a clamped-clamped beam could expand enough to reach the yield strength in the cross section. The expansion of a steel element due to heating can cause damage to connected concrete walls or columns when they restrict the expansion. As concrete has a low tensile strength these walls and columns could crack or break. As a steel member expands it will also increase the stresses in connections which could result in failure of a connection. [10]

The coefficient of thermal expansion is defined as the elongation of a material per increase of temperature. The Eurocode describes three distinct domains for the relative thermal elongation ($\Delta l/l$) of steel.

For $20°C \leq \Theta_a \leq 750°C$ $\quad \Delta l/l = 1.2*10^{-5}\,\Theta_a + 0.4*10^{-8}\,\Theta_a{}^2 - 2.416*10^{-4}$
For $750°C \leq \Theta_a \leq 860°C$ $\quad \Delta l/l = 1.1*10^{-2}$
For $860°C \leq \Theta_a \leq 1200°C$ $\quad \Delta l/l = 2*10^{-5}\,\Theta_a - 6.2*10^{-3}$

l is the length of the element at 20°C

Δl is the elongation due to temperature
Θa is the steel temperature in °C.

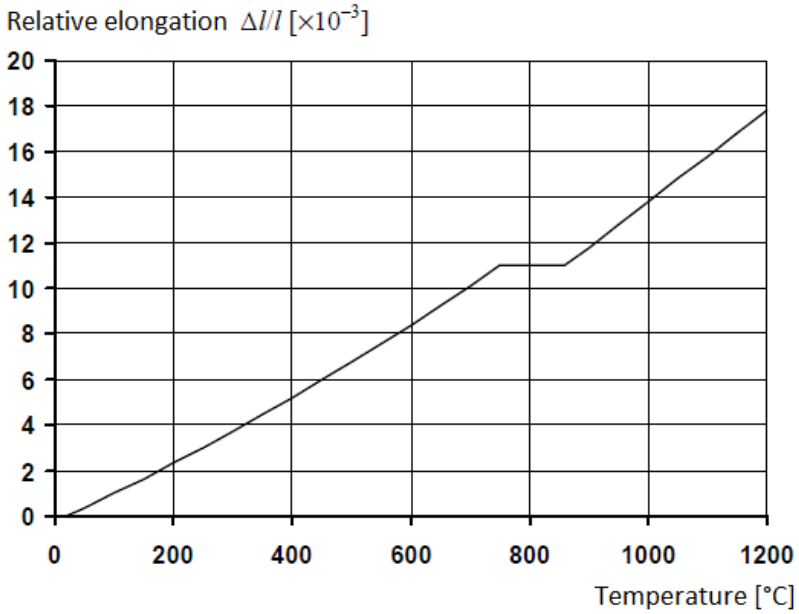

Figure 2.3.7.4-1: Relative elongation of steel as a function of temperature. [2]

2.3.7.5. Emissivity

Emissivity is the energy radiated by a material compared to the energy radiated by a black body at the same temperature. This factor is dimensionless and the Eurocode prescribes a value of 0.7 for normal carbon steel [17][2].

In a study performed by Sudheer and Prabhu [23] different emissivity factors have been researched for flammable liquids. The emissivity of a flammable liquid can be measured in two ways. Either infra-red cameras can be used or the rate of mass burning can be calculated. Sudheer and Prabhu conclude that the burning rate increases exponentially as the diameter increases as well as the emissivity. The emissivity measured at the top of the flames is less than that at the base of the fire.

2.4. Section factor

When calculating the fire safety of a structure the section factor is an important aspect. The section factor is used to take into account the effect of the geometry of the steel section on the steel temperature during fire conditions. The section factor is defined as the heated surface, A (in m2 per unit length), of the section divided by the volume of the section, V (in m3 per unit length), expressed in m-1. Simply stated the section factor is the heated perimeter of the section (m) divided by the cross sectional area (m2) [2][35].

In case of an unprotected H or I section a shadow effect must be taken into account. As the fire is directed on one side of a section the other side will be shaded from the fire by the section itself. In the formula this is implemented as a factor. A/V becomes $(A_m/V)_{sh} = 0.9(A_m/V)_b$. In case of any other section the factor 0.9 is set to unity and we obtain the equation as described before. [31].

A stocky section with a very small section factor will heat up slower because it has more material compared to a very compact section. This effect is described in the section factor. A section with a high section factor will reach the temperature of the standard fire curve faster than a section with a low section factor. The BCSA and TATA Steel [8] have developed a report in which they have researched that hot rolled structural

sections exposed to their full design load will be 15 minutes fire resistant when exposed to a standard fire curve as described by the Eurocode 3 [2] if the section factor fulfils the following criteria:

Beams supporting concrete floors:	section factor	<	230 m-1
Sections exposed to fire on four sides:	section factor	<	180 m-1
Bracing:	section factor	<	210 m-1

Most of the hot rolled sections will meet this set of criteria. Sections that have a higher section factor can still be used as long as the applied loads at room temperature are decreased in the ultimate limit state [8].

2.5. Heat transfer mechanisms

Research of heat transfer is a very important part when determining structural performance during a fire. There are three ways in which heat transfer can occur. These being: radiation, convection and conduction. Conduction occurs in solid materials on a molecular level. Convection is the transfer of heat in a fluid or by movement of a fluid. Convection occurs at heat differences in between fluids or at the edge of a fluid. An average fire will lose about 70% of its energy through convection and about 30% through radiation. Convection will cause the hot smoke to rise which directs upward, radiation is emitted in all directions. This means that objects which are not in the fire itself can still ignite due to radiation from the smoke layer [17].

2.5.1. Convection

Radiation and convection are the governing cases of heat transfer to steel structures [11] [18]. Heat transfer by convection is one of the most complex challenges in science. Convection is difficult to study because it is highly unpredictable in nature. Convection can occur in two ways: natural or forced. Forced convection can be caused by a pump or a fan. Natural convection occurs when differences in density appear due to temperature differences in a fire for example [17]. Eurocode 1 prescribes a value of α_c which is different per fire curve [1].

2.5.2. Radiation

If an element has a higher temperature it will emit electromagnetic radiation, we call this the heat radiation. Important aspects of heat transfer by radiation are absorption, reflection and transmission of the material [17]. Heat transfer to a concave element can cause for a blocking or reflecting effect by the different surfaces. To understand the effect of radiation on a concave element the geometry of the element is very important. Due to the concave element a shadow effect must be taken into account when creating a thermal energy balance. This means that due to the concave geometry this becomes a complex task to complete. The current Eurocode for fire loads overestimates the temperature in an unprotected steel section in a fire situation. The effect of geometry with respect to radiation has first been studied by Wickstrom. The “shadow effect coefficient” was designed to take into account the area between flanges of a section. After multiple tests this factor has been introduced in the Eurocode. Up to this point in time the actual solution to the geometry effect of H-sections using shadow factors and multiple reflective planes remains unknown. Test results by Wang [16] show that the estimations of temperatures made according to Eurocode 3 are higher than shown in models or reality.

2.5.3. Damage

Heat radiation can cause visible damage to structural elements and if the intensity of the radiation is big enough ignitions could occur. Below a certain level, the critical radiation intensity, no ignition will occur; even when the radiation is applied for an infinite amount of time. Any radiation intensity higher than this level will result in damage/ignition of the element. A very high intensity will result in a low resistance time.

When the element is made of steel or glass it will break or fail sooner than ignition. [7]. In Publicatiereeks Gevaarlijke Stoffen [7] a list has been presented showing the critical radiation intensity of different materials. Failure of a steel structure due to radiation will only occur in load carrying members. This will occur when the heat radiation has increased the temperature of the steel structure to about 550°C. To translate radiation energy to surface heat in a structural element is a very complex task because heat losses and different geometric effects are usually present.

In the end it really does not matter in which of these ways an object is heated, the most important question is: does it reach the combustion temperature? When people are exposed to radiation the exposure time, the radiation level and the physical condition of the person is of great importance. Enduring a radiation level of 2.5kw/m^2 for about 20 seconds will reach the pain threshold. Enduring a radiation level of 4-5kw/m^2 will result in skin burns. For comparison, on a sunny day the sun emits about 1kw/m^2 in the Netherlands. To be able to safely flee from a fire situation a maximum of 2.5 kw/m^2 can be acceptable for a few minutes. Usually this is equal to a smoke layer of about 200°C. [36]

2.5.4. Radiation of a hydrocarbon pool fire

It is very important to understand the effects of a hydro carbon pool fire. One important parameter is to know the amount of heat radiation sent from the fire. There are multiple methods to measure and calculate this, for example the “solid flame model”. In the past many tests have been performed on small pool fires but relatively little is known about larger pool fires. This means we get to endure more uncertainties in large pool fires because parameters cannot be determined accurately. In large hydrocarbon pool fires big amounts of smoke are produced which cause a blocking effect on the heat radiation. [20]. As a result of thick smoke it could occur that the radiation emitted from a small hydrocarbon pool fire is more than that of a large fire. [21]. Another method to measure the heat flux of a hydrocarbon pool fire is to model the fire as a cylinder or a conical shape. The height of the flames can be estimated by test results and then used for the shape. In this thesis a compartment will be chosen in which a pool fire could occur. This means that the amount of liquid which could ignite would not be in the order of a really large pool fire.

2.5.5. Thermal gradient

A construction element which is exposed to a fire load on less than four sides will develop a thermal gradient in its cross section. This can influence its behaviour in the structure and the resistance of the element. These parts of the construction can experience axial forces and moments due to the fact that deformations will be restricted. Because of the heat from one side, a column will start to bow towards the fire causing an eccentricity which then causes extra moments. The plastic resistance of a column experiencing an axial force and a moment could be different than the Eurocode predicts because of the thermal gradient. The Eurocode assumes that the cross section experiences a uniform temperature distribution. The methods described in the current Eurocode to test columns are too conservative for columns in the perimeter of a compartment. These methods will not accurately predict the failure mechanism of the columns as they do not take into account the thermal gradient which will be developed. [33]. The fact that this has been stated in other literature makes it an interesting subject to take into account for this thesis.

2.6. Fire scenario

For a fire there are three conditions necessary, combustible material, oxygen and heat. Combustible material and oxygen will react with each other if the temperature is high enough. During this reaction heat will be produced and if this heat production is large enough the reaction will continue. During a fire situation the number one reason for fatalities is not the flames itself but the production of smoke and toxic gasses. [35][36].

The lifecycle of an actual fire consists of three phases being: the growth phase, the fully developed fire phase and the decay phase. The growth phase is the only phase in which it is still possible to escape from a fire. When a fire is detected in this early stage the chances are bigger that it can be successfully fought. During this phase there is smoke production and temperatures are only locally very high. The most dangerous moment is flashover. This marks the point where the fire has reached the fully developed fire phase. During flashover hot gasses and smoke which are in the compartment reach such high temperatures that they ignite instantaneously. Temperatures can reach up to 1000°C in the compartment. After this moment it is no longer possible to fight the fire and fire fighters can only protect the surrounding compartments and areas. To be able to successfully fight the fire it is of great importance that the fire gets reported at an early stage. When most of the combustible material in the compartment has burnt, the decay phase sets in. This phase marks the near end of the fire and nearly all of the combustible material has been burned. [35][36].

2.6.1. Fire curves

Fire curves are used to describe the air temperature during a fire. Over the past years different fire curves have been invented and implemented. The ones which are most commonly used in fire safety practice will be discussed below. These include curves which are used by the Eurocode and curves which are more often used in Fire Safety Engineering practices.

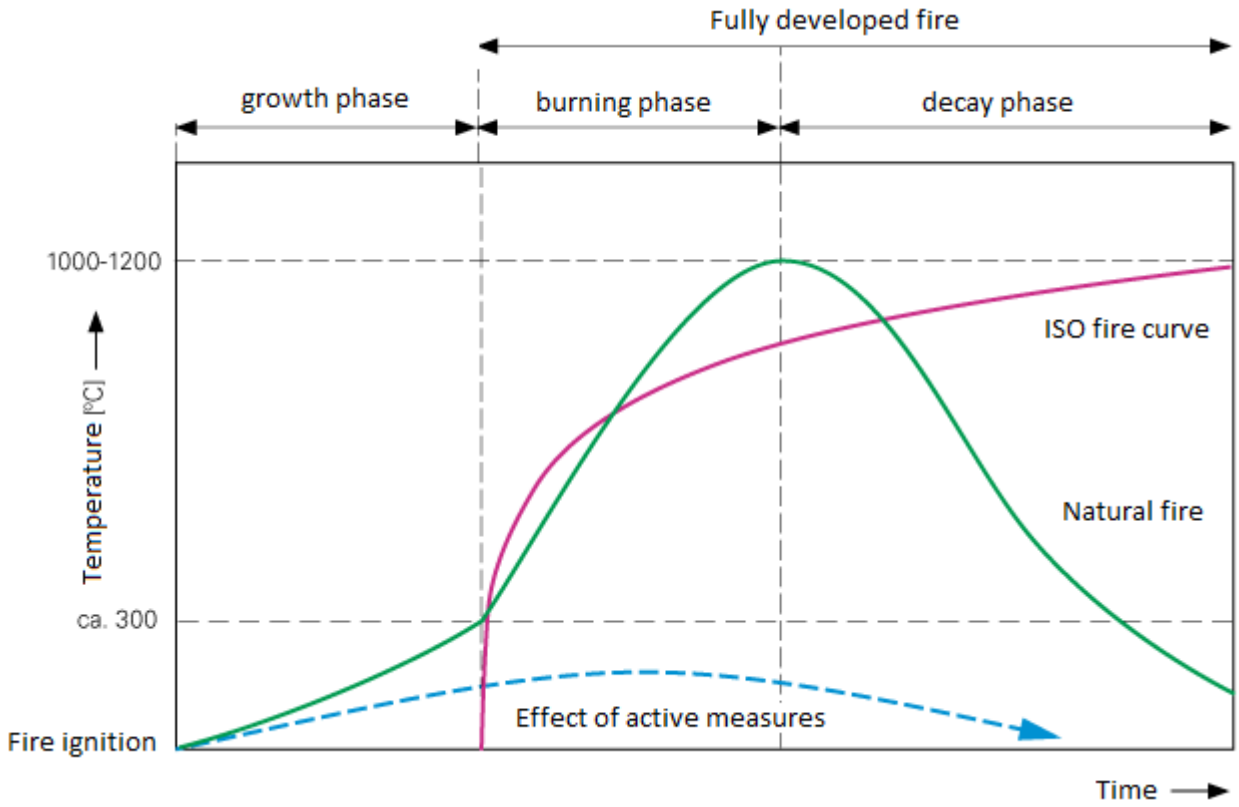

Figure 2.6.1-1: Comparison of natural fire to ISO standard fire curve [37]

2.6.1.1. Standard fire curve (ISO)

When the fire safety of a structure has to be determined the standard fire curve, otherwise known as the ISO fire curve, is usually assumed. This fire curve is fairly simplified compared to a real fire. The standard fire curve is a fire curve which is in the codes as leading curve for calculating fire safety of structural members. This curve omits the growth phase and actually starts right at the point of flashover. This fire curve has been designed in the 1920's and based on the amount of relevant materials usually in compartments. At that time this was mainly cellulosic products like wood and paper. Due to the fact that many materials in buildings and

offices have changed it could be that the standard fire curve is showing less or more favourable results depending on the type of materials in the compartment. The downside of using the standard fire curve is that when testing a member without fire protection it will most likely fail within a few minutes. [3][35].
The formula given by the Eurocode for the standard fire curve is the following (see figure 2-4):

$$\theta_g = 20 + 345log_{10}(8t + 1)$$

Θ_g is the temperature in the compartment as a function of time in minutes.
20 is the room temperature at which the fire will start.

2.6.1.2. Reduced fire curve

This fire curve closely resembles the standard fire curve; the main difference is that it levels out a lot sooner. At about 650°C the reduced fire curve stays at this level and thus deviates from the standard fire curve. This fire curve can be used whenever a fire is on the outside of a building and thus heating the compartment from the outside. See figure 2-4. An example describing this phenomena is included in reference [36].

2.6.1.3. Parametric fire curve

The parametric fire curve is the only fire curve in the Eurocode that takes into account a decay phase. These phases exist of the growth phase, the fully developed fire phase and the decay phase. During the growth phase of the fire only locally high temperatures are apparent. Due to human action or not enough combustible material it could happen that the fire does not pass through to the fully developed fire phase. The fully developed fire phase has been reached once flashover has occurred. After this time all combustible material in the compartment has ignited. The amount of time that the fire is in this phase depends on the amount of combustible material and the ventilation in the compartment. During the decay phase the fire is dying and nearly all the combustible material has been burnt. In this phase we also notice that the temperature in the compartment starts to decrease. [17][36]

2.6.1.4. Natural fire curve

The natural fire curve unlike any of the other fire curves starts at the ignition of the fire. All the other fire curves start from flashover and therefore do not really implement a start phase. The natural fire curve is a curve often used in Fire Safety Engineering to model the fire as accurately as possible. The speed of the growth phase and the rate of heat release of the fire depend on the type of combustible material and the compartment. The amount of time the fully developed fire phase is applicable also depends on the type of material. When 70% of the combustible material has been burnt the decay phase sets in. In this final phase the last 30% of the combustible material will burn and the fire will cease to exist.

During this thesis a natural fire curve will be implemented based on a liquid which has been spilled. This will result in a more accurate result than can be obtained by the standard fire curve. This will further be discussed in the chapter about Fire Safety engineering.

2.6.1.5. Hydrocarbon fire curve

The hydrocarbon fire curve is fit for use in structures which are exposed to burning hydrocarbon liquids. These include poolfires in the petrochemical industry or accidents involving flammable liquid tanks. The hydrocarbon fire curve is a curve which has an extreme fast temperature raise in the beginning. After that it slowly levels out at around 1100°C and can be seen in figure 2-4. Just like the standard fire curve this curve does not take into account a growth phase or a decay phase. [36]

2.6.1.6. The Rijkswaterstaat (RWS) fire curve

The Rijkswaterstaat curve is a curve designed bij Rijkswaterstaat in the Netherlands to more closely model fires in tunnels. It is based on the worst case scenario that a 50 m^3 tanker is on fire in a tunnel producing 300MW of fire load. The curve has been produced after multiple tests and has since development been implemented in many European countries as well as in Dubai and the USA. [36]

In the following figure the three main curves shown in the Eurocode can be seen. It is clear that the shown curves have a quick growth phase and maintain a very high temperature up to infinite time. A realistic fire will start to decrease in temperature as the amount of combustible material decreases.

Figure 2.6.1.6-1: Fire curves described by Eurocode 3 [2]

2.6.2. Fire load

When determining the fire load in a compartment many parameters must be taken into account. First of all the fire scenario or type of combustible material must be investigated. The type of material and possible reduction in strength properties at higher temperatures are of great importance. Fire load is described by many parameters including: rate of heat release, smoke production and size of the fire, temperature, emitted radiation and the burning time of the fire. The OGP Risk Assessment data directory states tables with characteristic values of heat radiation and emissivity of certain common fluids. [6][36].

2.7. Fire protection

When a steel member is exposed to a standard fire curve it could result in a fire safety of only a couple of minutes. This is the reason that steel members are often protected by certain fire protection materials. Even though in this thesis we will look only at unprotected steel columns it is worth knowing different types of fire protection and how they work. Fire proofing can be done in multiple ways, the easiest is to apply a cover that does not burn and does not create toxic smoke or gasses. It should have a certain insulating effect so the

material behind it stays cooler for a longer time. Needless to say, these fire proofing materials should have a good resistance to the natural elements and degradation.

2.7.1. Sheet material

To protect structural steel sheet material is often used. The steel will then be covered causing for an insulating layer. The connection between the steel and the sheeting is very important for the correct functioning of the insulating material. [27]

2.7.2. Sprayed material

Materials which increase the fire resistance of steel can also be sprayed on. There are two types of materials available for this: A sprayed on material which has enough thickness to cause an isolating effect or an intumescent coating. When this type of coating reaches 200-250°C it expands by a chemical reaction creating a layer which has a very low conduction coefficient. [27]

2.7.3. Concrete encasement

This method of fireproofing can be done in two ways. One option is to completely encase the entire profile in concrete and the other is just to fill the gap in between the flanges. The first of the two will have a longer fire resistance as the steel is covered by a layer of concrete. The concrete will in this case act as an insulating layer. [27]

2.7.4. Membrane effect

When a suspended ceiling has been installed in a compartment this can cause a membrane effect. Due to the fact that a layer of cool air is trapped in between the suspended ceiling and the actual structure it will have an insulating function. A fireproof suspended ceiling also has the function to keep the flames away from the structural members preventing direct contact. [27]

2.7.5. Heat shields

The main function of a heat shield is to prevent the direct contact of radiation on the structural steel members. By placing a shield in front of a structural member the radiation will first meet the shield and it will take longer for the structural members to heat up. [27]

2.7.6. Heat sinks

Heat sinks divert heat to other parts of the construction so the steel will not increase in temperature as fast as normal. Usually tubular structures will be filled with a liquid or concrete. Liquids which are applied must satisfy certain conditions, for example they must be resistant to frost and should not affect the steel in a negative way. A tubular section filled with concrete will have reinforced concrete as its core. In this case when the steel has reached yielding strength in fire conditions the concrete can take over the load. [27]

2.8. Structural behaviour

Before discussing the structural behaviour of a steel structure in fire it is important to understand what will happen to an individual column in a fire situation. A stocky column experiencing an axial force will be crushed or when made up of plate material local buckling will occur. A slender column will behave elastically and will fail by buckling. Tests conducted by Olawale and Plank [26] show that the slenderness of an element has big effects on the behaviour in a fire situation. In 1975 this was already researched and

experimentally proven by Witteveen and Twilt. Residual stresses are known to influence the buckling load at room temperature of an element but testing has shown that this effect does not increase in a fire situation. [26]

During full scale fire tests which have been conducted in the past years it has become clear that it is very important to check the behaviour of a structure opposed to just the behaviour of an element. Tests conducted on a column which is on the outside of a structure proved that the heat which was transferred to the column was also released rapidly to the outside air. Results show that maximum temperatures in these columns will be lower than that of an internal column because they are outside the compartment. [11]

A loaded column subjected to fire from one side only will due to temperature expand on that side. This side is the side which is closest to the fire. Because of this expansion the column will bow towards the fire and causes an eccentricity when an axial force is applied on the column. The eccentricity due to bowing creates a moment which could in certain circumstances add on to moments created by imperfections of the column and eccentric loads. In short, this means that in a fire situation a column could fail a lot faster through the failure mechanism of buckling. [11]

In Kirby and Wainman [11] different test setups have been made to test the fire resistance of steel members. The most important difference in these setups is that individual elements are compared to the behaviour of elements which are in a structure. A structure will have a better fire resistance than an individual element. The failure load of a structure will be higher than that of an element because in a structure load distribution will occur and because elements are connected they will aid each other. A negative effect of this is that connections will be loaded even higher and could result in failure. When checking a structure for fire resistance the fire scenario and the properties of the elements must be kept in mind. In the end the failure of the structure is not dependant on the failure of a single element but the behaviour of the structure. [11][12]

2.8.1. Calculation methods

There are multiple ways to test if a construction can cope with a certain fire. This can be done either by testing in a furnace with a known/calculated fire curve or using the calculations in the Eurocodes. The decision for testing or calculating depends on the type of material and the complexity of the structure. For standard load carrying members it will probably be cheaper and faster to use the Eurocodes then testing. In the other case, a member could be of such complexity that the Eurocodes do not describe the member well enough and full scale testing is the best option. The approach of the calculation methods for fire resistance of construction elements given in the Eurocodes can be described in five steps.

Step 1: Defining the loads on the construction during a fire situation. This load will be relatively low as safety factors are set to unity and the influence of any other large loads like storm or snow are omitted.
Step 2: Defining the thermic load on the structure. This could be the standard fire curve described in the Eurocode or a calculated fire curve depending on the type and amount of fuel available.
Step 3: Determining at what location and how fast the structure will be heated.
Step 4: Determining whether the residual load carrying capacity after heating of the structure.
Step 5: Checking whether the residual load carrying capacity is sufficient to resist the loads acting on the structure.

2.8.2. Eurocode

Eurocode 3 [2] states that the fire resistance can be proved with simple methods such as tables, graphs and simple calculations or using a more sophisticated Fire Safety Engineering approach. This latter approach is more focussed on the natural fire concept, describing the fire in a more realistic manner.

Using the natural fire concept the constructions fire resistance is evaluated through single elements and using the temperatures given by the standard fire curve. Using this fire curve the temperature will always keep rising, so eventually the elements properties will have decreased enough to fail. Whilst checking beams and floors only the bending moments are taken into account. The normal and shear forces in these elements are left out because they are usually not governing in case of a fire situation. Columns will be calculated only on compression or bending of the element by exceeding of the load carrying capacity.

The Eurocode implies that the event of a fire is an exceptional load case in which the chance of occurrence is small but the effects could be very severe. This means that when the fire load is in the design no other incidental loads have to be taken into account as the likelihood of both occurring at the same time is close to zero. Because fire is an exceptional load case the safety factors in design for self-weight and loads may be set to unity as described in the Dutch national annex to NEN-EN 1990. [1][15][35]. NEN-EN 1991-1-2 shows that when using the standard fire curve any physical forces caused by the fire do not have to be taken into account. [35]. Research done by Wang and Tan [19] has concluded that the calculation procedure described by Eurocode 3 shows steel temperatures which are higher than found by testing. The temperatures found in the web and in the flange both result in lower values than described by the Eurocode 3 procedure.

Drawbacks of these simple methods are that the forces created by expansion of members are not taken into account acting on the rest of the structure and the temperature of the fire follows the standard fire curve instead of the fire safety engineering approach.

2.8.3. Buckling

The Euler buckling formula which has been formulated by mathematician Euler in 1757 can calculate the maximum axial compressive force in a slender column without geometrical imperfections and residual stresses. The downside to this formula is the fact that this is only applicable to ideal perfect columns which have no imperfections. In reality all materials will have some imperfections which may arise during manufacture or installation. Since the formulation of the Euler buckling curve many buckling calculations have been based on it. Chapter ten will describe different methods for calculating the buckling strength in a steel column including the method in the Eurocode without a temperature influence and Euler's formation of the equation. In this chapter however the method described by the Eurocode will be briefly reviewed.

NEN-EN 1993-1-2, section 4.2.3.2 notes a specific formula for the buckling curve for fire. In this formula the effect of the reduced stiffness has been taken into account through a dimensionless relative slenderness.

$$\bar{\lambda}_\theta = \bar{\lambda}\sqrt{\frac{k_{y,\theta}}{k_{E,\theta}}}$$

Relative slenderness $\bar{\lambda}$ is equal to buckling calculations at room temperatures:

$$\bar{\lambda}_y = \frac{\lambda_y}{\lambda_1} \text{ and } \bar{\lambda}_z = \frac{\lambda_z}{\lambda_1}$$

In this equation λ is the slenderness for direction y or z and λ1 is dependent on the type of steel used. Slenderness λ is equal to:

$$\lambda_y = \frac{l_{fi,y}}{i_y} \text{ and } \lambda_z = \frac{l_{fi,z}}{i_z}$$

L_{fi} is the buckling length in fire and i the radius of gyration. NEN-EN 1993-1-1 section 6.3.1.3 shows that the slenderness value to determine the relative slenderness, which takes into account the steel grade, is equal to:

$$\lambda_1 = 93.9\varepsilon = 93.9\sqrt{\frac{235}{f_y}}$$

With two parameters, α and φ_θ, NEN-EN 1993-1-2 the buckling factor X_{fi} can be determined and after that the maximum allowable compression force $N_{b,fi,t,Rd}$.

$$\alpha = 0.65\sqrt{\frac{235}{f_y}} \text{ and } \varphi_\theta = \frac{1}{2}\left(1 + \alpha\bar{\lambda}_\theta + \bar{\lambda}_\theta^2\right)$$

$$X_{fi} = \frac{1}{\varphi_\theta + \sqrt{\varphi_\theta^2 - \bar{\lambda}_\theta^2}}$$

$$N_{b,fi,t,Rd} = X_{fi} A k_{y,\theta} f_y$$

In a braced structure the buckling length may be reduced in certain fire situations. This reduction is valid only for columns which are continuous or which are stiff or semi stiff connected to the structure. The fire must be retained to one floor only. The top column in a layered structure may be reduced to 0.7 times the length. Any intermediate columns may be reduced to 0.5 times the length. The same reasoning can be done for columns connected to the floor by an endplate, and can in certain situations be seen as a clamped connection. The circumstance under which this may be done is that the eccentricity of the load must be small. Usually in a braced structure this will be the case. [35]. The figure below shows in which cases the buckling length may be reduced. In the top story $l_{buc} = 0.7\ l_{sys}$ and an intermediate column $l_{buc} = 0.5\ l_{sys}$.

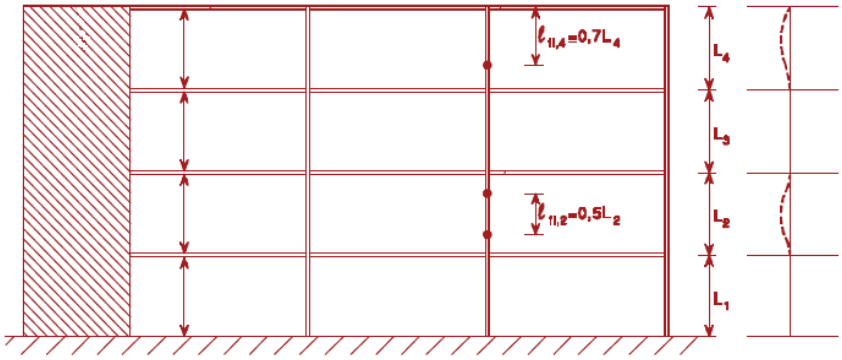

Figure 2.8.3-1: Reduced buckling lengths in a structure.

2.8.4. Rankine approach

Modelling of column failure with a temperature influence is a complex job due to the fact that many material parameters change as temperature increases. Due to these complex parameters it is not a very obvious choice to try and create a mathematical formulation of the problem. Still some have tried to add onto known formulas like the Euler buckling formula or the Rankine approach. [13]. In 1866 Rankine developed a formula for calculating the failure load of a bar in compression at room temperature. Toh, Tan and Fung [29] have investigated this approach and extended it so it can be used in the design of unprotected columns during a fire. Temperature deformations, plastic and elastic buckling mechanisms can be taken into account to define the strength and stability of a column at a certain temperature. Later Yao and Tan [30] have extended the Rankine method further to incorporate multiple loads on a column. Comparing results to finite element models it showed good similarities.

The Rankine formula developed resulted in the following equation:

$$\frac{1}{P_c(T)} = \frac{1}{P_p(T)} + \frac{1}{P_e(T)}$$

In this equation P_p defines the column strength as rigid plastic collapse load at a particular temperature. P_e is the Euler formula for buckling indicating the maximum elastic-critical load that an ideal column can resist in axial compression.

2.8.5. Heat transfer

The methods available to calculate the transfer of heat in a construction element require a process in which reliable analytical and numerical solutions must be used to describe the heat flow. Numerous methods have been invented to calculate this for solid objects. When trying to calculate the heat flow in a steel member due to a standard fire curve some extra challenges arise. The fact that the standard fire curve is a time dependant boundary condition causes formulating the temperature to be a complex task. Only a few 1D analytical solutions are known in literature that can apply a boundary condition consisting of the standard fire curve. These methods include the separation of variables by Wickstrom, the Laplace transform by Malinek and Thomas, and the Green's function method by Wang. In Wang and Tan [14] an analytical method has been developed which allows calculating the temperature changes in 2D or 3D elements. Testing showed a difference in comparison of about 4%. The expansion of the 1D formula to a 2D or 3D formula causes the method of calculation to be even more complex.

When pool fires are likely to occur it is much more difficult to calculate the amount of heat released and absorbed by an element. Large pool fires produce a lot of smoke and depending on the type of fluid almost 20% of the fuel could go to waste as smoke. This amount of smoke blocks the flames which are the main cause of radiation. Usually this effect only happens at very large pool fires with inefficient burning. Modelling of a pool fire can be done in two ways. A central point in the fire can be assumed from which all heat and radiation is coming from; the 'point source' method. Or the 'solid flame' method can be used. In this last case a cylinder is used to model the fire from which heat and radiation is coming from. Research has concluded that the "rate of heat release" is the best estimator for damage due to fire. The RHR is easier to calculate than the actual fire temperature or the size of the fire because it is depending on the mass burning rate which can be measured. [24].

2.9. Modelling tools

Different types of software exist to model temperature flow through an element. Many of these rely on complex mathematical equations or finite element software. In this chapter some of the available models will be explained. During this thesis the use of a CFD model or the Finite Element approach would most likely yield in the best result. A zone model is also fairly accurate for a small compartment fire and a preliminary calculation but will not give as accurate results as can be obtained by CFD or FEM.

2.9.1. Computation Fluid Dynamics (CFD)

CFD is the analysis of systems involving fluid flow, heat transfer and accompanying phenomena such as chemical reactions by means of computer based simulation. This technique is very powerful and can be used in a wide range of fields. Some of these fields include: aerodynamics, hydrodynamics, electrical engineering and external and internal environment of buildings: wind loads and heating.

The aerospace industry has applied CFD techniques since the 1960's in the design and manufacture of aircraft engines. Later these techniques have been used in the design of internal combustion engines and

combustion chambers of gas turbines. The main reason why CFD has only entered the industrial community since the 1990's is the fact that its underlying behaviour is extremely complex. As high performance computing hardware and user friendly interfaces were getting more available the interest in CFD began to grow. Using CFD models for fire purposes many times these are based on heat radiation and a fire curve. In fire safety engineering a CFD model is the most complete model available for calculating air temperature in a compartment. It will result in the most detailed output related to the conditions of a fire. Creating CFD calculations requires a lot of skill and experience to obtain results which are reliable.

CFD models can be used for multiple reasons. They can calculate if the Available Safe Egress Time is enough or if secondary fires can ignite. Also they can model smoke production and thickness or determine if load carrying members will fail. Each of these reasons requires a different model and its own approach. The software can handle fluid flow problems through numerical algorithms. To be more efficient in use, these software programs come with a sophisticated user interface which allows users to input problem parameters and examine results. All CFD software includes three main elements: a pre-processor, a solver, and a post processor. The equations used in the software are based on the conservation laws of physics and will be elaborated on in the following paragraphs. [36][39]

Where CFD is often used to calculate velocities, temperatures and concentrations of fluids or gasses, its main advantage over finite element models is the ability to calculate heat radiation and being able to use a combustion model. The approach to solving a problem is quite similar for FEM and CFD. When using a finite element method the stresses and strains in a structure can be calculated, which is not possible in CFD. When the load carrying capacity of a structure is to be determined using FEM, usually a thermal analysis is done in advance separately. After this the data is used in the finite element method.

2.9.1.1. Pre-processor

In the pre-processor all the input and parameters describing the model must be given. This includes the geometry of the model, the mesh and definition of the fluid properties. At the boundary of the domain specific boundary conditions must be assigned. Each domain will be divided in a number of cells which are all interconnected by nodes. These nodes are the points at which the CFD software calculates its values. This implies that the amount of cells and therefore the nodes will define the accuracy of the solution. In general this means that the bigger the amount of cells in the domain is the more accurate the solution will be. A specific disadvantage which comes to this is that when the amount of cells increase the calculation time will increase as well. As a result the build-up of a mesh will be very significant in the accuracy of the solution and the calculation time needed. Meshes which are well defined are usually non-uniform; they will have smaller cells in areas where large variations occur from point to point. In areas which are of less importance the mesh can be created to be coarser. It is possible to assign a cell size in certain areas and allow the CFD software to create a mesh that connects to this area. [39]

2.9.1.2. Solver

Numerical solution techniques come in three methods: finite difference, finite element and spectral methods. ANSYS CFX uses a specific finite difference method called the finite volume method. The solving sequence of this method consists of three steps. First the governing equations of fluid flow will be integrated over all the control volumes of the domain. The second step is to convert these equations to a set of algebraic equations in a matrix form. The set of algebraic equations is complex and non-linear so solving them will be done using an iterative method and is done in the last step of the process. [39]

2.9.1.3. Post-processor

The post processor allows the user to visually interpret the results of a calculation. Using vector plots for flow diagrams and contour plots for temperature for example results can easily be shown. In the pre-processor phase monitor points can be added to the model in which the exact results can be presented as output in a file. As an example temperature can be given at certain locations so the output file registers hard temperature data which can be used for further research. The advantage of using these monitor points is that the exact temperature is given instead of having to look on a plot or animation. [39]

2.9.1.4. Solving with CFD

Problem solving using CFD methods is a complex tasks and the accuracy of the results rely heavily on the physics and chemistry in the software and the knowledge and expertise of the user. To reduce the complexity of a model to a manageable level assumptions have to be made. It is important that these assumptions do not negatively affect the accuracy of the model. To be able to perform a computation with CFD software is a whole different skill. At the input stage the grid design is one of the most important parameters to obtain a successful computation result. As the solution is obtained using a numerical method a successful computation result is defined by grid independence and convergence of the solution. Guidelines to how to model a certain grid for a certain problem do not exist. Prior knowledge to the problem and a good idea of problem areas is important to obtain a good grid. This is a specific field which relies on the expertise of the designer. The field of expertise can only be obtained by extensive use of the code and so will take a lot of time to get a grip on. A good grid design will be based on insight, prior knowledge and expected flows in the problem.

The equations in the software used to solve the CFD problem are mass conservation in three dimensions, the momentum equation in three dimensions, and the energy equations in three dimensions. These equations all follow the conservation laws of physics. Mass conservation in three dimensions is based on the fact that the mass of a fluid is conserved. The momentum equation in three dimensions is based on Newton's second law: the rate of change of momentum equals the sum of the forces on a fluid particle. The energy equation in three dimensions is based on the first law of thermodynamics: the rate of change of energy is equal to the sum of the rate of heat addition to and the rate of work done on a fluid particle.

Heat transfer occurs in three modes, these being: conduction, convection and radiation. Energy emission in the form of electromagnetic waves or streams of photons causes thermal radiation. CFD calculations often neglect radiative heat transfer because in engineering problems usually convective heat transfer is prevailing. In some cases however radiative heat can be governing and must be taken into account. These cases include manufacturing processes where materials are exposed to radiation with very high energy density. Another example is combustion equipment, usually convective heat transfer is very forceful in combustors and the temperatures generated are sufficiently high for radiative heat fluxes to be of a similar magnitude. Air at room temperature is transparent to infrared radiation. This air-fluid at room temperature will not participate in the radiative heat exchanges because the molecules in clean air do not absorb heat easily. When a fire is present in a compartment the air will mix with products of combustion. These products contain large amounts of carbon dioxide and water vapour which are strong absorbers and emitters of infrared radiation. When the combustion process produces particulate matter such as soot scattering radiation may occur. In this case the fluid is called a participating medium. This means that in the energy equation an extra term will be added which takes into account the radiation. [39]

2.9.2. Zone models

A zone model is a model which is built up a compartment divided in two zones. The top zone is the hot air and smoke layer with a uniform temperature and smoke density. At the bottom there is a smoke free layer

which is the cold zone with a uniform temperature. The rising plume of smoke causes for the supply of air from the cold zone. A zone model gives us information about the formation of the smoke layer in time. This way we can calculate the height of the smoke layer at any time, the temperature of the smoke layer and the density of the smoke.

Calculation methods used in zone models rely heavily on the conservation laws being, the law of conservation of mass, conservation of energy and conservation of particles. Programs like Ozone (created by ArcellorMittal) incorporate the current Eurocodes. This means it can compute temperatures according to the standard fire curve. It is also possible to include a custom fire curve. In this case the exact fire curve must be known. A downside to the results obtained by this software is that the column will always be heated from four sides and the influence of a thermal gradient will not be taken into account.

The drawbacks of using a zone model are that when there are multiple fires it cannot be used and the geometry of the compartment must be simple. Natural airflows existing in the compartment are very difficult to take into account and horizontal smoke travel is not taken into account. Fires modelled in a zone model can be designed as a constant fire load or a t2 curve. In the latter case the fire is modelled as an exponentially growing fire load. When using a zone model a few thoughts need to be kept in mind. Since the geometry of the compartment is usually simplified are the results still reliable? Are assumptions and restrictions included in the model factual? When examining the results of a zone model a few checks can be made to see if the results are plausible. When looking at a temperature graph of the compartment, unrealistic temperatures (2000°C) should not be seen. Also kinks in graphs showing smoke thickness or temperatures are highly unlikely. When temperatures arise which could ignite secondary fires the zone model is no longer accurate. [36]

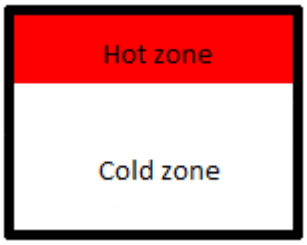

Figure 2.9.2-1: Cross section view of two zone model showing two zones [37]

The figure above shows a compartment during a zone model calculation. The upper layer is described by the hot gas layer formed by the fire and the smoke. The lower layer is the cool layer of air which is unaffected by the fire.

2.9.3. Finite element models (FEM)

Finite element methods are especially used in calculating stresses in construction elements. Using a FEM program it can be calculated if or when a construction member will fail. This software will divide a member in “finite elements”. When solving all the equations for these finite elements the stresses and temperatures will be calculated in the construction element. The smaller the elements used, the smaller the error will be. The downside of using a lot of elements is that when we double the amount of elements, the calculation time will increase quadratic.

Using a thermal model the temperatures of the element can be obtained. A mechanical model differs from a thermal model in the way that the modulus of elasticity, the expansion coefficient and the boundary conditions must be entered. Using a combination of the two will yield in a more complex and complete model but the calculation time will also be longer.

The most important parameters to be included in a FEM model are the temperature dependent parameters, size of the timestep, heat transfer coefficient and the boundary conditions of the system. The boundary conditions and the initial conditions have a great influence on the outcome of the calculations. In a mechanical calculation a boundary condition would be the type of supports on each end of the element while in a thermal calculation the boundary condition would describe a set temperature at the edge of the element. Due to a natural fire curve it could be that this boundary condition is also a function of time. The results of a FEM analysis should always be checked for credibility and should match simple hand calculations [36].

To find the temperatures in an element or the compartment CFD analysis would best suit. Once these temperatures are known a FEM analysis can be made to check the structure on strength.

2.10. Fire Safety Engineering (FSE)

Fire safety engineering is the study of describing the properties of a fire and the influence it has on a structure and its occupants. The actual response of a structure in a fire can differ significantly than test results or simple calculations. The purpose of fire safety engineering is to describe the response of a structure due to a more realistic fire curve and linking this to the response of the system. [35]

Using fire safety engineering the first and most important data is a realistic fire scenario. Using the rate of heat release or the temperature versus time graph the temperature and the behaviour of the structure can be examined. [9]. FSE gives us the advantage of modelling fires more realistically but also to study the structural behaviour. In earlier codes and guidelines individual members were tested and these results would govern the amount of time a structure is fire resistant. Because the structure has connections and loads can be transferred these results do not model reality very closely. [35]. To describe the fire scenario the amount and type of fuel need to be described as well as the compartment, the heat release and the smoke production. [36].

When modelling a fire in an FSE model a certain worst case scenario must be used. This case is governed by the most unfavourable load combination and location of the fire with an adequate probability of occurrence. In fire safety it's difficult to determine which scenario is the worst case scenario. Usually many different worst case scenarios will be investigated. Because this can lead to excessive costs some scenarios can be pre-calculated to find which scenario has a high probability of being the worst case. A model of a fire in a room is a more simplified representation of a real fire. It differs from reality in the sense that a real fire is very complex and has a lot of variables to keep in mind. Creating a very complex model does not necessarily mean the outcome will be more realistic, due to the difficulty of applying all the variables. Being able to change the parameters of a model is the main advantage of using them. It means that we can change the settings of a fire and get results fairly quickly without having to test every single setup in a laboratory. Both a calculation and a model are models of reality based on assumptions and simplifications. [36]

During this thesis the method of fire safety engineering shall be used to test the influence of a thermal gradient on a steel column in a compartment. Using a fire curve which has a rapid growth phase, a fully developed fire phase and a decay phase the temperature of the steel column can be modelled to be closer to reality. After this it can be investigated what the influence of the thermal gradient is with respect to the buckling load.

3

Case study

To investigate the influence of a thermal gradient in a column due to a pool fire a representative model has to be created. The model chosen is a steel structure creating a large compartment. This structure is based on an ongoing project by Tebodin. The dimensions of the compartment can be seen in the figures below. The length and the width of the compartment are both 12 meters whilst the height of the compartment is 6.4 meters. The two figures also show the columns which are of interest on the field of buckling. These columns have the same section size as the columns used in the walls but as they carry most of the load in the current design they will be governing. In the top view figure the two columns are indicated by the red circles and in the cross section the red ellipsoid shapes indicate the columns. The figures are created using AutoCAD files and also display the profiles which have been used in the design. The floor of this structure is assumed to be flat and not a sloped surface. Using this assumption we can create situations in which the fire is in different locations.

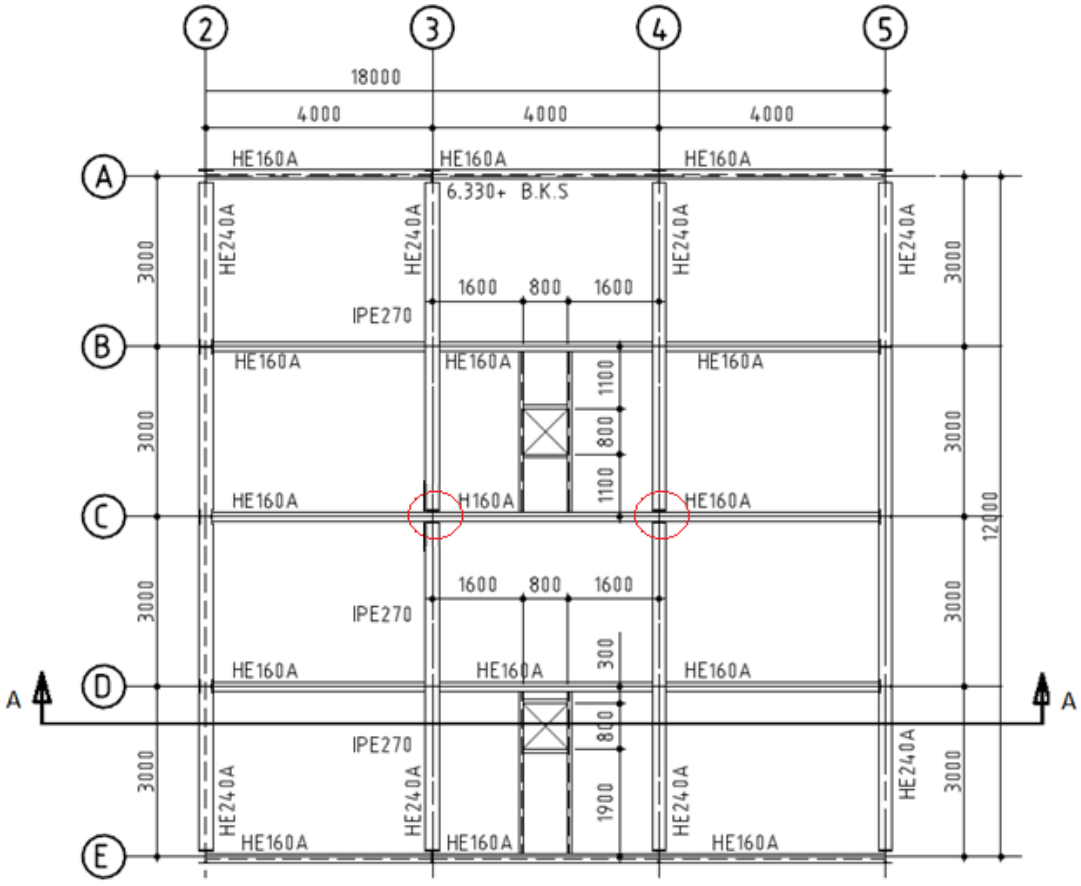

Figure 3-1: Top view model

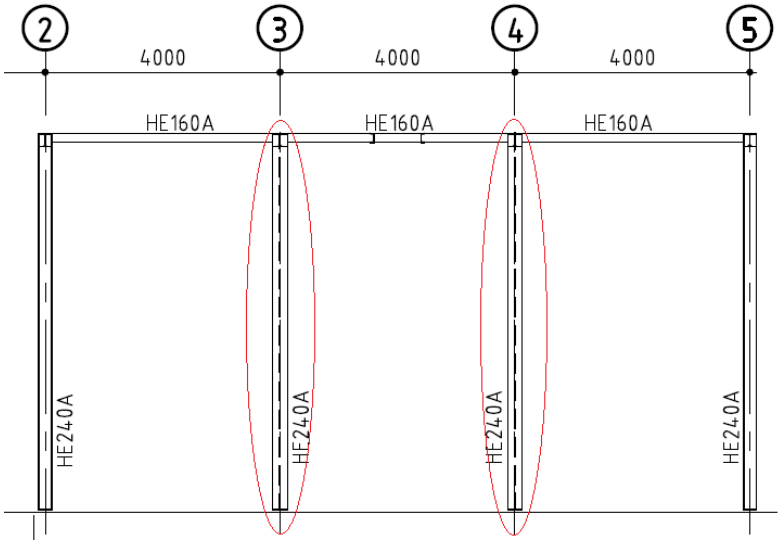

Figure 3-2: Cross-section A-A showing columns

The model which will be considered also has openings in the structure. A large overhead door, windows and roof openings are included. The following figure show the location of the overhead door and the window in one side of the structure. The other side of the structure has a window which has the same dimensions. For more information on the model which has been used please refer to the appendix.

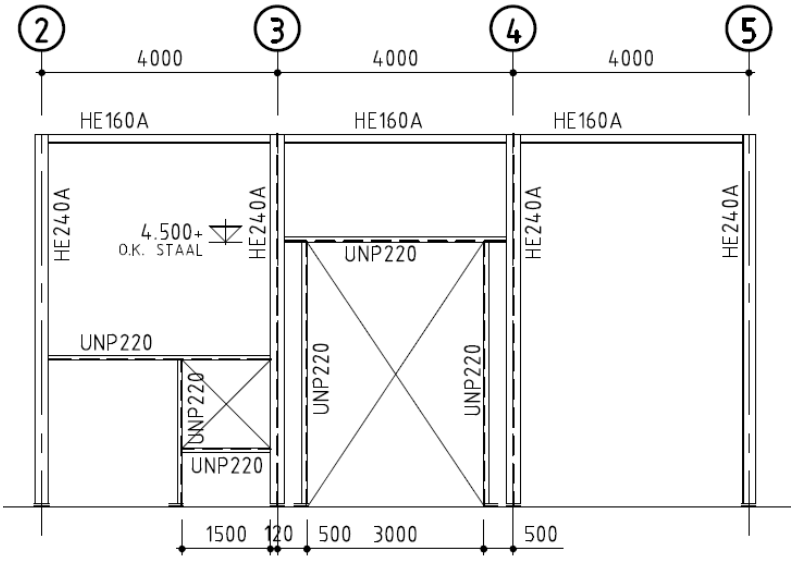

Figure 3-3: Side view showing openings.

At the points where the columns meet the roof and ground floor connections must be realised. There are multiple ways to model the supports of these columns in the structure. The simplest way is to assume a simply supported column which is axially loaded. In a more realistic schematization the supports can be interpreted as rotational springs.

Figure 3-4: Schematization rotational springs

Figure 3-5: Schematization simply supported column

In the chosen model at first the column with hinges at the ends will be investigated. This case will not take into account the connections at the floor and at the roof. After this has been done the study can be expanded to take into account the effect of the connections on the column. This will mean that the effective buckling length of the column changes, and will result in a different buckling load.

The connections connecting the column to the roof and the floor must be checked according to the Eurocode 3 in a fire situation. Eurocode 3 states that it is not necessary to assess the failure of connections on the subject of surface area. This is due to the fact that connections have more material and the temperature in the connection will be lower. The bolts in a connection which are loaded in shear or tension must be checked to make sure they can resist the elevated temperatures. Welds which have been applied must be checked according to Eurocode 3 as well. The focus of this thesis is mainly on the column itself and therefore the connections shall not be treated extensively.

3.1. Columns

To support the roof structure of the compartment columns have been added to the structure. These two columns are located in the near centre of the structure. The roof structure will be supported by both the columns and the walls surrounding the compartment. When calculating all columns and walls individually the model will get many different types and sizes of sections. In this case it has been chosen to apply a minimal of different section sizes so connections and installation will be faster and easier. This means that the columns in the walls and the columns in the middle of the compartment are also the same size. The permanent load of the roof structure as well as the variable load on top of it results in forces on all columns. As the loads acting on the roof structure are transferred to the columns it seems legitimate to assume that the columns in the centre will carry the majority of the load, therefore these columns are very important in the design.

The columns in the centre of the compartment just like those in the walls are HE 240A sections. These sections are 230 mm tall and 240 mm wide. The grade of the columns is S235; this means that the yield strength of this grade is 235 MPa or 235 N/mm^2. Often steel columns in a structure will have fire protection to gain more fire resistance time. As discussed in the literature review there are many different types of fire protection available for use. The columns which will be discussed in this model and this thesis will be unprotected. This means that the heating rate is not slowed down by any means. The heating rate of the column depends solely on the section factor of the section. The section factor is defined as the heated circumference of the section divided by the cross sectional area. For I- shaped sections the shadow effect needs to be taken into account. This is done by multiplying the previous factor by 0.9. A HE240A section will then have the following section factor:

$$P = 0.9 * \left[\frac{A_m}{V}\right]_b = 0.9 * \frac{230 + 230 + 240 + 240}{7680} * 10^3 = 110 m^{-1}$$

Very slender sections will have a high section factor meaning they heat up faster. Stocky sections have a low section factor and due to the amount of material which is present in the section it will heat up slower.

3.2. Fire description

In this thesis the focus will be on the type of fire which consists of hydrocarbon fluids. When these types of fluids ignite they have an ultra-fast growth rate due to the high combustibility and nature of the material. As stated in the literature review there is many types of fire curves which can be used to predict the temperature in a compartment. In this thesis the focus will be laid on a method with a more realistic approach to modelling fires. This means that a representation of a natural fire curve will be used. The main difference to the standard fire curve is the fact that the natural fire curve has a growth phase, a fully developed fire phase and a decay phase. This more realistic approach also takes into account the amount and type of combustible material which is in the compartment. [36]

The growth phase in a natural fire curve is defined by a so called t2 -curve. The growth rate of the fire is usually defined by the time it takes to reach 1MW. The t2 –curve assumes that the growth rate is constant and equal in two dimensions, the surface of the combustible material. As the fire progresses with a constant rate over the length and width of an item, the area of the fire will increase quadratic. Items which are highly combustible will have a steep increase in growth and items with a relatively low combustibility will have a slower growth. The curves have been split in ultra-fast, fast, medium and slow depending on the amount of time needed to reach 1MW of power. The ultra-fast t2 curve reaches 1MW in 75 seconds and the slow t2 curve in 600 seconds for example.

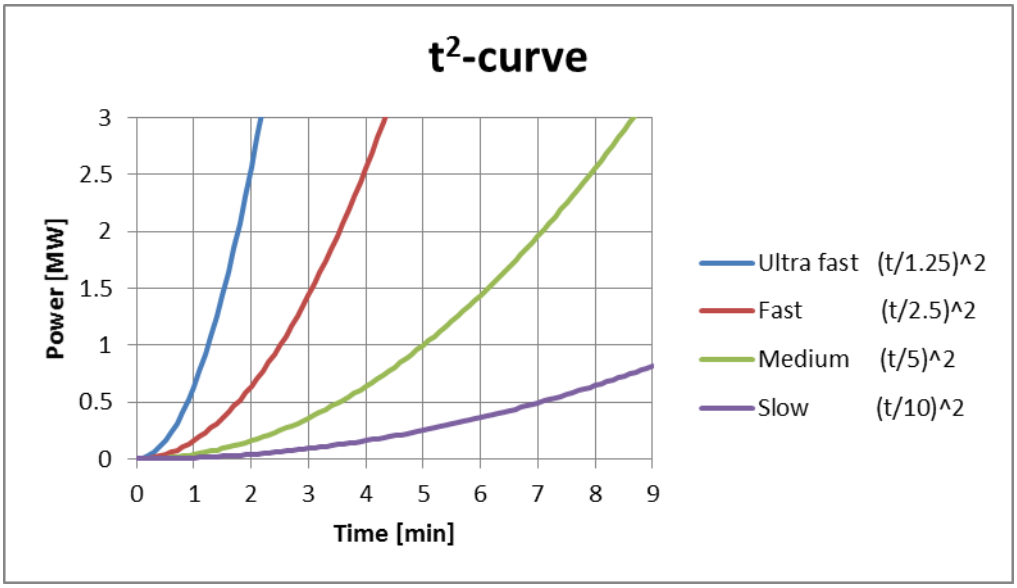

Figure 3.2-1: Standard t2-curves for an ultra-fast, fast, medium and slow developing fire.

In certain situations this approach cannot be used; for example when the fire progresses in three dimensions. This is the case in a storage compartment where material is stacked and so the fire will progress over the surface area of the floor but as well in the height. (a t3-curve would best describe this). [36]

3.3. Fire dimensions

To conduct the research on a thermal gradient a certain fire must be assumed. The type of fluid must be set and the dimensions of the fire area. These parameters can then be used in the national annex to develop the natural fire curve. The type of fluid and its rate of heat release can be calculated to find the height of the plateau in the fire curve. Using the mass burning rate of the liquid and the amount of fluid which is used the burning time of the fire can be calculated. This means that also the time can be calculated at which the decay phase sets in according to the national annex of the Eurocode [1].

The chosen dimension of the pool fire surface is three meters in diameter. Research has concluded that this diameter of a circular pool fire the most energy is released. Any smaller and the energy released will be less while any bigger diameters will result in more production of smoke and thus increasing the blocking effect. A diameter of three meters results in a total surface area of 7.06m^2. A liquid on this area which is 2.5 cm deep will result in a volume of 177 litres of liquid. The reason that the chosen depth of the pool fire is 2.5 cm is that any deeper than this there will be energy loss towards the ground. The chosen liquid which is used during this thesis is heptane. This is a highly flammable hydrocarbon liquid which is often used at test facilities to mimic the effects of a hydrocarbon fire. A calculation example for the amount of energy released by this liquid and area is given below.

The next item is to determine the position of the fire in the structure. This will be set up in two different locations. The first fire location is at a distance from the weak axis of the column which will be focussed on this side. In this setup the thermal gradient will develop over the width of the flanges. The second location is at a distance from the major axis of the column resulting in a thermal gradient which is from one flange to the other.

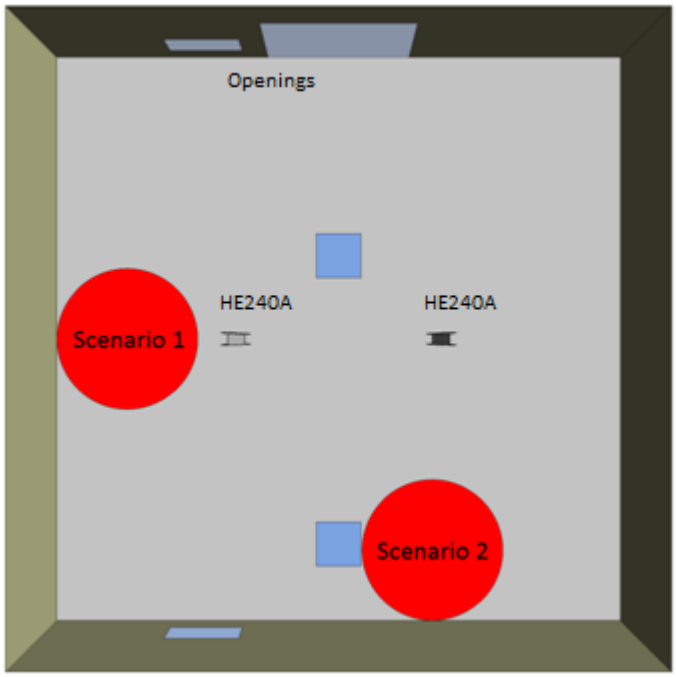

Figure 3.3-1: Top view of model in perspective indicating the fire scenarios.

The figure above shows a top view of the compartment and the two fire scenarios. The red circles indicate the fire locations. Fire scenario 1 has the fire on the weak axis of the column and scenario 2 has the fire situated on the strong axis of the column. Blue rectangular and square shapes indicate the openings in the compartment. The walls have two window openings and a large door, the roof shows two square openings.

3.4. National annex to NEN-EN 1991-1-2

The t_2-curves have been categorized in four rates; being ultra-fast, fast, medium and slow. In case of a hydrocarbon pool fire the ultra-fast case would be the most obvious. Eurocode 1-1-2 and the Dutch national annex provide a first step towards calculating a natural fire curve. It provides guidelines for creating a growth phase and the height of the plateau in the fully developed fire phase. The growth part of the function is described by the following formula and is also the same as the t_2 -curves:

$$Q = 10^6 \left(\frac{t}{t_\alpha}\right)^2$$

Q= fire load density in [W]
t= time in [s]
t_α= time needed to reach a fire load density of 1[MW]

The factor t_α is defined as either 75, 150, 300 or 600 seconds. These values are chosen through tables in the national annex based on the use of the building and the type of material which is in it. The ultra-fast curve which is applicable in this case would mean that tα equals 75 seconds.

The fully developed fire phase is defined by a horizontal plateau connected to the growth curve. When 70% of the combustible material has been consumed by the fire the decay phase sets in. The decay phase can be described by a linear segment with a negative slope until all material has been burnt and the final rate of heat release is zero. The height of the developed fire phase is constant and can be calculated by:

$$Q = RHR_f * A_s$$

A_s = maximum surface of the fire in [m2]
RHR_f = maximum fire load density per m^2 fire in a fuel controlled fire in [kW/m^2]

According to the national annex, RHR must be multiplied by a factor (δ_{qf}) which takes into account the activation risk and the effect of the active fire safety systems in the compartment. The same factor must be applied to the value of the fire load [MJ/m^2]. [1]

3.4.1. National annex worked out

3.4.1.1. Fire load and fire load density

The national annex allows us to calculate the fire load and the fire load density for a given compartment and the amount of material which is inside. The following calculation is a worked example for the compartment we are discussing. This calculation is according to a three meter diameter poolfire which is 2.5cm deep. The total area of the poolfire is in this case 7.06m2 and the volume of the liquid is 177 litres. In the chapter “fire dimensions” these parameters are explained and argued.

The design value for the fire load density $q_{f,d}$ is given by:

$$q_{f,d} = q_{f,k} * m * \delta_r$$

The characteristic fire load $Q_{fi,k}$ in MJ is given by:

$$Q_{fi,k} = \sum M_{k,i} * H_{u,i} * \psi_i$$

$M_{k,i}$ = 177*0.684 = 121.068 kg mass of combustible item
$H_{u,i}$ = 45 [MJ/m2] heat of combustion of heptane

Ψ_i = 1.0

$$Q_{fi,k} = 121.068 * 45 * 1.0 = 5448.06\ MJ$$

The characteristic fire load density $q_{f,k}$ in MJ/m2 is given by:

$$q_{f,k} = Q_{fi,k}/A = 5448.06/7.06 = 770.74\ MJ/m^2$$

The design fire load density $q_{f,d}$ in MJ/m2 is given by:

$$q_{f,d} = q_{f,k} * m * \delta r$$

m = for cellulose based products a reduction of 0.8 may be used. In this case 1.0 will be used.

δ_r = factor based on the fire resistance time needed as set per building type.

R [min]	20	30	60	90	120
δr	0.33	0.5	1.0	1.5	2.0

For halls which have no storey floors higher than 5 meters above ground level no requirements for fire resistance have been set. Because of this we will use R equal to 20 minutes.

$$q_{f,d} = q_{f,k} * m * \delta_r$$

$$q_{f,d} = 770.74 * 1.0 * 0.33 = 254\ MJ/m^2$$

The calculation value of the fire load density is the design fire load density multiplied by a risk factor which takes into account the activation risk of the fire and the types of active fire protection systems in the compartment.

$$p_{tot} = p_1 * p_2 * \prod_i^n p_{ni}$$

p_1 = floor area of the compartment divided by 25

p_1 = 144/25 = 5.76

p_2 = factor for the risk of activation of a fire

p_2 = 100 for very high risk class. Used for e.g. chemical laboratories, paint production companies.

P_{ni} = factors taking into account the chances of failure for the active fire protection systems.

In the national annex to NEN-EN 1991-1-2 table NB.3 different active fire protection systems have been explained and the factors given. In our case we assume that as for a normal building only the government fire brigade is available and the fire will automatically be reported to the authorities.

This gives us two factors for p_{ni} being: 0.25 for the automatic reporting and 0.1 for the government fire brigade.

p_{ni} = 0.1*0.25 = 0.025

p_{tot} = 5.75 * 100 * 0.025 = 14.4

Using linear interpolation δ_{qf} can now be calculated from table NB.1 resulting in a value of 1.56. This value incorporated in the equation to find the calculation value for the fire load density.

$$q_{f,r} = q_{f,d} * \delta_{qf}$$
$$q_{f,r} = 254 * 1.56 = 396.24\ MJ/m^2$$

In the fire area of 7.06m^2 [1]

3.4.1.2. Heat release rate

The rate of heat release can be found in the national annex for different types of materials and use of the compartment. In table NB.10 different use of compartments show heat release rates which can be used. These may only be used if the factor p^2 in the equations above is equal to unity. This is only the case when the risk class for the activation chance of a fire is "normal". In our case we are dealing with a risk class which is "very high" which means we may not use this table and must calculate the rate of heat release based on the type of fluid and area of fire.

The total area of the liquid is 7.06m^2 filled with 2.5 cm of heptane. The burning rate of this liquid is assumed to be 4.5mm/min, the density is 684 kg/m^3 and the heat of combustion is 45MJ/kg [35]. In one minute a total volume of 4.5*10^{-3}*7.06m2 = 31.77*10^{-3} m^3 is burnt. The mass of this volume is 31.77*10^{-3}*684=21.7 kg. This mass creates an energy of 21.7 * 45 = 977 MJ. Dividing this energy by 60 seconds gives us the heat release rate of the fire. 977/60 = 16 MW. Using the given data we can also calculate the amount of time this fire will burn. The depth of the liquid is 2.5 cm and the burning rate is 4.5 mm per minute. This means the fire will burn for 5.55 minutes not taking into account the dacay phase after 70% has been burnt. In this method the liquid is only burning from the top which represents reality in the case of a contained liquid. [35]

Another method to calculate the burning time is to use the amount of mass burnt per second. This method takes into account that all material is on fire at the same time. The formula used to calculate this time is:

$$t_b = \frac{V * \rho}{m'' * A}$$

V is the volume of the combustible material
Rho is the density of the combustible material
m" is the mass burning speed
A is the area of the combustible material

$$t_b = \frac{7.06 * 0.025 * 684}{0.101 * 7.06} = 169\ seconds$$

Obviously this burning time is much less than calculated before, but is also less accurate in the case that the liquid is contained in some area.

4

Thermal gradient study

4.1. Introduction

To investigate the thermal gradient which occurs in the cross section due to a pool fire a study has been performed in cooperation with ONE Simulations. ONE Simulations is an engineering company which has made advanced simulations in the field of fluid dynamics their speciality. Using Computational Fluid Dynamics software and experience from studies and projects ONE Simulations has gained expertise in the field of fluid dynamics, fire safety, the environment and energy. The CFD software used at ONE Simulations is ANSYS CFX. This high performance fluid dynamics program has been widely used to solve fluid flow problems and challenges for over 20 years. ANSYS claims this particular CFD programme is so highly developed that it could possibly model and solve any problem related to fluid flow. The geometry and mesh has been created with ANSYS Workbench, this tool will be further explained in the following subheading.

4.2. Setup of the model

4.2.1. Geometry and meshing

In the first stage of the analysis the geometry of the model must be entered in the software. As discussed before the model which is of interest is a compartment with the following length by width by height respectively, 12m by 12m by 6.4m height. At this stage all dimensions which are relevant to the model are introduced, this includes all windows, doors, openings, relevant objects inside the compartment and the area of fire in this case. When all the dimensions of the model have been entered the next step is to start creating a mesh. It is worth noting that as the temperature in the column is of great interest the mesh will be much finer than that of the fluid at a further away location. To create a good mesh the solid columns will be meshed with a very fine mesh while the fluid surrounding the column (the air) is allowed to be coarser. The software provides the possibility to create an inflation layer. This layer is started from the face mesh and creates elements with increasing thickness away from the boundary in order to accurately predict the velocity profile and heat transfer near walls. Because the columns are relatively thin-walled the maximum cell size in the cross-section has been set to 0.2mm and the height to 10mm resulting in rectangular cells. The following figure shows the mesh which was created for the column in top view. In this view the inflation layer around the column can clearly be seen.

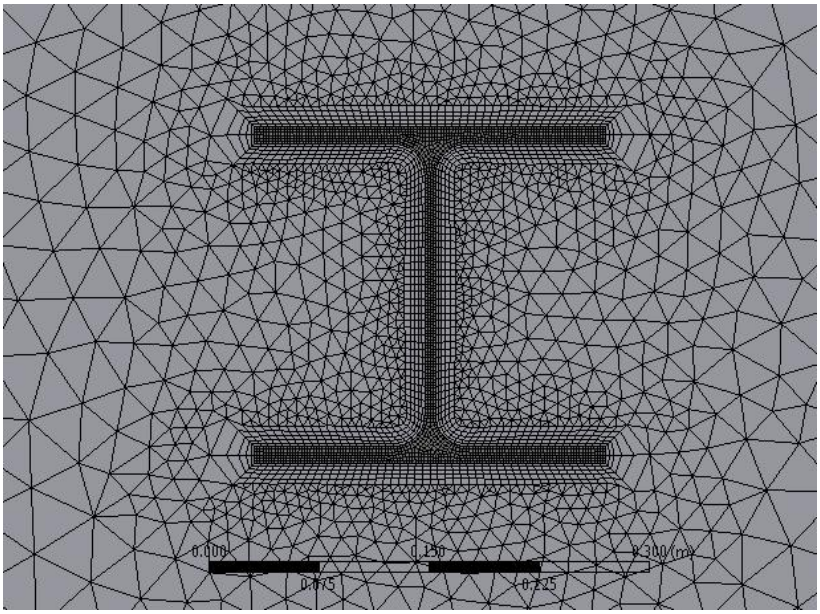
Figure 4.2.1-1: Mesh of column and surrounding fluid.

At first the meshing generator created over 25 million elements which would result in a huge calculation time in the solver phase. The reason for this large number was the fact that the meshing generator would connect cells to the column and allow them to grow as it gets more to the centre of the model. This in combination with the fact that tetrahedron cell shapes were used caused the model to be filled with tiny cells. After a revision of the mesh the cells would be of triangular prism shapes around the columns and a prescribed inflation the following figure was obtained.

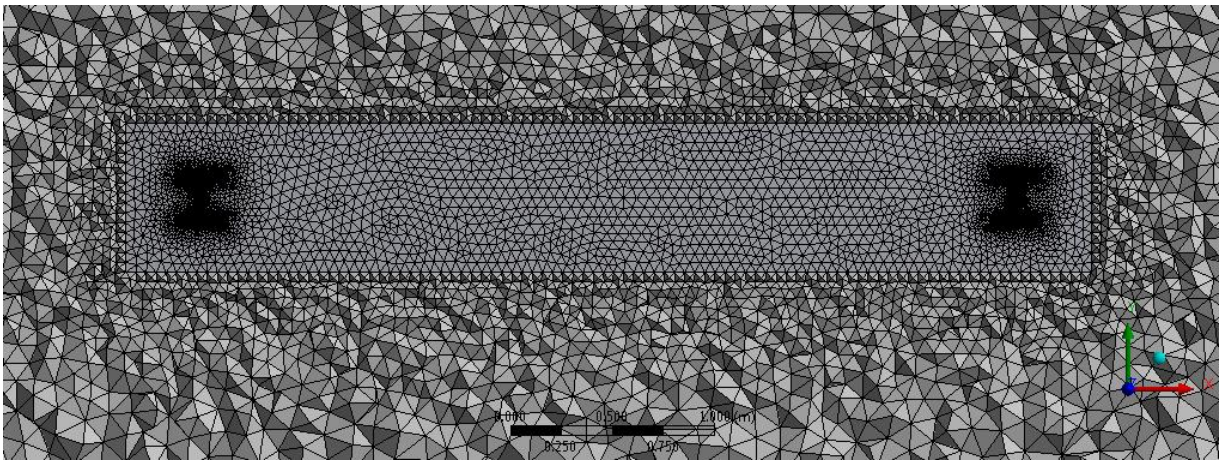
Figure 4.2.1-2: Mesh of area around columns.

Due to this slight and mostly smart modification of the mesh and cell type the amount of cells has been reduced to 5 million. The figure clearly shows the area around the columns made up of prisms and the area outside of that which is made up of tetrahedron cells. The cells surrounding the column start at 0.5cm and increase to 5 cm further away from the column and the height of these cells is set to 5cm. At the area in which the fire is present it is of importance to create a well-defined grid because many changes occur in this area during the fire simulation. The element size for the fire surface area has been chosen to be 10cm and built up of tetrahedron elements. All other elements in the fluid domain (air) have been set to tetrahedron elements and the maximum length of the elements set to 25cm.

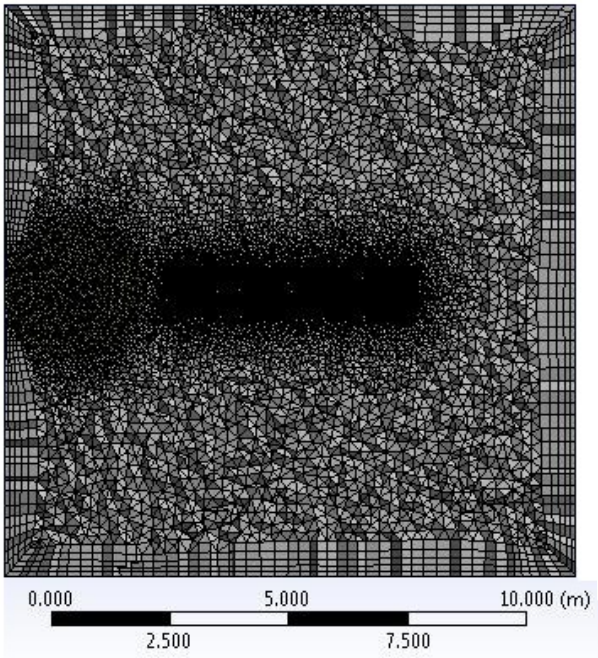

Figure 4.2.1-3: Cross-section top view case 1

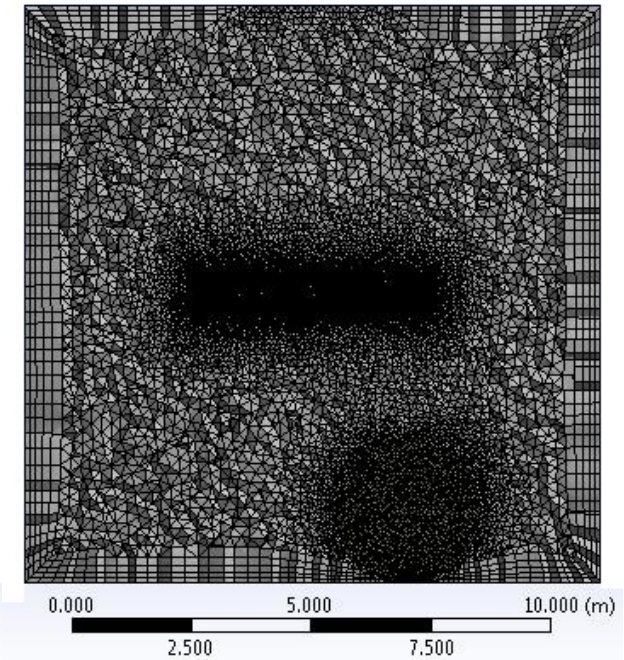

Figure 4.2.1-4: Cross-section top view case 2

When all the elements discussed before are implemented in the model the above figures show the different setups of the fire situation. On the left the fire area has been set up near the wall directed from the weak axis of the column. On the right figure the fire has been modelled near the wall directed from the strong axis of the column. Both figures clearly show a dense mesh where the columns and the fire are situated and a courser mesh in the fluid domain of the model. Near the walls of the model the inflation layer can clearly be seen which consists of triangular prism shapes and may be up to 5 cells thick.

4.2.2. Pre-processor

The pre-processor phase consists of all the input parameters and defining of the model. This phase is the final step before calculating through the entire model and as such all relevant information to the model must be known and entered. This includes the setup of the different bodies in the geometry and the individual parameters which are linked to material properties. The input parameters for the two bodies which are in the model will be discussed in this chapter. The fluid domain consists of the air in the compartment and the solid domain consists of the steel columns supporting the roof. In the pre-processor phase also monitor points have been placed in the model. Temperatures which have been calculated in the solver will be given for these monitor points at a time interval which is specified. In the cross section of the column 13 monitor points have been set up: 5 in each flange and 3 in the web of the column. These monitor points have been set up at every 10cm of height of the column resulting in 845 monitor points per column.

4.2.2.1. Fluid domain

The fluid domain consists of all the air in the compartment, the openings and the fire area. During the simulation all openings are assumed to be open, this has been chosen so the fire will not be ventilation controlled and the compartment allows for greater temperature differences inside. In the case that the openings are closed the compartment would very quickly become a two zone model in which a hot layer of smoke is on top of the cooler air resulting in a smaller or no thermal gradient in the column. Wind conditions which are outside the compartment can have a large effect on the way the fire develops. It could either provoke the fire or cause the temperatures to be lower. In this model it has been chosen to have no wind influence from outside the compartment and thus no wind is applied. The fluid domain has been set to an initial temperature of 20º Celsius.

As the fuel is in the fluid domain an air-fuel mixture is present in the domain. In ANSYS CFX this mixture follows the ideal gas law which describes the behaviour of an ideal gas under the influence of pressure, volume, temperature, and the amount of particles. Also gravity is taken into account as to take into account that hot air will rise. The turbulence model which has been applied is the shear stress transport model. This is a hybrid turbulence model which consists of a κ-ε two equation model and a κ-ω two equation model. The κ-ε model is for free flow and the κ-ω takes into account turbulence near walls. [40]

The combustion model which has been used in the ANSYS CFX calculation is the Eddy dissipation combustion model. If the chemical reaction is fast compared to the processes in the flow this model can be applied. This model is based on the idea that when oxygen is available the combustible material will burn. Radiation has been modelled according the discrete transfer model which states that any material present which has a temperature will contribute in heat transfer through radiation. The liquid heptane has been modelled in ANSYS CFX using the reaction of combustion for heptane. As the heptane is released in the model it reacts with the oxygen creating the fire. In the model the heptane has been modelled as a mass source of the fuel. This mass source is based on the energy released by the fire and the fire curve which is used. In the following tables more information is given about the fire which has been modelled and the amount of energy released.

Pool parameters		
Diameter	3,000	[m]
Radius	1,500	[m]
height	0,025	[m]
Area	7,069	[m2]
Volume	0,177	[m3]
Mass	120,873	[kg]

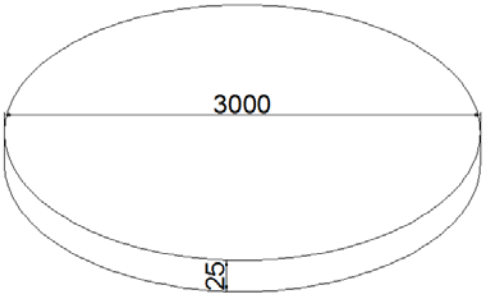

Figure 4.2.2.1-1: Hydrocarbon pool parameters

Pool fire parameters		
Burning rate	0,0045	[m/min]
Burning rate	0,0001	[m/s]
Volume burnt per second	0,0005	[m3/s]
Density of fluid	684	[kg/m3]
Mass burnt per second	0,3626	[kg/s]
Energy release per kg	44560000	[j/kg]
Total heat release	16,16	[MW]
Heat release per m2	2285,93	[kW/m2]

Figure 4.2.2.1-2: Hydrocarbon pool fire parameters

From the figures we can conclude that as expected heptane is a hydrocarbon liquid which produces a lot of energy when ignited. In this case where we assume a three meter diameter pool fire the total heat release is 16.16 megawatts. Based on the burning rate of 4.5 mm per minute the fire would burn 333 seconds which is 5.55 minutes. As described by Eurocode 1 part 1-2 annex E, the decay phase may be assumed to start when 70% of the combustible material has been burnt. The decay phase is described by a negatively sloped line which proceeds until all combustible material has been burnt. 70% of the combustible material has been burnt after 233 seconds, the last 30% of the combustible material is burnt after that in another 200 seconds. This means the total burn time in this case is 433 seconds or approximately 7.2 minutes. Due to the fact that heptane is an extremely flammable liquid which burns at an extremely fast growth rate the decision has been made to not model the growth phase of the fire as this will be mere seconds until the maximum heat release is reached. The figure below illustrates the fire curve which has been used in the calculation.

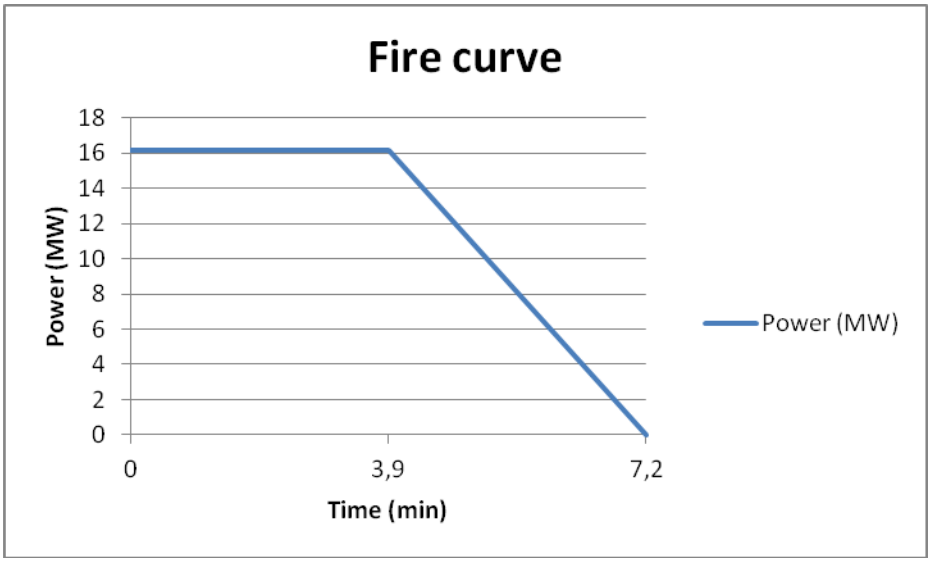

Figure 4.2.2.1-3: Fire curve used for calculation

Soot is an important contributor to radiation and reduction of visibility in case of a fire. Soot is not in the standard calculation methods in ANSYS CFX and as such had to be introduced as an added variable. The air that rises from the fire is smoke and a part of this smoke is soot. To take into account the effect of soot in the smoke a certain fraction of the smoke is labelled to be soot. This means that a part of the mass reduction of the fuel is turned into soot which contributes to heat radiation and also absorption. The amount of soot yield has been set to 0.0149 based on an article by NIST [41].

4.2.2.2. Boundary and Interface conditions

The boundaries of the system consist of the exterior walls, roof and the floor. The openings which are present in the walls and the roof have been modelled in such a way that air can move through these areas. As the entire system has been given a global pressure of 1 atmosphere the relative pressure in the openings has been set to 0 Pa. In this phase of the process also the heat transfer coefficients have to be introduced. Based on the thermal conductivity of the material this can be calculated by ANSYS CFX. For the walls and the roof the same values have been used as they are made of the same materials. The floor however is made of concrete and the bottom side isn't in contact with air so this factor has to be different.

Due to the fact that there are multiple bodies in the model in which there are two different materials to be addressed automatically an interface arises. The interface is the entire area where the cells of the fluid modelled air are in contact with the solid modelled steel column cells. At this location energy transfer occurs based on the properties of the materials. As the hot air from the fire comes in contact with the steel column it will heat up due to the effects of radiation and convection.

4.2.2.3. Solid domain

The solid domain consists of the two columns which support the roof structure in the compartment. This domain is a steel solid domain and heat transfer inside the steel occurs through conduction and is based on the parameters of steel. Inside this domain no air or radiation only conduction is present which reduces the amount of calculations needed to solve the problem in this domain. As there is no fluid for example no turbulence can occur. The time needed to complete the calculation is governed by the domain which has the most calculations and would be the fluid domain. The calculation takes into account the density, specific heat and the thermal conduction coefficients of the material.

4.2.3. Post-processor

The burn time of the fire was calculated and found to be 433 seconds. Based on this it was chosen to perform a calculation with a time of 600 seconds which would show the stationary phase, the decay phase and some of the cooling of the compartment after the fire is extinguished. The calculation has been made on a basis of a 0.25 second time step in which each time step consists of two to 10 iterations. The amount of iterations is determined by if the calculation has met its convergence criterion. This criterion is met when the root mean square of all control volumes falls below $1*10^{-4}$ for each equation during an iteration. The calculation has been performed on a 32 core computer which is solely used for calculating fluid flow problems at ONE Simulations and even then took over four days per fire scenario to complete. Temperature calculated at the monitor points which have been discussed before have now been placed in an out-file, which can be copied to an excel worksheet. Using this data the thermal gradient can be investigated which in the end is the purpose of the investigation. The final calculation file is a file in which all the parameters, model setup and iteration process has been saved. In total the model including the final calculation file consists of 40GB of data for each fire scenario. This means that in total the model is over 80 GB of data.

With ANSYS CFD-post it is possible to visualise the results in the form of static or motion pictures at any time. In the motion picture results have been written every second to create a video which has a fluent image. It is worth noting that even though the visual results are presented per second, the time step in the calculation was still 0.25 second. The figure below shows an example of a possible output scenario with ANSYS CFD-post. In this case a cross sectional view is shown in the zx-plane. From this image the temperature of the air in the compartment can be seen using the scale provided.

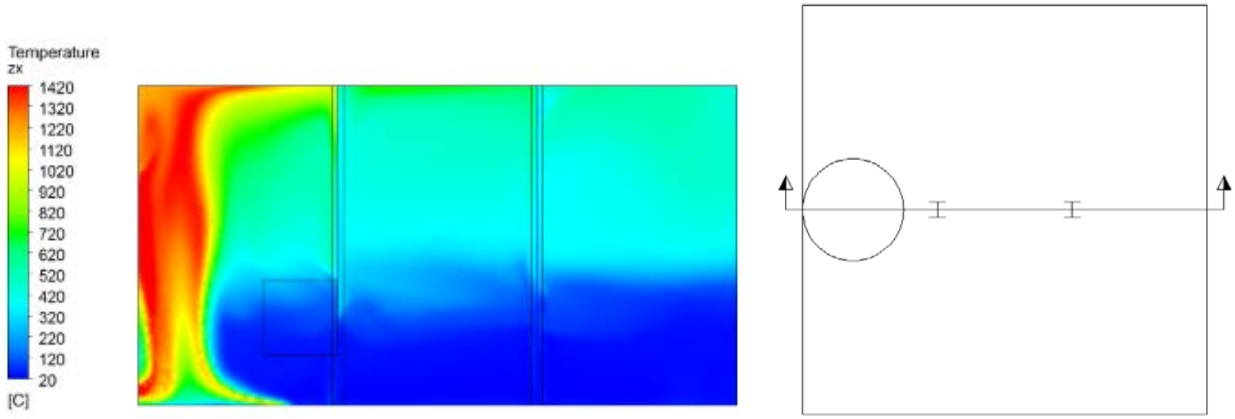

Figure 4.2.3-1: Image of compartment showing hot air at 25 seconds

4.3. Thermal gradient study results

To be able to show the temperature gradient which develops in the column monitor points have been set up in the steel column. These monitor points provide temperature data at each time step of the calculation. These temperatures can then be imported in MS excel and then processed to find the thermal gradients in the cross section during this particular fire situation. The monitor points have been set up as shown in the figure below. In the cross section 13 monitor points have been modelled. Of these 15 points 10 are included in the flanges and the remaining three are positioned in the web of the column. The following figure shows the monitor points in the cross section of the column with their individual dimensions. As the thermal gradient in the column will be investigated the amount of monitor points is rather important. Too little monitor points could cause a result which is not reliable, showing a linear thermal gradient where in fact it isn't linear for example. On the other hand, too many monitor points will only result in a longer calculation time. To gain a result which shows the thermal gradient in an appropriate way it has been chosen to use five monitor points in each flange which are spaced at 60 mm. The web will also have a total of five monitor points; two of these are also in the flanges. These being monitor points 3 and 11. In the flanges and the web it has been chosen to

apply the monitor points only in the length and width of the section and not in the thickness of the flange and web. The reason for this is that the web and flanges have small thicknesses which result in a more or less uniform temperature over the thickness. This in combination that the thermal gradient of interest is over the cross section and not over the thickness of the flange led to the decision to only model one row of monitor points and not two.

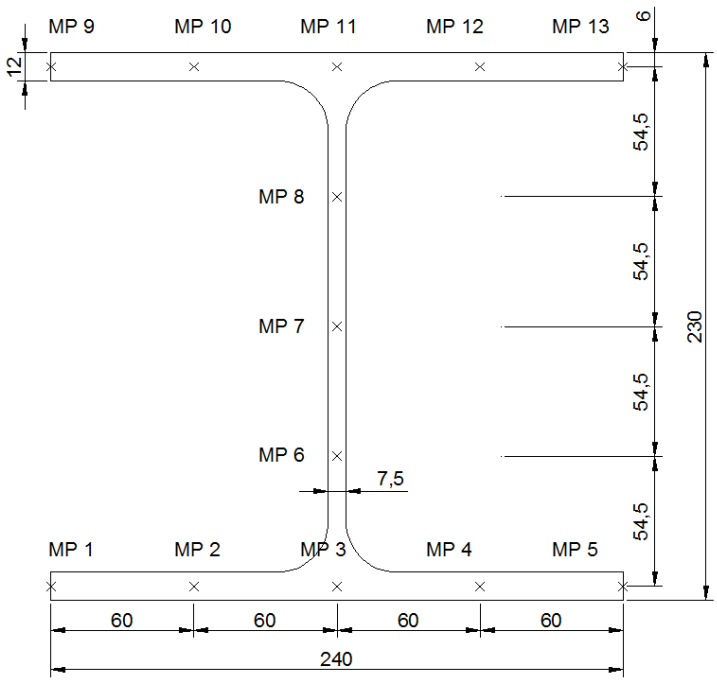

Figure 4.3-1: Cross section of steel column including monitor points.

The following table illustrates the coordinates which have been used to set up the monitor points in the model. The first column is positioned four meters from the wall in x- direction and six meters from the wall in y- direction. As the centre of the column is positioned at coordinate (4000, 6000) it makes sense that monitor point seven has the same coordinates. From this point the local dimensions of the monitor points in the column can be used to obtain the global coordinates of the monitor points in the column.

Monitor point	x (mm)	y (mm)	z (mm)
1	3880.0	5891.0	0, 100, 200, … , 6400
2	3940.0	5891.0	0, 100, 200, … , 6400
3	4000.0	5891.0	0, 100, 200, … , 6400
4	4060.0	5891.0	0, 100, 200, … , 6400
5	4120.0	5891.0	0, 100, 200, … , 6400
6	4000.0	5945.5	0, 100, 200, … , 6400
7	4000.0	6000.0	0, 100, 200, … , 6400
8	4000.0	6054.5	0, 100, 200, … , 6400
9	3880.0	6109.0	0, 100, 200, … , 6400
10	3940.0	6109.0	0, 100, 200, … , 6400
11	4000.0	6109.0	0, 100, 200, … , 6400
12	4060.0	6109.0	0, 100, 200, … , 6400
13	4120.0	6109.0	0, 100, 200, … , 6400

Figure 4.3-2: Coordinates of monitor points in cross section of column.

The model which has been used consists of two columns supporting the roof. The second fire situation has been modelled with the fire near the second column on the strong axis. The monitor points which have been applied in the first column will also be used in the second situation. In the second fire situation the fire is situated at a distance from the strong axis of the column. In this case the second column will be reviewed,

meaning that the monitor points must be shifted to this column. Using the same coordinates as the monitor points in the first column but moving them by four meters in the positive x-direction will move the points to the second column.

4.3.1. Thermal gradient weak Axis (Z)

The thermal gradient on the weak axis of the column is the thermal gradient which occurs from one edge of a flange to the other edge of a flange. The figure below illustrates the direction of the thermal gradient in the flange of the column due to the fire.

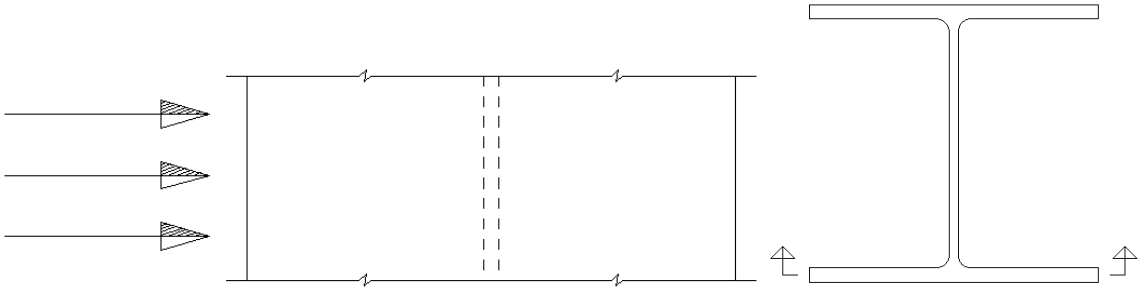

Figure 4.3.1-1: Direction of thermal gradient in column at the given cross section.

The temperature data calculated by the simulation was exported to excel which made it possible to investigate the maximum thermal gradient in the column. While searching for the maximum thermal gradient one must keep in mind that this thermal gradient in the cross section will be different over the height of the column as well as in each time step. To investigate the maximum thermal gradient in the cross section first the temperatures at an interval of 30 seconds were checked at every meter height of the column. After this an indication could be found at which height of the column and near which time step the maximum thermal gradient would occur. Using this iterative procedure eventually the maximum thermal gradient can be found in the column. When reusing the same table the thermal gradient can then be found for each height of the column. A much simplified table showing the results of this investigation has been included below. In the table the thermal gradient has been included per elevation.

Delta temperature in column		
Height (m)	**Gradient (C°)**	**Time (s)**
6.4	181.39	210
6	150.73	180
5	118.83	265
4	85.95	265
3	83.27	265
2	94.62	270
1	87.42	265
0	86.40	270

Figure 4.3.1-2: Maximum thermal difference per elevation.

From the table we can conclude that the maximum thermal gradient per elevation is around 265 seconds from ignition. After this time the thermal gradient will start to decrease again. Near the top of the column the thermal gradient will get to its maximum faster than the rest of the column. This can be explained due to the fact that the hot air from the fire travels along the roof of the compartment and comes in contact with the top of the column quickly. The highest thermal gradient over the flanges of the column has been found to be 184 °C at 180.25 seconds and occurs at 6.3m height.

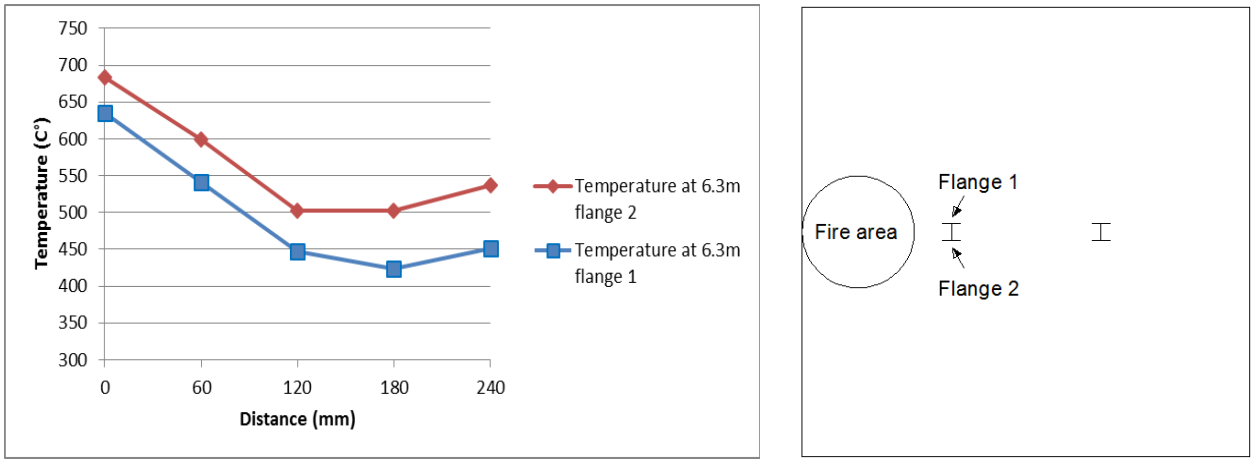

Figure 4.3.1-3: Temperature distribution in flanges during shown fire situation.

The figure above shows the maximum thermal gradient which occurs in the flange due to fire scenario one. We can clearly see that the temperature of the steel is not uniform. The left side of the graph displays the edge of the flange which is closest to the fire. This edge will therefore heat up more compared to the edge on the right. As expected a thermal gradient occurs through the flange as the hot air heats up the steel.

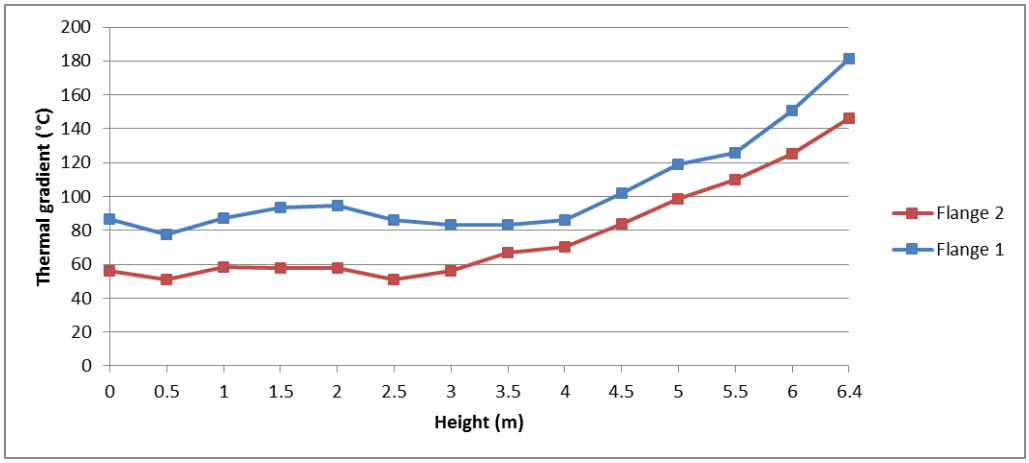

Figure 4.3.1-4: Temperature differences in flanges at elevation in column.

The maximum thermal gradient which has been found in the cross section does not appear throughout the entire cross section. The figure above shows us the thermal gradient which has been found in the cross section at each 0.5m height of the column. On the horizontal axis the height of the column is displayed and on the vertical axis the thermal gradient which occurs. Interpreting the graph we can conclude that the highest thermal gradients occur near the top of the column and will decrease drastically when looking at a lower point in the column. Up to about 4.5 meters in column height the maximum occurring thermal gradient is around 90 °C while any higher along the column the thermal gradient will increase rapidly.

4.3.2. Thermal gradient strong axis (Y)

The thermal gradient on the strong axis of the column is the thermal gradient which occurs from one flange to the other through the web of the column. The figure below illustrates the direction of the thermal gradient in the web of the column due to the fire.

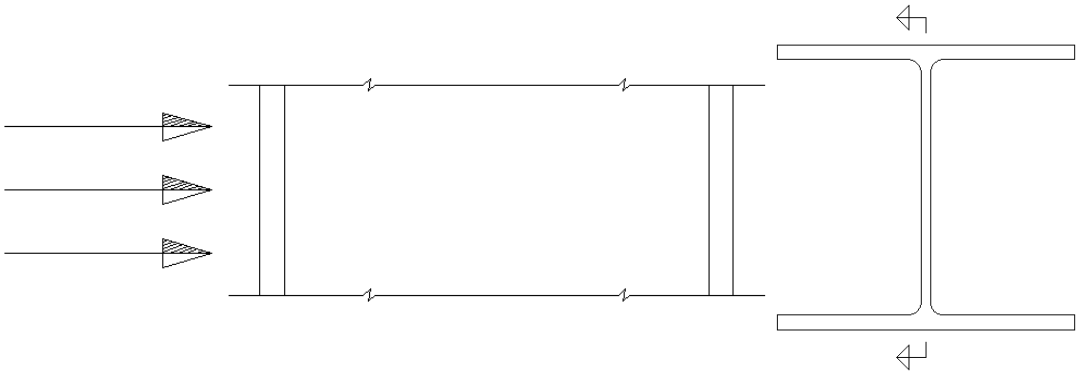

Figure 4.3.2-1: Direction of thermal gradient in column at given cross section.

The method described in the previous sub heading to obtain the maximum thermal gradient in the cross section is also applied in this case. The only difference is that the monitor points which have to be compared are different. In this case the thermal gradient over the web will be investigated. Using the same iterative method to find the maximum thermal gradient has been used. Looking at the different elevations and time steps the maximum thermal gradients per height in the web were found. A much simplified table showing the results of this investigation has been included below. In the table the thermal gradient has been included per elevation.

Delta temperature in column		
Height (m)	**Gradient (C°)**	**Time (s)**
6.4	112.96	270
6	94.35	240
5	42.30	295
4	25.84	325
3	39.03	360
2	66.05	365
1	63.72	365
0	60.66	350

Figure 4.3.2-2: Maximum thermal difference per elevation.

From the table we can conclude that the maximum thermal gradient per elevation is around 300 seconds from ignition. After this time the thermal gradient will start to decrease again. Near the top of the column the thermal gradient will get to its maximum faster than the rest of the column. This can be explained due to the fact that the hot air from the fire travels along the roof of the compartment and comes in contact with the top of the column quickly. The highest thermal gradient over the web of the column has been found to be 116 °C at 150.0 seconds and occurs at 6.3m height.

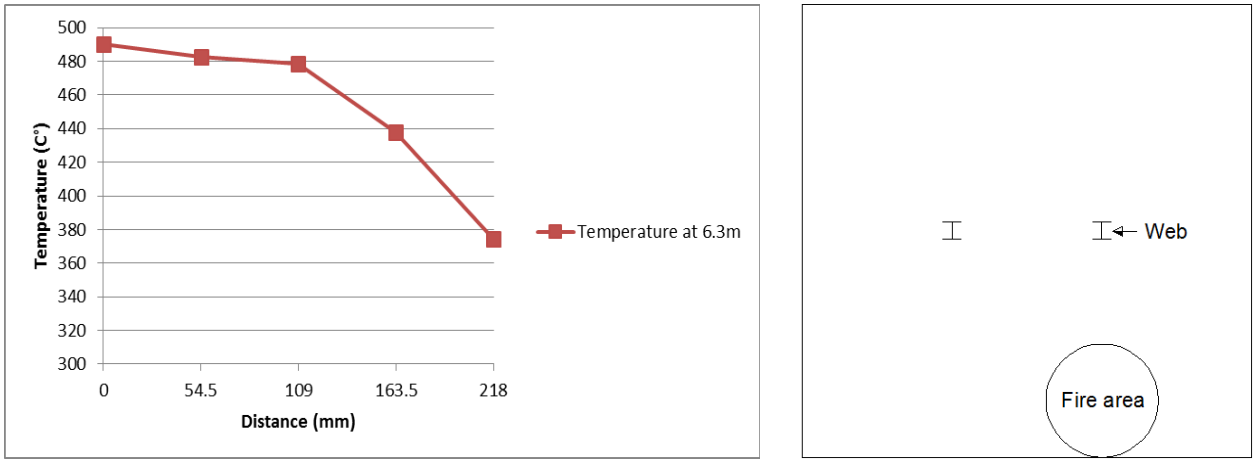

Figure 4.3.2-3: Temperature distribution in web during shown fire situation.

The figure above shows the thermal gradient in the web of the column which has been developed through fire scenario two. In this case the fire is directed at a flange. It can clearly be seen that over the cross section a thermal gradient develops through the web. The left side of the graph shows the flange which is closest to the fire and therefore heavily under influence of the hot air. As we move further away from this flange we see that the temperature decreases and has its lowest temperature in the opposite flange. As expected a thermal gradient occurs through the flange as the hot air heats up the steel. The shape of this graph is probably due to the fact that the entire flange will heat up all this heat will slowly be transferred through the web. When we move further away from the flange we will see the temperature drop rapidly and reach its lowest point at the flange which is the furthest away.

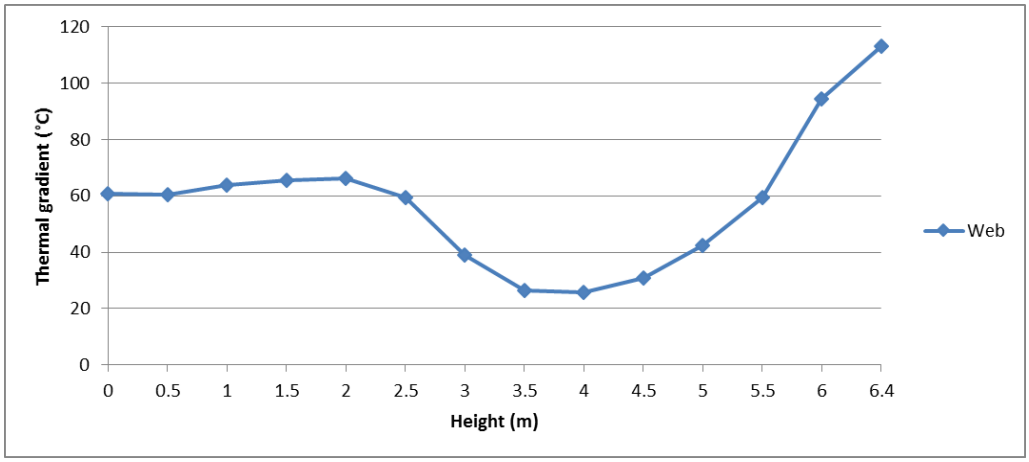

Figure 4.3.2-4: Temperature differences in web at elevation in column.

The maximum thermal gradient which has been found in the cross section is not the same over the height of the column. The figure above shows us the thermal gradient which has been found in the cross section at each 0.5m height of the column. On the horizontal axis the height of the column is displayed and on the vertical axis the thermal gradient which occurs. From the graph we can conclude that the highest thermal gradients occur near the top meters of the column and the lowest near the middle of the column.

4.4. Comparison CFD to Ozone

4.4.1. Input

Ozone is a tool created by ArcelorMittal to determine the temperature development in a compartment using either a fire curve prescribed by the Eurocode [1] or a user defined fire curve. Once the temperature in the compartment is known the tool can calculate the fire resistance of the structure depending on the type of exposure and the fire protection which is applied. The tool is set up to have an easy to use interface which works like a flow chart. Following the individual steps will result in the temperatures which are in the compartment during and after the fire situation. This chapter will focus on Ozone and how the results have been obtained.

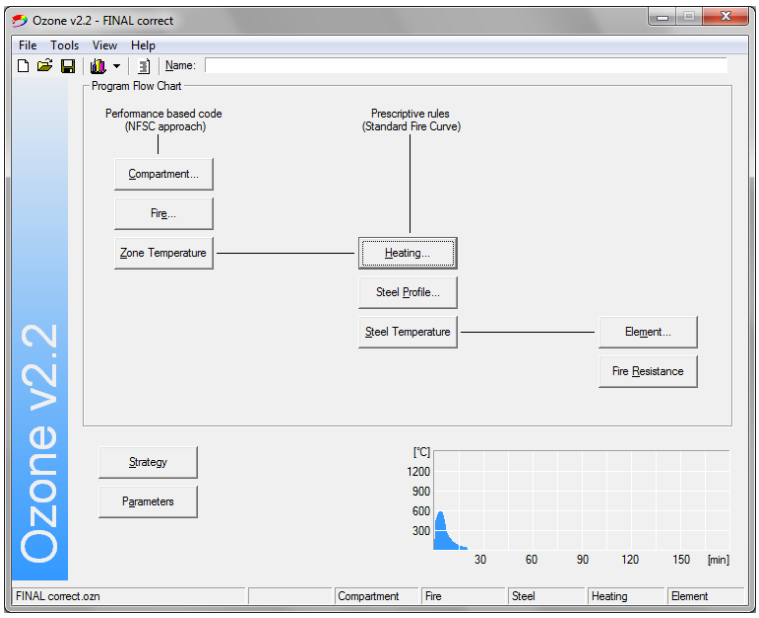

Figure 4.4.1-1: Ozone interface

The figure above shows the interface of Ozone. In this interface we can see the flow chart which needs to be completed to obtain the zone temperatures in the compartment. The flow chart can be started from two points being the Natural Fire Safety Concept (NFSC) approach or the Standard fire curves prescribed by the Eurocode [1]. The difference to these two approaches is the fact that the NFSC approach takes into account the specific type of fire which is present and the compartment type and dimensions. The idea to this approach is to determine the fire safety of a structure based on the characteristics of a real fire. In this case the type of material in the compartment must be known to set up a fire curve which closely represents the fire in that specific case.

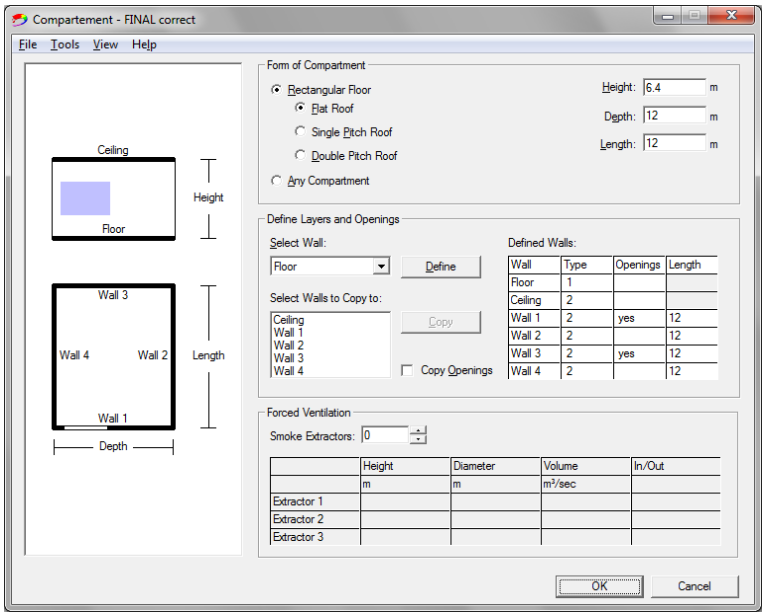

Figure 4.4.1-2: Ozone Compartment tab

The Compartment tab in Ozone consists of all the characteristics of the compartment. In this tab the shape and dimensions of the compartment are inserted. After this the walls floor and ceiling will be specified. Using the “define” button materials and thicknesses can be specified for the individual pieces. Openings can be specified in this tab as well. In our case we have a 12 x 12 x 6.4 m compartment which has openings in

walls 1 and 3. As there are no smoke extractors in this particular compartment this part is left empty and set to 0.

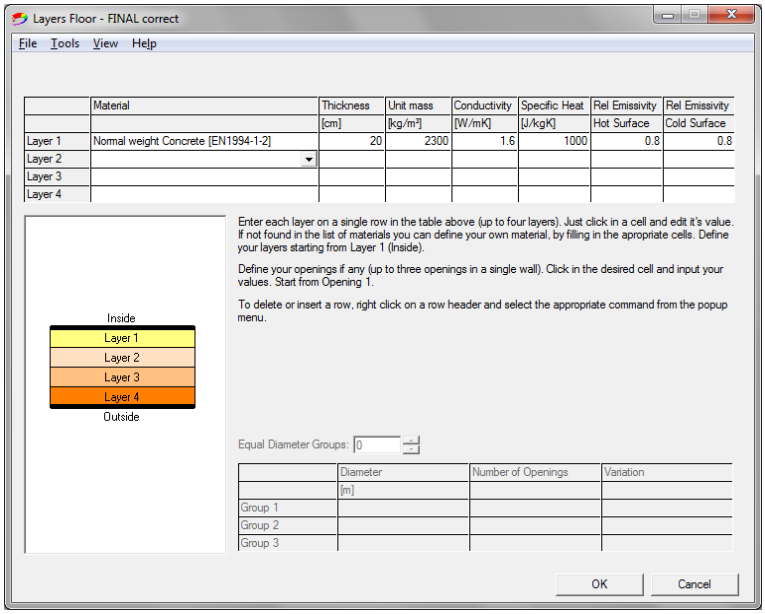

Figure 4.4.1-3: Ozone define layers and openings

Every wall must be defined in Ozone, this includes the ceiling and the floor. Depending on the type of walls many layers can be applied so a custom insulated wall can also be modelled in Ozone. In our case we have steel walls and ceiling which are made of thin sheeting, the columns have been left out as they cannot be input and the floor is modelled as a normal concrete. This tab also allows the user to specify openings in the walls.

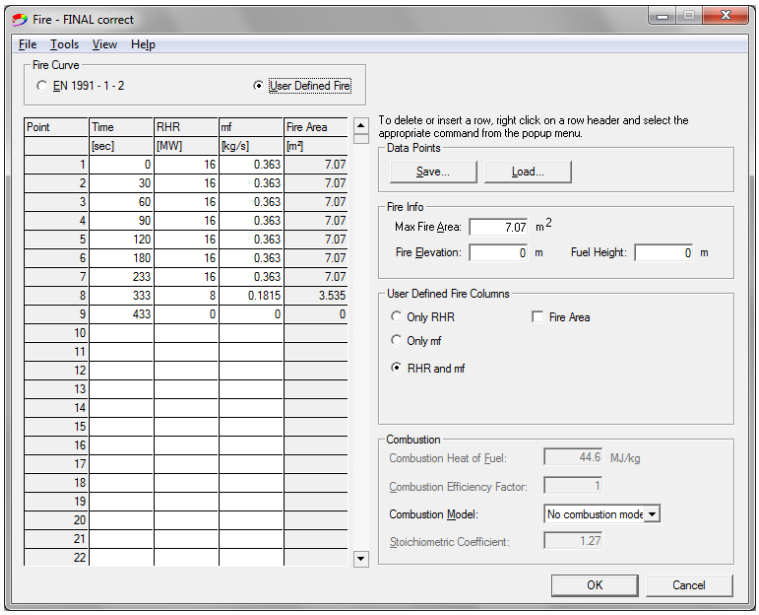

Figure 4.4.1-4: Ozone User defined fire description

Under the button “Fire” the screen above is displayed. This tab allows the user to select either the standard fire curve from the Eurocode [1] or a user defined fire curve. Selecting EN 1991-1-2 will open a window which allows the user to specify the type of occupancy. A set value for the fire growth rate and rate of heat release will pop up. After this the active firefighting measures can be incorporated in the calculation which include reduction factors for the type of protection. Selecting the User Defined Fire will open the window as

shown above. This window allows the user to use a specific type of fire if its fire curve, rate of heat release, burning rate and fire area is known. The fire curve and the burning rate as can be seen in the figure is the same fire curve and data as discussed in chapter 6.2.2.1. This fire curve consists of a 16MW fire up to 233 seconds and after that slowly decays until it extinguishes at 433 seconds.

4.4.2. Output

Having filled in all the necessary input parameters we can now use the button “Zone Temperatures”. This will calculate the given situation and compute the temperatures in the compartment in a hot zone and a cold zone. Also it will show the elevation of the zone interface. The graphs produced can then be compared to the data collected by the CFD calculation.

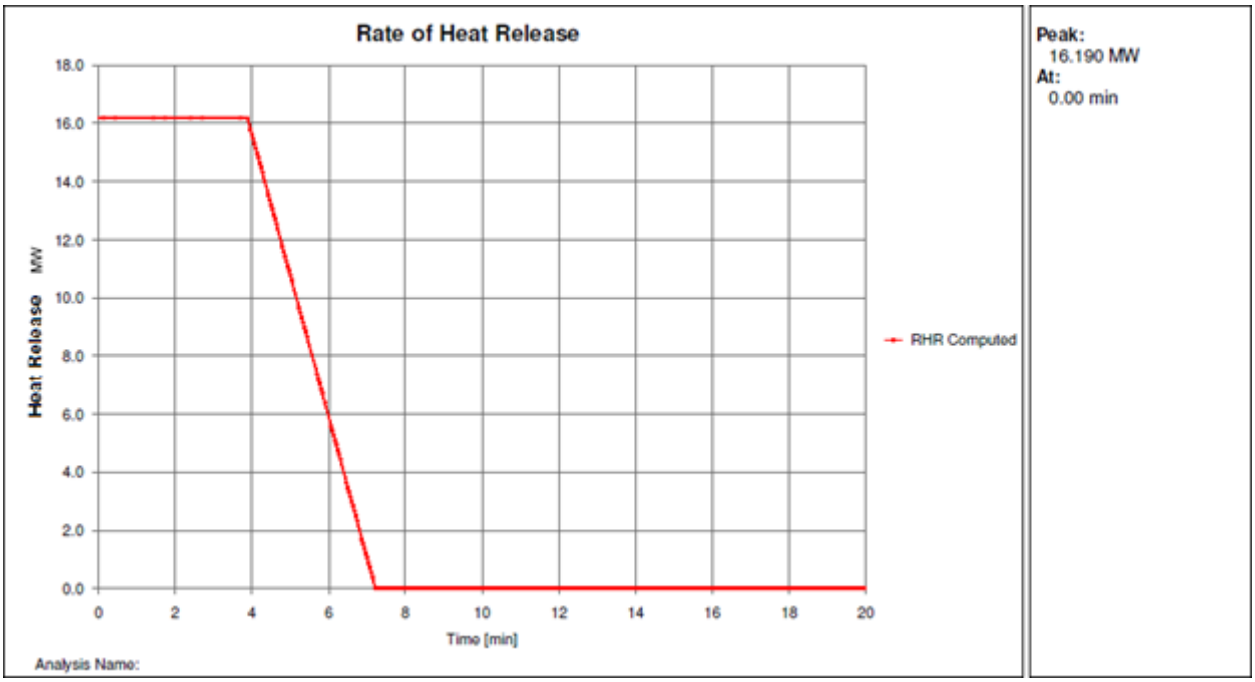

Figure 4.4.2-1: Ozone rate of heat release

As we can see from the graph above which is a result from Ozone the input for the fire curve yields the same result as the fire curve which has been discussed in chapter 6.2.2.1. The heat release of 16MW is continued until 3.9 minutes (233 sec) after which the fire starts to decay and finally extinguishes at 7.2 minutes (433 sec). To make sure Ozone can cope with such a sudden release of energy a test calculation has been made in which the heat release is set to zero at the zero seconds mark and the full load applied at 30 seconds. This test showed only minor differences in temperature indicating Ozone is capable of calculating with this sudden release of energy.

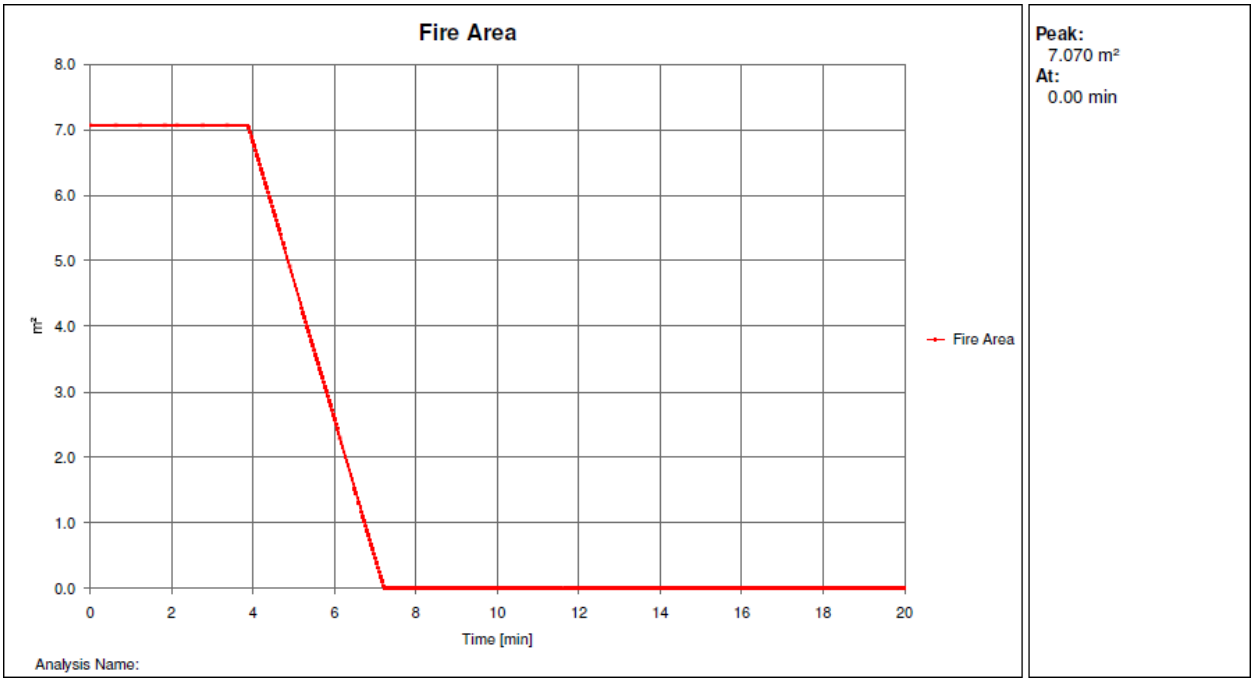

Figure 4.4.2-2: Ozone fire area

The way the fire is modelled in Ozone is the same as it has been modelled in the CFD software with respect to fire curve. The fire area in the Ozone model will decrease after 3.9 minutes and extinguishes at 7.2 minutes. Using this fire area the fire curve which is shown in figure 6-23 has been calculated by Ozone.

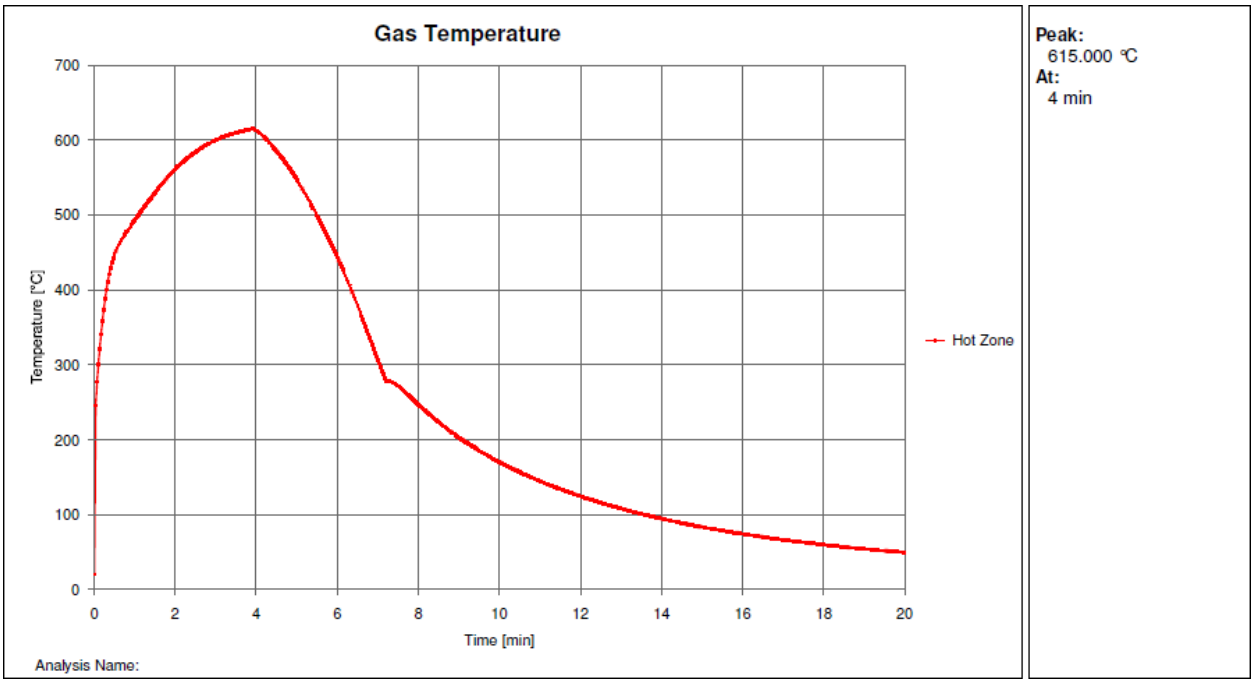

Figure 4.4.2-3: Ozone Hot zone temperature

As Ozone computes the temperatures in the compartment it uses a combination of a two zone model and a one zone model. As the fire first ignites, the temperatures in the compartment will increase near the top of the compartment. This creates a hot air layer which will further be described as the hot zone. As the fire continues the hot zone will get hotter and thicker. The height at which this hot zone starts will be shown in one of the figures below. When the temperatures in the compartment cause the hot zone to be very large Ozone switches to a one zone model as now the temperatures in the compartment are nearly the same everywhere. From the graph which has been displayed above we can see the temperatures of the hot zone.

Interpreting the graph we can state that the temperatures in the compartment increase very rapidly as long as the fire burns. As the fire starts to decay at 3.9 minutes (233sec) we can see that the temperature will start to decrease as well due to the fact that the fire is now emitting less energy.

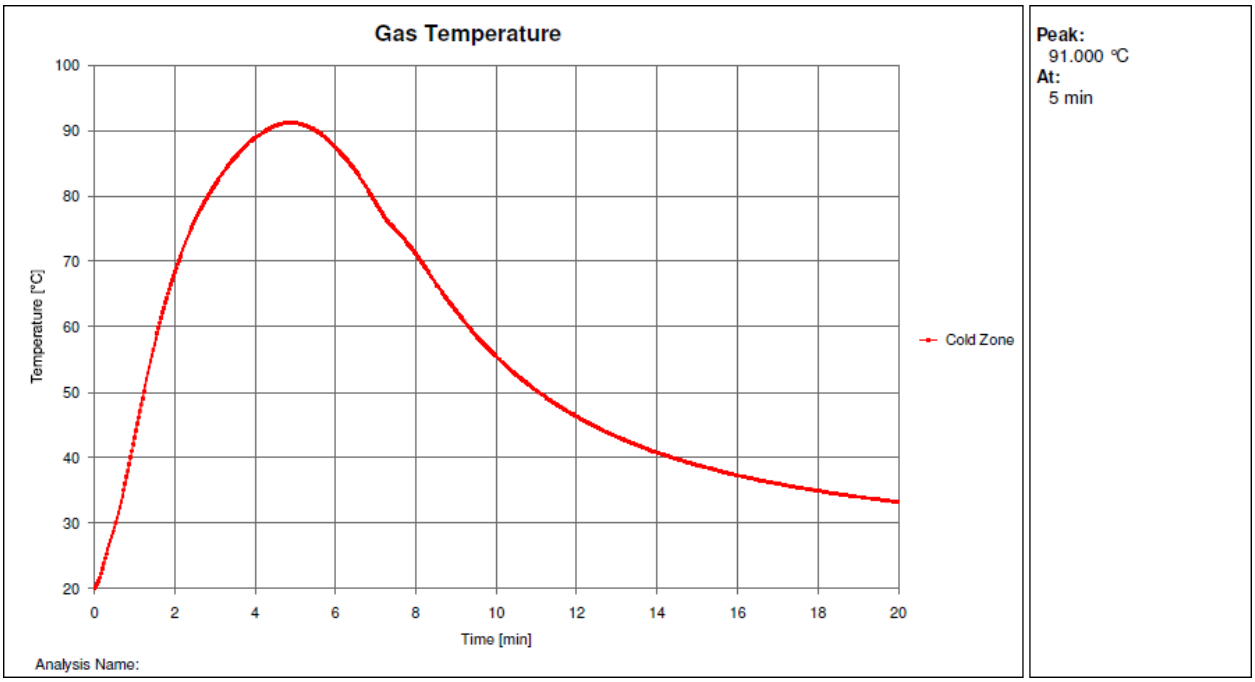

Figure 4.4.2-4: Ozone cold zone temperature

Throughout the duration of the fire we can see the temperatures in the cold zone increase rapidly until the point where the fire enters the decay phase. After this which occurs at 3.9 minutes we can clearly see the temperatures will no longer increase as fast as before and the temperatures in the zone will start to decrease.

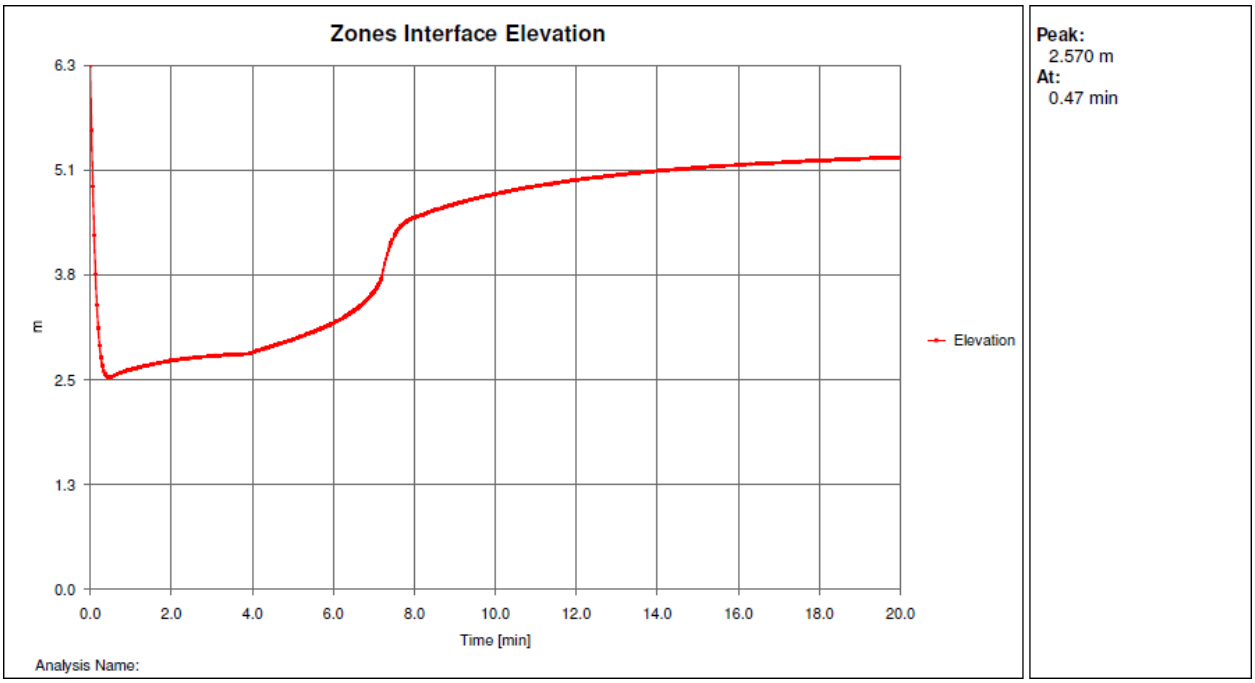

Figure 4.4.2-5: Ozone zone interface elevation

As the hot air from the fire rises it will create a hot layer of air near the top of the compartment which is the hot zone. The cold air underneath this layer is the cold zone in the compartment. The graph displayed above indicates the elevation at which the cold zone meets the hot zone. At the zero minutes mark the air in the

compartment has a uniform one zone temperature. As time goes by we can see a hot zone developing rather quickly due to the hot air produced by the fire. At first a peak develops at 0.50 minutes at which the height of the zones interface is 2.57m. After this the hot and cold zone will become more in equilibrium and levels out at around 3 meters in elevation. When the fire is extinguished at 7.2 minutes in time we can clearly see the interface rise indicating the hot zone will get thinner because the hot air moves out of the compartment through the openings. After 7.2 minutes the interface increases rapidly in height because the fire is now extinguished.

4.4.3. Comparing the results CFD to Ozone

Now that these results have been obtained we can start comparing them to the results obtained from the CFD model and calculation. The results obtained from Ozone, which are graphs, can be read and compared to the visual representation of the temperatures in the compartment calculated by CFD. The temperature of the hot zone in the Ozone calculation is around 615°C and the cold zone is around 88 degrees at 4 minutes in time.

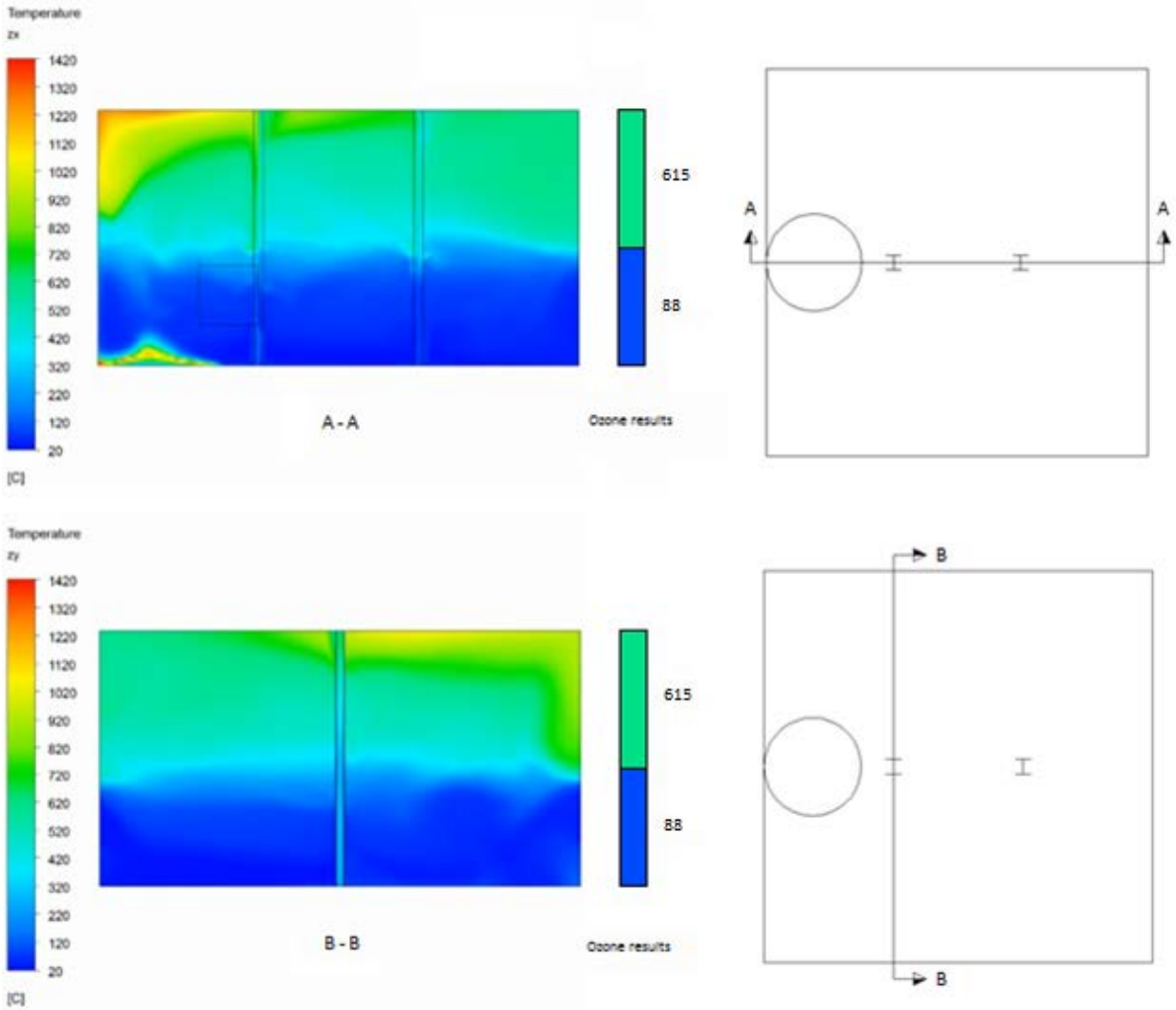

Figure 4.4.3-1: CFD results at 4 minutes compared to ozone results.

Interpreting the temperatures in the figure above with the given scale we can conclude that the temperatures of the hot zone are between 350°C and 850°C throughout the compartment. Ozone had calculated a hot zone temperature of 615°C at 4 minutes in time which coincides with the temperatures calculated by CFD when taking an average temperature of the hot zone in the compartment. The cold zone in this figure is in between 20°C and 350°C which develops slowly until the interface and then rapidly increases to 350°C. Taking an

average of this zone and comparing it to the 88°C which has been calculated by Ozone shows good similarity between the two. Knowing the compartment has a height of 6.4 meters we can judge the interface of the zones to be just under 3 meters. The calculation performed by Ozone shows an interface height which is at 2.8 meters and thus shows good similarity.

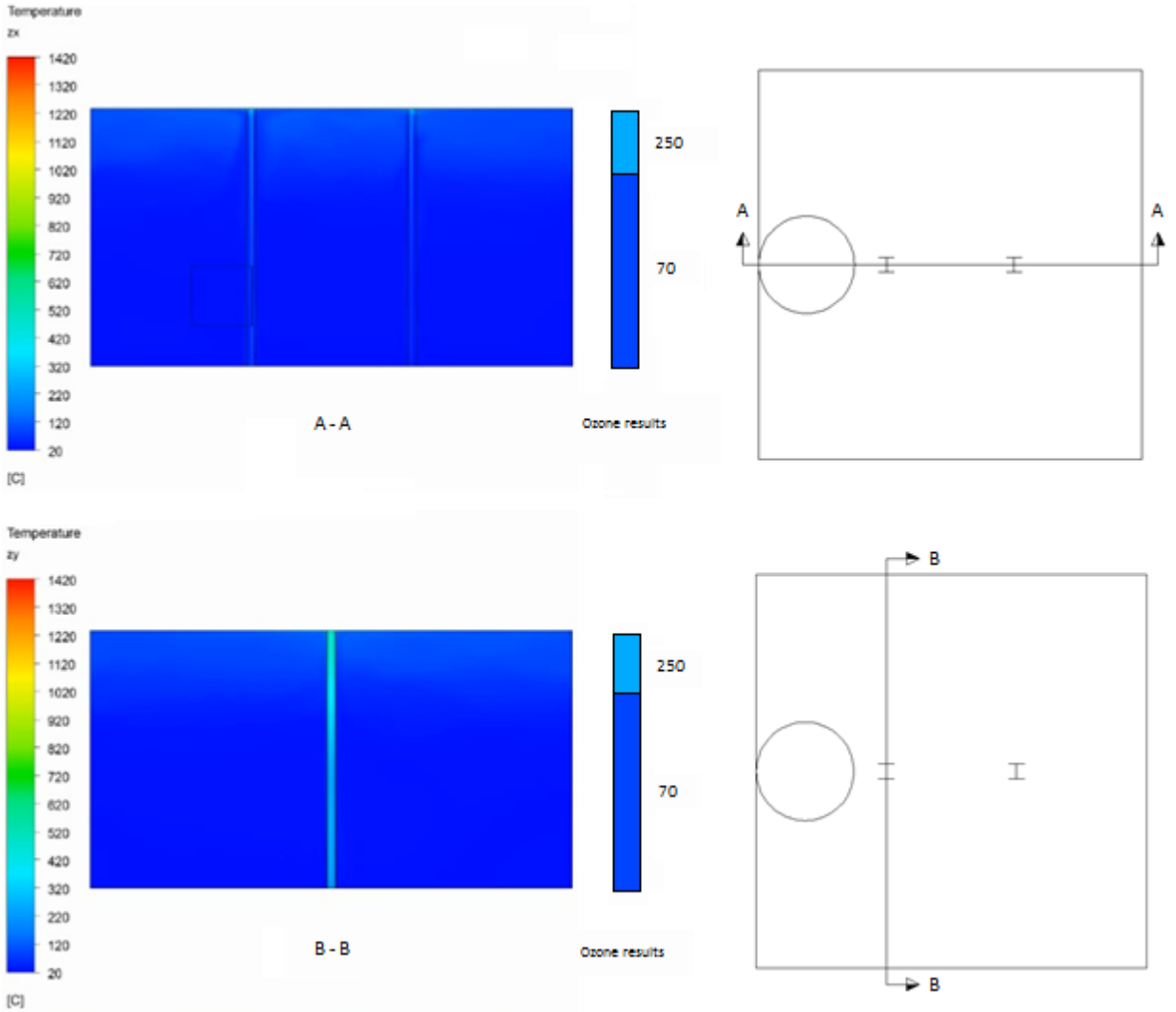

Figure 4.4.3-2: CFD results at 8 minutes compared to ozone results.

As the fire has decayed the temperatures in the compartment will decrease rapidly. As can be seen in the graphs produced by Ozone after the 4 minute mark the temperatures drop very fast. During the CFD calculation and the Ozone calculation the temperature in the compartment started to decay once the fire starts to decay. At the 8 minute mark the Ozone calculation showed a temperature which was dropping fast but still showed a temperature around 250°C in the hot zone and 70°C in the cold zone. The CFD calculation showed the hot air cooled faster, or moved out of the compartment faster than was calculated by the Ozone calculation. Ozone still predicts a hot zone and a cold zone at this point in time while the CFD calculation shows a more or less uniform temperature of around 100°C. The difference in the two can be explained by what has been noted before. An important difference between the two is that the CFD calculation is a much more complex calculation which takes into account the location of openings, flows and roof vents while Ozone will only take the ratio of openings to walls into account.

5

Required cross section (strength)

The load bearing capacity of a column has to be checked in two ways. This being stability of the column and strength of the column. In many cases stability issues will arise before strength problems are encountered. In a fire situation the strength and the stiffness will reduce due to the heating of the steel column which means that the strength of the column is an important parameter as well. Based on the temperatures which have been found in the simulation we can calculate the amount of load which the column can resist solely on the field of strength based on the strength reduction. Due to the thermal gradient which develops in the column the strength of the column does not decrease uniformly over the cross section. The sides facing the fire will decrease in strength faster than the other sides of the column. In the following sub headings both fire scenarios will be evaluated on the field of strength. As discussed before fire scenario one consists of the case in which the fire is directed at the web of the column and fire scenario two consists of the case in which the fire is directed at a flange of the column. This chapter focuses solely on the strength of the column; stability is not taken into account at this point.

When looking only at the strength of the column and using a yield strength of 235N/mm^2 an HE240A column with a cross sectional area of 7680mm^2 will have a yield load of 1804kN. At this point the entire cross section has yielded.

5.1. Strength the column during fire scenario one.

During this fire scenario a thermal gradient develops through the flanges from one edge of the flange to the other. This means that the yield strength of the column does not decrease uniformly. One side of the column will decrease faster than the other side. At this point the decision has been made to use the maximum thermal gradient which has been found in the simulation as well as the temperature distribution belonging to the highest temperature. The column has been divided in five segments and using the temperature of the steel the load bearing capacity of the column can be calculated.

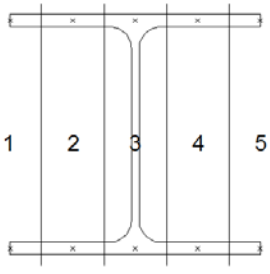

Figure 5.1-1: Top view of column divided in five sections.

This approach has been used for the highest thermal gradient which occurs in the column and the temperature distribution belonging to the highest temperature occurring in the column. The following table shows the result of this calculation. The first table is based on the highest temperature found in the simulation and results in a failure load of 549.7 kN at which the entire cross section is yielding. The

maximum temperature difference occurring in the cross section due to the fire is not the same as the highest temperature recorded. In the second table which looks at the maximum temperature difference in the cross section the yield load of the column is 1468.5 kN at which the entire cross section is yielding. From this we can conclude that the maximum temperature difference does not necessarily mean that it is also the governing situation. In the case the column is tested only on strength the temperature in the column is the most important factor as the higher the temperature the weaker the column becomes.

Strength at raised temperatures with maximum steel temperature					
Section	Temperature (°C)	Reduction	Yield strength (N/mm2)	Area (mm2)	Force (kN)
1	785	0.128	235.000	720.000	21.658
2	730	0.194	235.000	1440.000	65.650
3	651	0.352	235.000	3360.000	278.255
4	643	0.381	235.000	1440.000	128.998
5	660	0.326	235.000	720.000	55.159
				Total force (kN)	549.720

Strength at raised temperatures with maximum temperature difference					
Section	Temperature (°C)	Reduction	Yield strength (N/mm2)	Area (mm2)	Force (kN)
1	635	0.386	235.000	720.000	65.311
2	540	0.656	235.000	1440.000	221.990
3	446	0.899	235.000	3360.000	709.692
4	423	0.949	235.000	1440.000	321.277
5	451	0.888	235.000	720.000	150.216
				Total force (kN)	1468.487

Figure 5.1-2: Calculation of yield load based on strength.

5.2. Strength of column during fire scenario two.

During this fire scenario a thermal gradient develops through the web of the column from one flange to the other flange. Which just like before implies that the yield strength of the column does not decrease uniformly. As one flange heats up faster than the other the yield strength of this part will decrease faster. Using the temperature data from the simulation the column has been divided in five sections. To investigate the yield strength of the column in this scenario the yield strength has been calculated for the temperature distribution with the highest temperature found and the temperature distribution with the biggest temperature difference. Using the temperatures in the sections the yield strength of the column can be calculated.

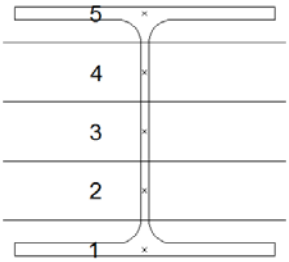

Figure 5.2-1: Top view of column divided in five sections.

The following table shows the results of the calculation performed for the two temperature sets. The first table is based on the highest temperature which has been found in the steel during the simulation. Using the provided temperatures and reduction factors we can calculate the yield strength of the column. The load the cross section can endure is 1441.3 kN. The maximum temperature difference in the cross section does not occur at the same time as the highest temperature. For this reason the maximum thermal gradient has also been checked for strength. In the second table the maximum load which the column can restrain has been calculated. Looking only at strength this is 1613.0 kN. Again we can conclude that when the column is tested on strength only, the governing situation is that in which the temperature is the highest. This is due to the fact that the strength of the steel decreases as the steel temperature increases.

Strength at raised temperatures with maximum steel temperature					
Section	**Temperature (°C)**	**Reduction**	**Yield strength (N/mm2)**	**Area (mm2)**	**Force (kN)**
1	532	0.681	235.000	3226.875	516.261
2	519	0.721	235.000	408.750	69.266
3	508	0.752	235.000	408.750	72.244
4	475	0.835	235.000	408.750	80.207
5	433	0.928	235.000	3226.875	703.338
				Total force (kN)	1441.316

Strength at raised temperatures with maximum temperature difference					
Section	**Temperature (°C)**	**Reduction**	**Yield strength (N/mm2)**	**Area (mm2)**	**Force (kN)**
1	490	0.80	235.000	3226.875	608.169
2	482	0.82	235.000	408.750	78.728
3	478	0.83	235.000	408.750	79.583
4	437	0.92	235.000	408.750	88.237
5	374	1.00	235.000	3226.875	758.316
				Total force (kN)	1613.032

Figure 5.2-2: Calculation of yield load based on strength.

When comparing these results to the load which could be applied to the column when there was no thermal influence we notice a huge decrease in strength due to the temperature. It must be noted that the failure loads found in these results are specifically for the simulations which have been done but can show a fair idea about the decreasing strength of a steel column. As long as the load is smaller than the loads which have been calculated in this chapter the column will not fail on strength. While the column can resist the load based on strength it may still fail due to instability. Buckling also relies on the stiffness of the material which will decrease as well.

6

Comparison with heat transfer according to Eurocode

NEN-EN 1993-1-2 allows us to use a relatively simple calculation method to determine the fire resistance of a structure. As steel warms up internal temperatures have only small temperature differences because steel is a good conductor. The steel surface which is exposed to heat will warm up due to radiation and convection and inside the cross section heat will propagate through conduction. According to Eurocode 3 the temperature may be assumed to be uniformly distributed in the cross section depending on whether the section is heated from one (bottom), three (bottom and sides) or four sides (all sides). For the most common unprotected steel sections that are exposed to a fire from three or four sides Eurocode 3 states that a uniform temperature distribution in the cross section is a good assumption. From the model performed at ONE Simulations the conclusion can be made that during a fire from one side of a column a thermal gradient definitely occurs. As Eurocode 3 does not take this thermal gradient into account an uncertainty arises whether this method is in fact less accurate than taking into account the thermal gradient. The formula described below is the method used by the Eurocode to calculate the uniform temperature increase in a steel section during a known time interval.

$$\Delta T_{steel} = q * \Delta t * k_{shadow} * \frac{\frac{Hp}{A}}{c * \rho}$$

In this equation the following parameters have been used

ΔT	is the temperature increase in °C or K
q	is the heat flux in W/m2
Δ_t	is the time interval
k_{shadow}	is the correction factor for the shadow effect
H_p/A	is the section factor in m-1
c	is the specific heat in J/(kg*K)
ρ	is the density of steel in kg/m3

By using a timestep of 10 seconds for example the uniform temperature in the section can be calculated at any point in time. Take note that the maximum timestep for this equation is 30 seconds. Any larger timestep which will be used results in a solution which is not accurate enough. As the temperature difference between the fire and the steel is larger, the heat flux (q) traveling to the steel will increase. From the formula we can conclude that as the heat flux and the section factor gets larger the heating of the steel will be bigger as well. A large density and specific heat will result in a slower heating and also cooling of the steel. In the following example the heating of a steel HE240A section will be calculated using the fire described in chapter 6 which means the heat flux to be used is 2290 W/m2. The section factor including the shadow effect has also been discussed before and results in 110 m-1. For the specific heat of steel we assume 500 J/(kg*K)

$$\Delta T_{steel} = 2290 * 10^3 * 30 * \frac{110}{500 * 7850} = 1925$$

If the modelled fire would be focused directly on the steel column it would result in a temperature raise of 1925+20=1945°C. Obviously this isn't the case as the fire is located at a distance from the fire and the full amount of heat flux is not concentrated on the column.

When the section is encased in concrete for most of the perimeter, the section will be heated from one side. The temperature in the cross section will then display a thermal gradient. These temperatures can be calculated using FEM models at any moment in time. This method is no longer a simple calculation which can be applied in a quick manner. The solution to still be able to use this method is to assume a uniform temperature in the cross section causing a very conservative result. In the case a beam in bending is being tested with the complex method, the cross section will be divided in slices of material. Taking the average temperature of such a slice the contribution to the moment capacity of the cross section can be calculated at a certain point in time. [35]

To find the buckling load of a column with a thermal gradient this same technique will be used. As the thermal gradient is known in this case we can divide the column in multiple slices with different temperatures resulting in multiple stiffnesses. A calculation method will have to be found or developed to be able to cope with such an inhomogeneous cross section in axial compression.

6.1. Temperatures found during CFD simulation

While the model was created monitor points have been placed in the cross section of the column. These monitor points will give the temperature in 845 points at every time step of the calculation. This means that every 0.25 seconds the temperature is written to a separate file. As the calculation is to be completed over 600 seconds each monitor point will get 2400 different temperatures. Using these sets of temperatures graphs can be made to illustrate the increasing temperatures in the cross section. In the following two sub headings the temperatures in the cross section will be shown per elevation in the column.

6.1.1. Temperatures fire situation 1

To show the temperatures in the cross section the following graphs have been developed. Each graph shows the increase in temperature of a cross section at a certain height. The lines indicate the temperature at the location of the monitor points as the time progresses. Fire situation 1 consists of the setup in which the fire is at the side of the weak axis of the column. This situation implies that we will expect the temperatures of the monitor points on this side to increase in temperature faster than the other side.

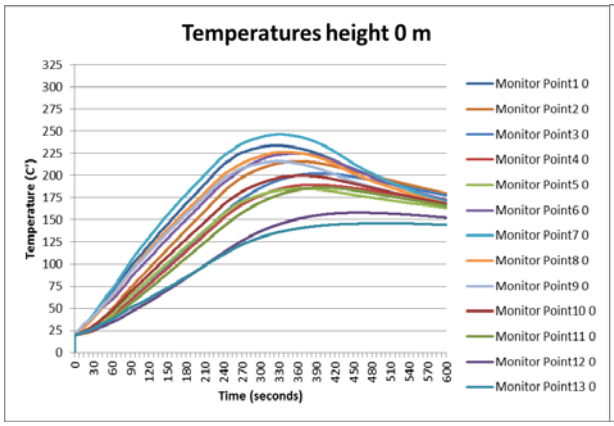

Figure 6.1.1-1: Steel temperature at 0m

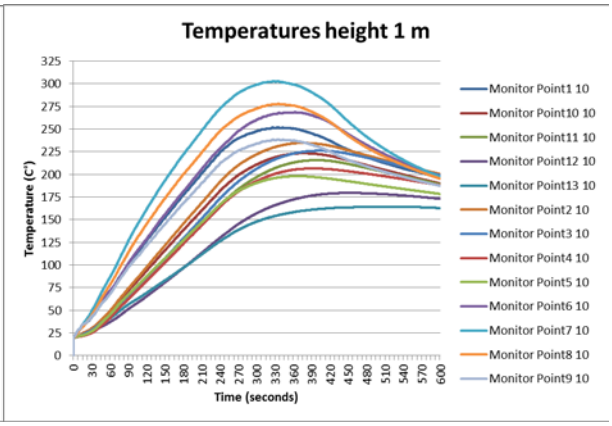

Figure 6.1.1-2: Steel temperature at 1m

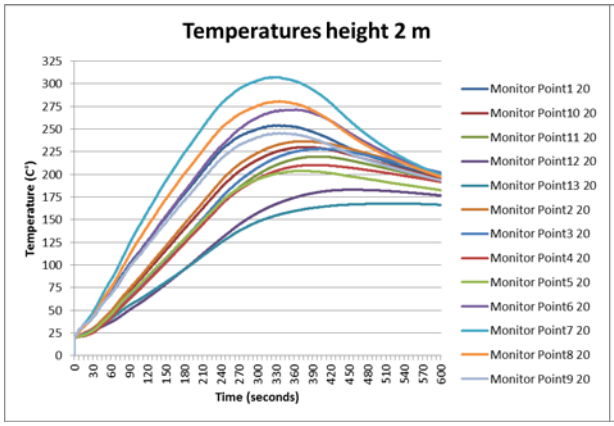

Figure 6.1.1-3: Steel temperature at 2m

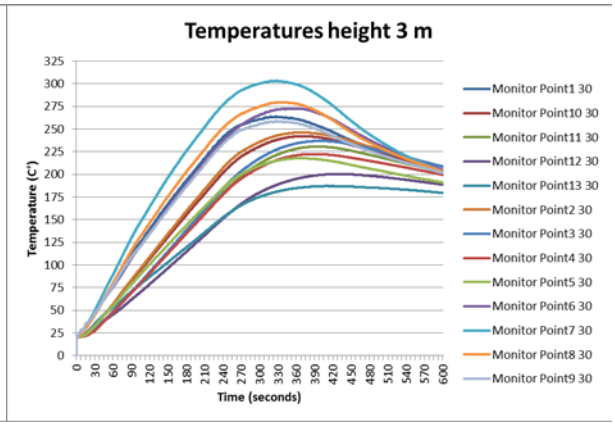

Figure 6.1.1-4: Steel temperature at 3m

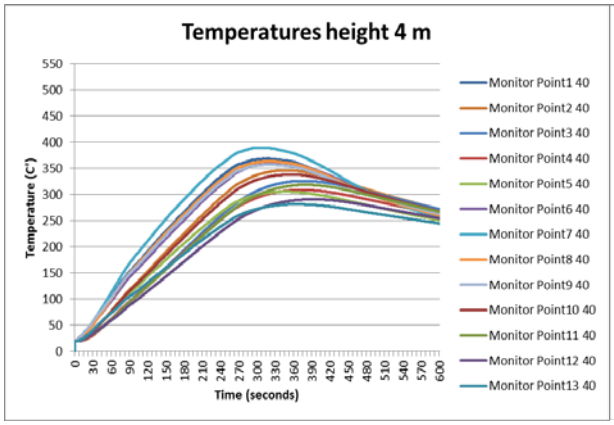

Figure 6.1.1-5: Steel temperature at 4m

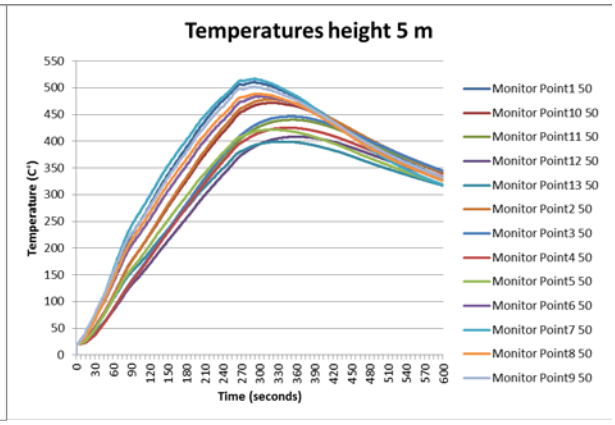

Figure 6.1.1-6: Steel temperature at 5m

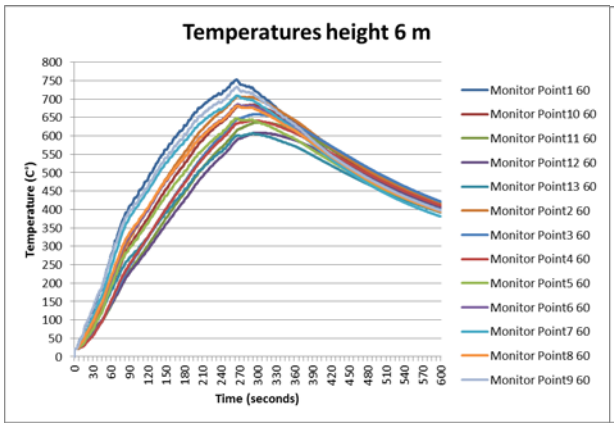

Figure 6.1.1-7: Steel temperature at 6m

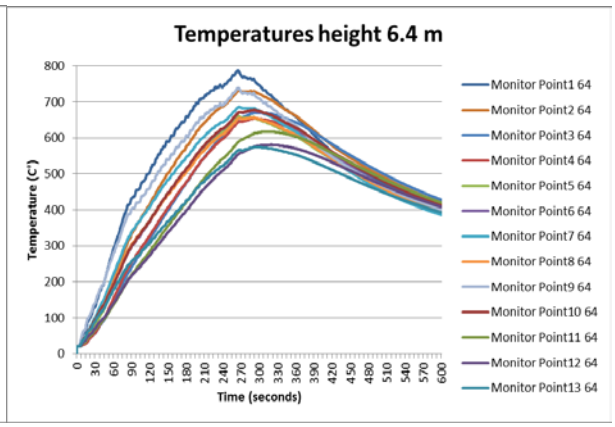

Figure 6.1.1-8: Steel temperature at 6.4m

The stationary phase of the fire continues for 233 seconds, after this time the decay phase sets in. From the graphs it clearly shows that when the decay phase sets in the steel will no longer heat up as fast as it did before. As the decay phase of the fire comes to an end we notice that every part of the column is cooling down.

6.1.2. Temperatures fire situation 2

In the second fire situation the fire is situated at a distance from the strong axis of the section and thus one flange will heat up faster than the other flange. This is due to the fact that the flange causes a blockage with respect to the radiation which is being emitted. In this situation we will expect the set of monitor points in the flange to increase faster than that of the other flange due to this blockage effect.

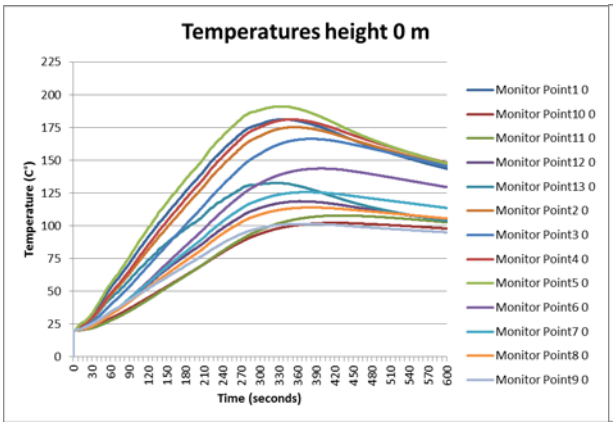

Figure 6.1.2-1: Steel temperature at 0m

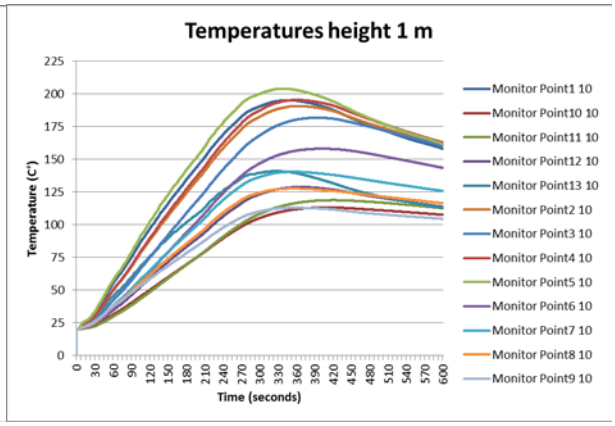

Figure 6.1.2-2: Steel temperature at 1m

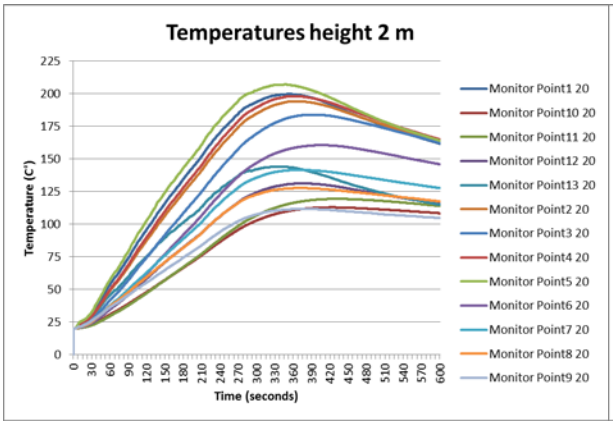

Figure 6.1.2-3: Steel temperature at 2m

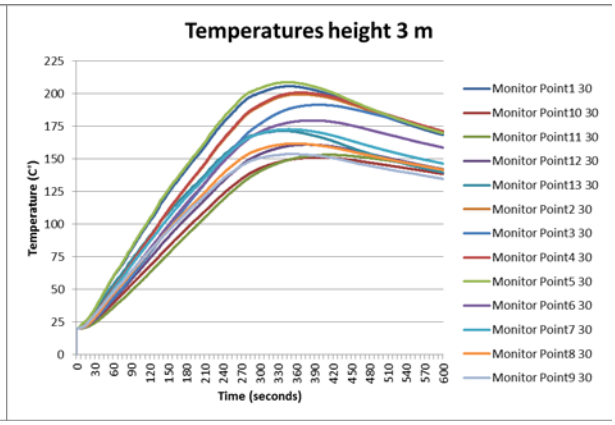

Figure 6.1.2-4: Steel temperature at 3m

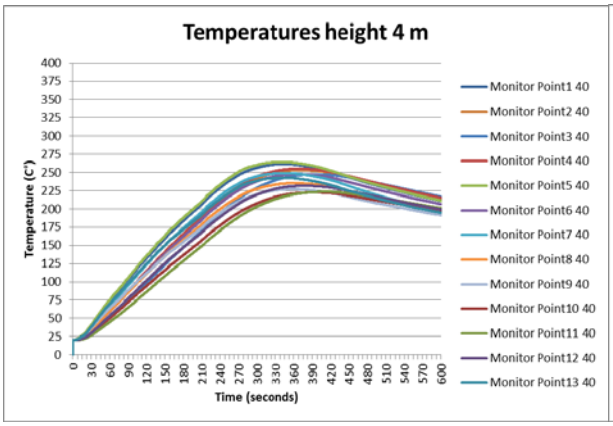

Figure 6.1.2-5: Steel temperature at 4m

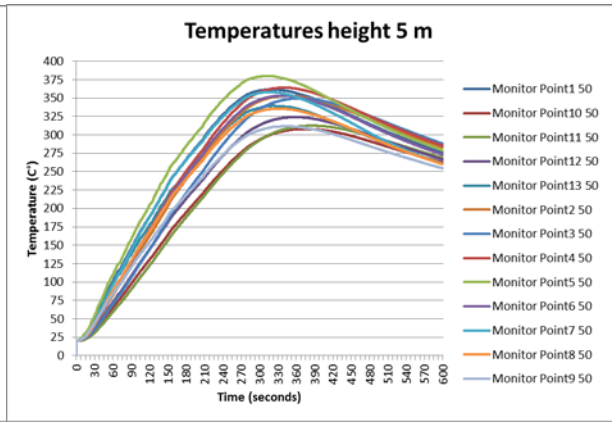

Figure 6.1.2-6: Steel temperature at 5m

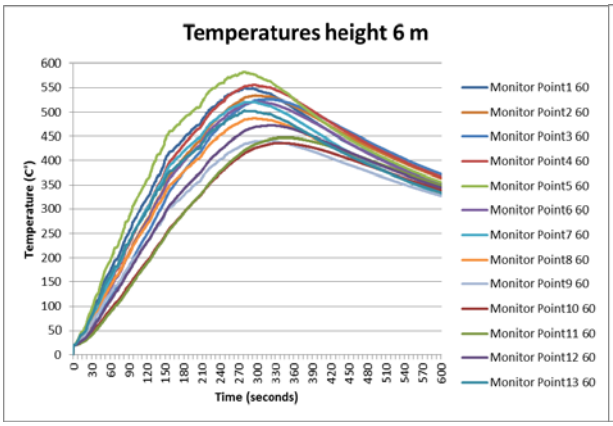

Figure 6.1.2-7: Steel temperature at 6m

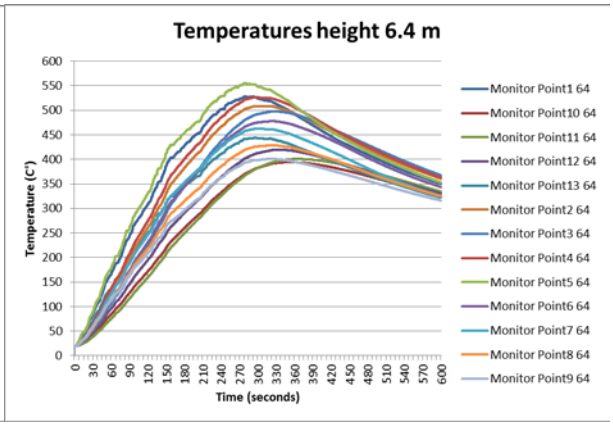

Figure 6.1.2-8: Steel temperature at 6.4m

As expected the flange located closer to the fire will heat up faster than the web and the flange at the rear of the profile. In the graphs showing the temperatures from height zero to three meters we can clearly indicate which lines belong to the flanges and which lines correspond to the web of the section. The five lines which show the highest temperatures correspond to the flange exposed to the most radiation and the bottom five to the flange which is blocked from the fire.

7

Buckling

7.1. Euler buckling

The buckling curves and forces which can be calculated using the Eurocode are derived from the Euler buckling calculation. The method of calculating the Euler buckling stress is given below. The values for the calculation are based on the model which will be treated. The column to be tested is an HE240A section which has the following parameters

Height: 6400mm
I_z: $2769*10^4$ mm^4
i_z: 60 mm
L_{buc}: 6400mm (pin ended column)
A: 7680 mm^2

The Euler buckling force is defined as:

$$F_{euler} = \frac{\pi^2 E I_z}{L_{cr}^2} = \frac{\pi^2 * 210000 * 2769 * 10^4}{6400^2} = 1.401.000N = 1401kN$$

The definition of a stress:

$$\sigma = \frac{F}{A}$$

The Euler buckling stress can now be written as:

$$\sigma_{Euler} = \frac{F_{euler}}{A} = \pi^2 E \frac{I}{A L_{cr}^2}$$

In this form the factor I/A, which is the radius of gyration, can be clearly seen. Using $i = \sqrt{\frac{I}{A}}$ the formula can be rewritten in the following form:

$$\sigma_b = \pi^2 E \frac{i^2}{L_{cr}^2}$$

The buckling stress will then be determined by the stiffness of the material, the Young's modulus, the column slenderness and the radius of gyration. This last ratio is called the slenderness of the section:

$$\lambda = \frac{l_{cr}}{i}$$

Finally the Euler buckling stress can be described by the following formula:

$$\sigma_b = \frac{\pi^2 E}{\lambda^2}$$

The buckling stress must always be smaller than the yield stress of the material. Using this equation the minimum slenderness λ1 of a certain steel grade can be determined.

$$f_y > \frac{\pi^2 E}{\lambda^2} \quad so \quad \lambda > \sqrt{\frac{\pi^2 E}{f_y}}$$

Steel grade S355 with a Young's modulus of $2.1*10^5$ N/mm2 and a yield stress of 355N/mm^2 will have the following lambda:

$$\lambda > \sqrt{\frac{\pi^2 * 210 * 10^3}{355}} = \lambda_1 = 76.4$$

Steel grade S235 with a Young's modulus of $2.1*10^5$ N/mm^2 and a yield stress of 235N/mm^2 will have the following lambda:

$$\lambda > \sqrt{\frac{\pi^2 * 210 * 10^3}{235}} = \lambda_1 = 93.9$$

For small slenderness values the yield stress will be governing while with high slenderness the Euler buckling stress is governing. As stated above, each steel grade has its own minimal slenderness. It would be inefficient to create buckling curves for each steel grade so a factor is introduced called the relative slenderness. The relative slenderness is the slenderness of the section divided by the minimum slenderness.

$$\bar{\lambda} = \frac{\lambda}{\lambda_1}$$

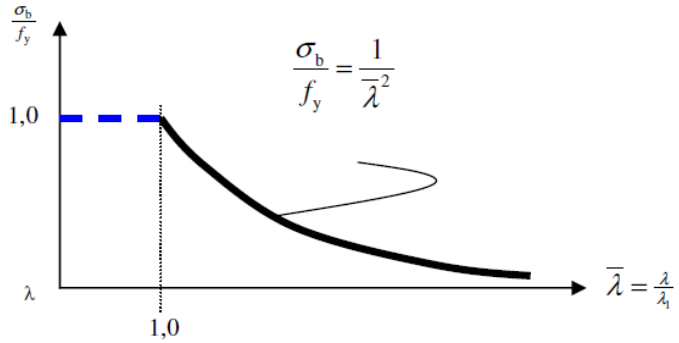

Figure 7.1-1: Dimensionless buckling curve according to Euler [38]

Dividing both sides of the Euler buckling stress by the yield strength of the steel the following equation will be obtained.

$$\frac{\sigma_b}{f_y} = \frac{\pi^2 E}{\lambda^2 f_y} = \frac{\lambda_1^2}{\lambda^2} = \frac{1}{\bar{\lambda}^2}$$

The effect of buckling is a stability issue which will cause the failure load of the column to be significantly lower than the load required to fully yield the cross section. This reduction which is shown by the buckling curves can be seen as a reduction factor for the yield strength of the material.

$$\sigma_b = \chi_{euler} f_y$$

The buckling reduction factor according to Euler is equal to the reciprocal of the squared relative slenderness:

$$\chi_{euler} = \frac{1}{\bar{\lambda}^2} \quad with: \quad \bar{\lambda} = \frac{L_{cr}}{i} * \frac{1}{\lambda_1} \quad and: \quad \lambda_1 = \pi \sqrt{\frac{E}{f_y}}$$

Unfortunately in reality the buckling curves are different than those predicted by Euler. As a column is never ideal and thus not perfectly straight the buckling curves which appear are lower than that created by Euler. This means that calculating according to Euler is unsafe. In Eurocode 3 the buckling reduction factor is defined by a different formula. [38]

7.2. Buckling according to Eurocode

The method described by the Eurocode for steel structures is slightly different than that described in the previous chapter but the Euler theory is still incorporated. According to the Eurocode a structure loaded in compression and tested for stability must satisfy the following unity check:

$$\frac{N_{Ed}}{N_{b,Rd}} \leq 1$$

N_{Ed} is the calculation value of the compression force due to the load.
$N_{b,Rd}$ is the calculation value of the maximum allowable buckling force for the cross section.

When calculating according to the Eurocode at first a buckling curve must be determined. This curve depends on the cross section and will describe a factor called “α”. Also known as the imperfection factor this factor takes into account natural imperfections in the section. The section class is 1 and according to the tables in Eurocode 3 the buckling curve which must be used for an HE240A section is “c”. This means the imperfection factor is 0.49 which will be used to calculate the buckling reduction factor.

At first the relative slenderness must be calculated using the properties connected to the specific steel grade. Using the relative slenderness the buckling factor can be calculated as shown below.

$$\lambda_1 = \pi \sqrt{\frac{E}{f_y}} = \pi \sqrt{\frac{210000}{235}} = 93.9$$

$$\bar{\lambda} = \frac{L_{cr}}{i} \frac{1}{\lambda_1} = \frac{6400}{60} \frac{1}{93.9} = 1.13$$

$$\Phi = 0.5\left[1 + \alpha\left(\bar{\lambda} - 0.2\right) + \bar{\lambda}^2\right] = 0.5[1 + 0.49(1.13 - 0.2) + 1.13^2] = 1.37$$

Using these constants we can now calculate the buckling factor for this section according to the Eurocode. This factor will take into account deviations in the material and imperfections which could be introduced due to residual stresses in the section.

$$\chi = \frac{1}{\Phi + \sqrt{\Phi^2 - \bar{\lambda}^2}} = \frac{1}{1.37 + \sqrt{1.37^2 - 1.13^2}} = 0.46 \quad \chi \leq 1.0$$

The ultimate compression strength of a cross section is defined in the Eurocode as:

$$N_{c,Rd} = \frac{Af_y}{\gamma_{M1}}$$

The maximum allowable buckling force of the cross section can be defined as the maximum force which can be applied on the cross section multiplied by a factor which takes into account the effect of buckling. The influence of buckling has been incorporated in the buckling reduction factor "χ".

$$N_{b,Rd} = \chi \frac{Af_y}{\gamma_{M1}} = 0.46 \frac{7680 * 235}{1.0} = 840\ kN$$

χ	Buckling factor
A	Cross sectional area of a section class 1-3
γ_{M1}	Stability control; 1.0 for structures

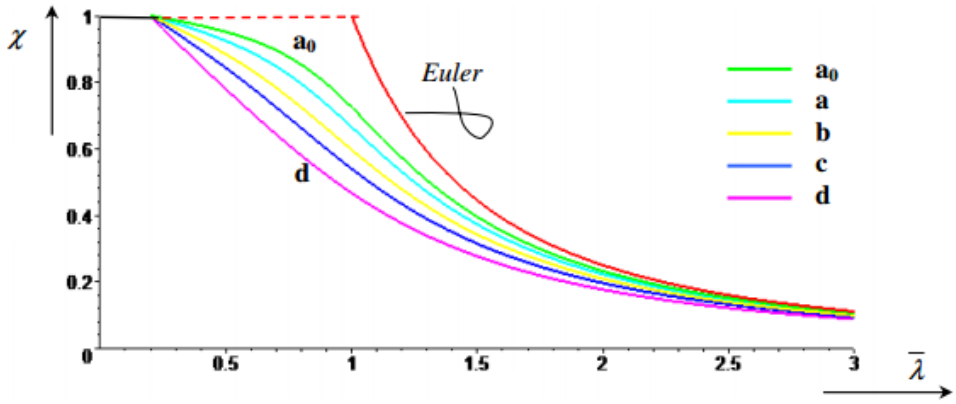

Figure 7.2-1: European buckling curves [38]

The failure load calculated by the Eurocode turns out to be a lot lower than that calculated by Euler. This result is due to the fact that the Eurocode takes into account residual stresses in the cross section, size effects and the inhomogeneity of the material. Instead of the Euler buckling curve the Eurocode defines five buckling curves depending on the type of section which is being tested. All of these curves for different cross sections are lower than the Euler buckling curve as can be seen in the figure above.

7.3. Buckling according to Eurocode at raised temperatures

As the steel section heats up the strength and stiffness will decrease. In case of buckling the decreasing stiffness is an important parameter for the stability of the section. The decreasing stiffness is taken into account in the relative slenderness specific for a certain temperature "$\bar{\lambda}_\theta$". In the calculation according to

Eurocode the temperature is an extra parameter which needs to be taken into account. To be able to calculate the maximum allowable buckling force in the section either the maximum temperature of the section must be known or the plastic degree of utilization. When the plastic degree of utilization is known the critical steel temperature can be calculated and checked against the temperature the steel will reach. In this case if the temperature exceeds the calculated temperature the column will fail. The second cased is if the maximum steel temperature is known the buckling force can be calculated. In this manner the buckling force can be calculated according to the maximum steel temperature during a fire.

Our model consists of a single compartment with two columns supporting the roof. These columns are 6,4m tall. The area of the roof that will be loaded on one column is 6m * 4m = 24 m^2. Assuming a permanent floor load of Gk,floor = 5 kN/m^2. The variable load will not be taken into account because for roofs ψ1, ψ2, ψ3 are set to zero in the Eurocode. To apply the calculation method described by Eurocode 3-1-2 the section must be either class 1, 2 or 3. According to Eurocode 3-1-1 the section class for an H section can be calculated with the ratio of height over web thickness. An H section in class 1 must comply with the following demand at room temperature:

$$\frac{c}{t} \leq 33\varepsilon = 33\sqrt{\frac{235}{f_y}}$$

In a fire situation this equation must be altered with a factor 0.85 which takes into account the influence of the rising temperature:

$$\frac{c}{t} \leq 0.85 * 33\varepsilon = 0.85 * 33\sqrt{\frac{235}{f_y}}$$

$$\frac{164}{7.5} \leq 0.85 * 33\varepsilon = 0.85 * 33\sqrt{\frac{235}{235}}$$

$$22 \leq 28$$

From this we can conclude that the cross section is in cross sectional class 1 and we can apply the method described by the Eurocode.

7.3.1. Plastic degree of utilization known

The force applied on the column is the area of the roof carried by the column multiplied by the permanent load. This results in $N_{\Theta,d,roof} = a(G_{k,roof}+\psi_2 * Q_{k,roof}) = 24(5+0*Q_{k,roof}) = 120kN$. The column is schematized as being simply supported and will have a buckling length equal to its own length, being 6400mm.

$$l_{fi} = 6400mm$$

$$\lambda_1 = 93.9\sqrt{\frac{235}{f_y}} = 93.9\sqrt{\frac{235}{235}}$$

$$\lambda = \frac{l_{fi}}{i} = \frac{6400}{60} = 106.67$$

$$\bar{\lambda} = \frac{\lambda}{\lambda_1} = \frac{106.67}{93.9} = 1.135$$

The plastic degree of utilization μ_{pl} can be calculated by the following formula:

$$\mu_{pl} = \frac{E_{fi,d}}{Af_y} = \frac{120000}{7680 * 235} = 0.06$$

Using the plastic degree of utilization and the relative slenderness calculated above the critical steel temperature can be found in tables such as in “Bouwen met staal publicatie Brand” [35]. In this case the critical steel temperature is found to be 700°C.

Arcelor has created a document which also calculates the critical temperature of a section based on the Eurocode. This method is the same as the one described in the Eurocode but uses different input parameters. The method in the Eurocode allows the user to calculate the buckling force of the section when the steel temperature is known. The method described by Arcelor will calculate the maximum steel temperature when the load on the section is known.

7.3.2. Maximum steel temperature due to fire known

When the plastic degree of utilization is unknown a slightly different approach can be applied using the known maximum temperature in the steel during a fire. When the temperature of the fire is known the reduction in strength and stiffness is known as well. Calculating with these values we can find the ultimate compression force which can be applied on the column. To illustrate this we will use the temperature of 700°C found before to calculate the allowable compression force in the column. This temperature results in a reduction factor for yield stress of 0.230 and a reduction factor for stiffness of 0.130. Using these values we can calculate the relative slenderness for this temperature.

$$\bar{\lambda}_\theta = \bar{\lambda}\sqrt{\frac{k_{y,\theta}}{k_{E,\theta}}} = 1.135\sqrt{\frac{0.230}{0.130}} = 1.51$$

$$\alpha = 0.65\sqrt{\frac{235}{f_y}} = 0.65\sqrt{\frac{235}{235}} = 0.65$$

$$\varphi_\theta = \frac{1}{2}\left(1 + \alpha\bar{\lambda}_\theta + \bar{\lambda}_\theta^2\right) = \frac{1}{2}(1 + 0.65 * 1.51 + 1.51^2) = 2.13$$

$$\chi_{fi} = \frac{1}{\varphi_\theta + \sqrt{\varphi_\theta^2 - \bar{\lambda}_\theta^2}} = \frac{1}{2.13 + \sqrt{2.13^2 - 1.51^2}} = 0.27$$

For χ_{fi} the smallest value must be taken, which is either the z or the y direction. For an H section the weak axis is usually around the z axis but can differ depending on the boundary conditions of the system. The buckling force at a known temperature can now be calculated to be:

$$N_{fi,t,Rd} = \chi_{fi} A k_{y,\theta} f_y = 0.27 * 7680 * 0.23 * 235 = 114kN$$

The second method can also be used to calculate the critical temperature in the cross section iteratively as long as the load on the column is known. Using the tables with k factors the temperature can be calculated by trying a certain temperature and matching it with the load on the column. After a couple of iterations the critical temperature can be found.

7.4. Euler buckling with thermal gradient in cross section

Due to the fire which heats up the steel section, from numbers 1 through 5 in the figure below, the Young's modulus will decrease non-uniformly throughout the section. To calculate the buckling force in this case the Euler buckling formula will be used and altered. The Euler buckling formula can be used for a homogenous cross section and is defined by:

$$F_{Euler} = \frac{\pi^2 EI}{l_{buc}^2}$$

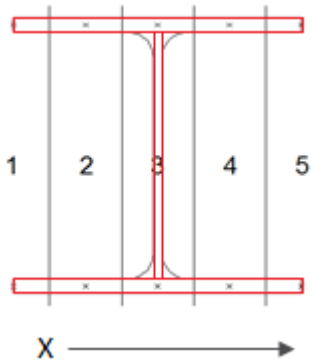

Figure 7.4-1: Sections indicating temperature differences

In this case we have a section which has a non-uniform Young's modulus and thus this formula can't be applied. This means a certain "EI" has to be created which is dependent on the temperature which in turn depends on the location in the section. The mass moment of inertia of the section can be calculated using the following formula:

$$I = \int_A x^2 \, dA$$

When the Young's modulus depends on the temperature and on the location in the cross section it must be taken in the integral in the following form to calculate "EI":

$$"EI" = \int_A E(T_x)\, x^2 \, dA$$

Taking into account the fact that the flanges will result in the same values only two integrals have to be calculated to find the final bending stiffness of the section with a thermal gradient.

$$"EI" = \int_{Aweb} E(T_3)\, x^2 \, dA + 2 \int_{Aflange} E(T_x) x^2 \, dA$$

The first integral describes the bending stiffness of the web of the section. The web is assumed to have one temperature and thus one Young's modulus because it is only 7.5mm thick and no thermal gradient will occur through the web. The second integral consists of the flanges of the section. These flanges have different temperatures which causes the Young's modulus to be different throughout the flanges. This means the young's modulus depends on the temperature and thus on the location in the cross section. As now there is a dependency on space it is no longer a constant and must remain inside the integral. Solving both

integrals the first integral which is the web of the section is the quickest to solve as E(T3) is constant it can be taken outside the integral. Using the height of the web 230 – 2 * 12 = 206mm and the width of 7.5mm we obtain:

$$E(T_3)\int_{-103}^{103}\int_{-3.75}^{3.75} x^2\,dx\,dy = 206E(T_3)\left[\frac{1}{3}x^3\right]_{-3.75}^{3.75}$$

$$"EI"_{web} = 7242.1875E(T_3)$$

To solve the second integral we make use of the fact that the temperatures at the five locations in the flange are known and use linear interpolation to determine the temperatures in between these points. In the following figure Y1 and Y2 are Young's moduli at locations X1 and X2.

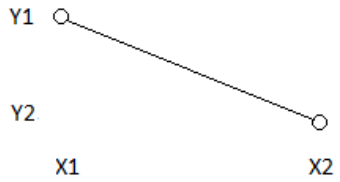

Figure 7.4-2: Linear interpolation diagram

Linear interpolation can be obtained using the following formula in which x is in between X1 and X2 representing distance and Y1 and Y2 Young's moduli:

$$\frac{Y_2 - Y_1}{X_2 - X_1}(x - X_1) + Y_1$$

Using this in the integral to solve the bending stiffness of the flanges results in a summation of four integrals as there are 5 known temperature points in between which the temperature can be linearly interpolated:

$$\begin{pmatrix} x_1 < x < x_2 \\ x_2 < x < x_3 \\ x_3 < x < x_4 \\ x_4 < x < x_5 \end{pmatrix}$$

Using these values for the points on the cross section also the influence of the neutral line will be taken into account changing the values for x1 through x5. As the Young's modulus of the material on one side of the section decreases the neutral line will shift to the right.

$$"EI"_{flange} = \int_{Aflange} E(T_x)x^2\,dA$$

$$"EI"_{flange} = 12\sum_{i=1}^{4}\int_{x_i}^{x_{i+1}}\left(\frac{y_{i+1} - y_i}{x_{i+1} - x_i}(x - x_i) + y_i\right)x^2\,dx$$

Evaluating this integral we get to the solution of the bending stiffness of the section with different EI over the flanges of the section:

$$"EI"_{flange} = 12\sum_{i=1}^{4}\left(\frac{y_{i+1}-y_i}{x_{i+1}-x_i}\left(\frac{1}{4}x_{i+1}^4-\frac{1}{3}x_i x_{i+1}^3-\frac{1}{4}x_i^4+\frac{1}{3}x_i^4\right)+y_i\left(\frac{1}{3}x_{i+1}^3-\frac{1}{3}x_i^3\right)\right)$$

Adding the solution to the integral composed of the web of the section the total "EI" has been calculated.

$$"EI" = 2"EI"_{flange} + "EI"_{web}$$

The "EI" which has been obtained in the calculation method shown above gives us the EI of the column which has the effect of the thermal gradient in the EI. When using this EI in the Euler formula for buckling the buckling force can be calculated for a column which has multiple Young's moduli over the cross section of the column. The following formula show the Euler buckling force with the new EI in it.

$$F_{Euler,thermalgrad.} = \frac{\pi^2 "EI"}{l_{buc}^2}$$

Having formulated the equations in Microsoft Excel the temperatures known in the cross section can be used as input after which the Euler buckling force with a thermal difference will be calculated. When the temperatures are input the file will calculate the stiffness of the steel material at that temperature using the reduction factors in the Eurocode. The total calculation file and Excel sheet are provided in the appendixes.

7.4.1. Results with temperatures obtained from CFD

The file which has been created in excel allows the user to use known temperatures in the flanges and cross section of the section to calculate the buckling force according to Euler. As shown in chapter 7 there are two possible temperature profiles which can be governing. These being the temperature distribution which arises at the maximum temperature in the section and the temperature distribution in the section at the time of the greatest temperature difference in the section.

Euler buckling calculation with thermal gradient in the cross section

Dimensions

Height of section	230	[mm]
Width of section	240	[mm]
Flange width	12	[mm]
Web width	7.5	[mm]

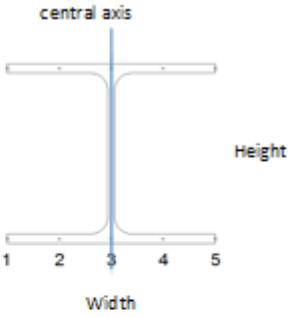

E*A*dist. 38064675600
EA total 287857710
Neutral axis x direction
E*A*dist/EA 132.2343445 mm from left
12.23434453 mm from central axis

	x (mm)	T (C°)	E (N/mm^2)	respect to NA	EI (Nmm^2)
1	-120	785	20160	-132.2343445	14212265669
2	-60	730	24780	-72.23434453	3880268997
3	0	651	45822	-12.23434453	1780615210
4	60	643	48846	47.76565547	17079487042
5	120	660	42420	107.7656555	

EI A1	4.43432E+11	[Nmm^2]
EI A2	10928387999	[Nmm^2]
Total EI	8.97792E+11	[Nmm^2]

Buckling length	6400	[mm]
Buckling force	216329.3129	[N]
Buckling force	216.33	[kN]

Figure 7.4.1-1: Excel file Euler buckling calculation with thermal gradient

When entering the temperature distribution of the maximum temperature difference the buckling load of the column is found to be 692kN. This shows quite a difference to the situation where we enter the temperature distribution which is apparent at the highest temperature recorded. As shown in the figure above this buckling force is calculated to be 216kN. Needless to say we can conclude that the higher temperature distribution is the governing situation. Due to the higher temperatures in the section the stiffness of the material will decrease rapidly and will negatively influence the buckling force of the section.

A disadvantage of this method is the fact that the column will only have a temperature difference in the cross section and not in the longitudinal direction of the column. This means that the highest temperature which has been recorded is in that entire section of the column even though in reality it could only be in a small part. This will cause results which show a buckling load which is lower than would be expected in a situation where a column is subjected to temperature gradients in the cross section and over the height.

7.5. Rayleigh buckling with longitudinal thermal gradient

7.5.1. Rayleigh method

The Rayleigh method is an approximation formula to calculate the buckling force. This formula is based on the amount of work produced by the force during buckling and the deformation energy needed to produce a buckled shape of the system. The amount of work produced by the force is energy which is taken from the surrounding and inserted in the system. If this amount of work is less than the energy needed to deform the system the system won't change its shape.

The deformation energy needed to buckle the system depends on the buckling shape, w(x), of the system:

$$\Delta E_v = \int_0^l \frac{1}{2} EI \left(\frac{d^2w}{dz^2}\right)^2 dz$$

The work produced by the force and the energy transferred to the system is:

$$A = Fu_f = F \int_0^l \frac{1}{2} \left(\frac{dw}{dz}\right)^2 dz$$

Buckling force F_k is the smallest value of F at which a buckled shape w = w(x) can be found such that the work produced is equal to the amount of deformation energy needed.

$$A = \Delta E_v$$

Or using the formulas stated before:

$$F \int_0^l \frac{1}{2} \left(\frac{dw}{dz}\right)^2 dz = \int_0^l \frac{1}{2} EI \left(\frac{d^2w}{dz^2}\right)^2 dz$$

To calculate the buckling force the deformation shape of the system must be found such that the force is minimal. Instead of finding the buckling shape of the system a deformation shape can be assumed and the buckling force, $F = F_R$ associated can be calculated.

$$F_R = \frac{\Delta E_v}{u_f} = \frac{\int_0^l \frac{1}{2} EI \left(\frac{d^2w}{dz^2}\right)^2 dz}{\int_0^l \frac{1}{2} \left(\frac{dw}{dz}\right)^2 dz}$$

This expression for F_R is known as the Rayleigh formula. It depends on the shape of the deformed situation and if this shape is chosen incorrectly it will produce a value which is higher than the actual buckling force. As the chosen deformation shape approaches the actual deformation shape the accuracy will increase.

7.5.2. Calculating the deformation energy

In this particular situation we are describing a column with a changing bending stiffness over the height of the column due to the temperature difference which is present. The moment of inertia in the column is the same at any elevation but the Young's modulus changes. This means that in the integral the Young's modulus is dependent on the height in the column. The equation for the deformation energy needed to buckle the system becomes:

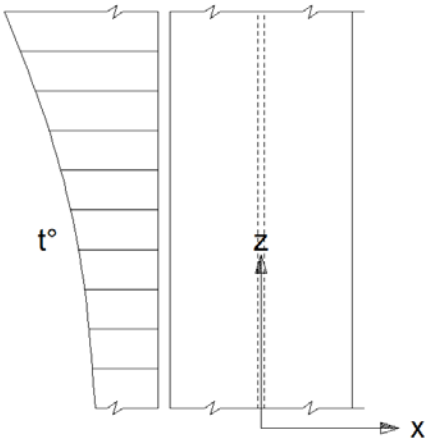

Figure 7.5.2-1: Temperature along longitudinal direction of the column

$$\Delta E_v = \int_0^l \frac{1}{2} E(z) I \left(\frac{d^2w}{dz^2}\right)^2 dz$$

The next step is to assume a deformation shape of the column as it buckles. We assume a parabolic buckling shape with the following equation in which C is an arbitrary constant:

$$w(z) = Cz(l - z)$$

To use this in the equations we need to find the first and second derivatives and the first and second derivatives squared.

$$\frac{dw}{dz} = C(l - 2z)$$

$$\frac{d^2w}{dz^2} = -2C$$

$$\left(\frac{dw}{dz}\right)^2 = C^2(l^2 - 4lz + 4z^2)$$

$$\left(\frac{d^2w}{dz^2}\right)^2 = 4C^2$$

Filling this into the equation for the deformation energy in the column and taking each term nondependent on z out of the integral results in the following equation:

$$\Delta E_v = \int_0^l \frac{1}{2} E(z) I 4 C^2 \, dz = \frac{1}{2} I 4 C^2 \int_0^l E(z) \, dz$$

The Young's modulus which changes over the height of the column will have to be formulated so it can be introduced in the integral. In this case the temperature is known at each 500 mm in the column. So from ground level to 6.4m height we get 14 temperatures. These temperatures will be linearly interpolated in the integral.

$$E(z) \begin{cases} z_1 < z < z_2 \\ z_2 < z < z_3 \\ z_3 < z < z_4 \\ : \quad : \quad : \\ \\ z_{13} < z < z_{14} \end{cases}$$

The integral consisting of E(z) can then be described as a summation of integrals of all the pieces in the height of the column. The evaluation of this integral and total equation can be found in the appendix.

$$\Delta E_v = 2IC^2 \sum_{i=1}^{13} \int_{z_i}^{z_{i+1}} E(z) \, dz$$

$$\Delta E_v = 2IC^2 \sum_{i=1}^{13} (z_{i+1} - z_i) \frac{1}{2} (E_{i+1} + E_i)$$

Take note that E_{i+1} and E_i both consist of the product of the Young's modulus of steel and a reduction factor. Thus the Young's modulus of steel can be moved outside the summation sign to create an equation which is more easily entered in Microsoft excel for example.

$$\Delta E_v = 2E_{steel} IC^2 \sum_{i=1}^{13} (z_{i+1} - z_i) \frac{1}{2} (red_{i+1} + red_i)$$

7.5.3. Calculating the amount of work produced by the force.

The amount of work produced by the force is equal to the force multiplied by the distance it has moved. The displacement of the point of application of F in the direction of F is:

$$u_f = \int_0^l \frac{1}{2} \left(\frac{dw}{dz} \right)^2 dz = \int_0^l \frac{1}{2} C^2 (l^2 - 4lz + 4z^2) \, dz$$

Solving the integral and filling in the boundaries results in the following equation for the amount of work produced:

$$A = F u_f = F \frac{1}{2} C^2 \left(l^3 - 2l^3 + \frac{4}{3} l^3 \right) = F \frac{1}{6} C^2 l^3$$

7.5.4. Calculating Rayleigh buckling force

The Rayleigh buckling force can be calculated by setting the amount of work done by the force equal to the amount of energy produced during deformation using the following formula:

$$A = \Delta E_v$$

As the amount of work (A) is equal to a force times a distance we can rewrite the equation in the following form to produce the Rayleigh buckling force. As the arbitrary constant C2 is in both parts of the equation it cancels out and the equation becomes:

$$F_R = \frac{\Delta E_v}{u_f} = \frac{2E_{steel} I \sum_{i=1}^{13} (z_{i+1} - z_i) \frac{1}{2} (red_{i+1} + red_i)}{\frac{1}{6} l^3}$$

Having formulated the equations in Microsoft Excel, the temperatures known in the height of the column can be used as input after which the Rayleigh buckling force will be calculated. When the temperatures are input the file will calculate the stiffness of the steel material at that temperature using the reduction factors in the Eurocode. The total calculation file and Excel sheet are provided in the appendixes.

7.5.5. Results with temperatures obtained from CFD

Having incorporated all the equations shown in the previous sections of this chapter in excel a simple tool has been created to calculate the buckling force according to Rayleigh. The excel file which can be seen in the figure below allows the user to calculate the buckling force according to Rayleigh when a thermal difference occurs in the longitudinal direction of the column. The highest temperature which occurs in the section during the CFD calculation was 785 °C. The temperature profile that goes with this temperature has been entered in the sheet and figure below.

Rayleigh method for buckling force
Simply supported column

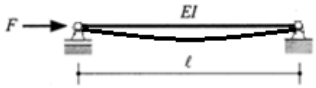

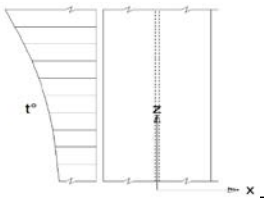

	Height (mm)	Temp (°C)	Reduction factor for E	Delta z (mm)	Average red	Product
1	0	224.24	0.8758			
2	500	235.05	0.8650	500	0.8704	435.1792
3	1000	238.10	0.8619	500	0.8634	431.7146
4	1500	239.73	0.8603	500	0.8611	430.5432
5	2000	240.04	0.8600	500	0.8601	430.0581
6	2500	235.89	0.8641	500	0.8620	431.0174
7	3000	253.55	0.8464	500	0.8553	427.6387
8	3500	304.38	0.7956	500	0.8210	410.5176
9	4000	355.53	0.7445	500	0.7700	385.0229
10	4500	422.74	0.6773	500	0.7109	355.4321
11	5000	505.15	0.5851	500	0.6312	315.5790
12	5500	618.27	0.2771	500	0.4311	215.5448
13	6000	751.58	0.1094	500	0.1932	96.6221
14	6400	785.84	0.0957	400	0.1025	41.0059

Section information (weak axis)		
Izz	27690000	mm^4
Esteel	210000	Nmm^-2

Total integral	4405.8756
Ev/C^2	5.1239E+16
u_f/C^2	43690666667

F_R	1172777.9918	N
F_R	1172.7780	kN

Figure 7.5.5-1: Excel file Rayleigh method for buckling force (longitudinal)

The sheet has been designed in such a way that it will calculate the buckling force according to Rayleigh with limited input parameters. As stated before the sheet is designed to calculate columns which are simply

supported and thus create a buckling shape which resemble a parabolic shape. Using this sheet the only input parameters are the height of the column and the temperatures at intervals, the mass moment of inertia of the section and the Young's modulus of the steel section. In the figure we can see the situation in which the temperature profile is shown which is related to the highest temperature recorded. This results in the buckling load according to Rayleigh of 1172kN. When changing the I_{zz} to I_{yy} the buckling force can be calculated for the strong axis as well but as this will result in a situation which is not governing it will not be displayed here.

This method only allows the user to apply a thermal gradient over the height of the column which is the case in which the fire is surrounding the column and the column heats up evenly in the cross section. In reality the fire will not always surround a column perfectly and could be on just one side of the column. This means that a thermal gradient could occur in the height of the column as well as in the cross section of the column. From this statement we can conclude that this method will show a buckling force which will be lower than when a thermal gradient is apparent in the height and width of the column.

7.6. Rayleigh buckling with temperature distribution in two direction

When calculating the buckling force in a column with a temperature distribution in the cross section and a temperature distribution in the height of the column it would be most accurate if both of these distributions could be taken into account. The calculations and excel files which have been discussed in the previous chapters only calculate the buckling load in a situation where a temperature distribution is only in one direction of the column. This implies that the next task at hand is to create a file in which the two previously discussed files have been moulded together. The expectation is that the buckling load which will be calculated will be higher than the ones found in the previous calculations. This assumption has been based on the fact that the column will have more stiffness leftover when the temperature field is predicted more accurately.

The best way to expand the sheets which have been created to cope with the temperature distribution in two directions would be to modify the sheet using the Rayleigh buckling method. This method allows the use of multiple stiffnesses in the longitudinal direction of the column and can be modified to cope with temperature distributions in the cross section. As a temperature distribution over the width of the column is apparent, multiple reduction factors for the Young's modulus are connected. Taking a weighted average depending on the area of these reduction factors an average reduction factor can be calculated per elevation in the column. The average reduction factor per elevation can be calculated using the following calculation.

$$average\ red. = \left\{2\left(\frac{1}{4}S_w * F_t\left(\frac{1}{2}Red_1 * Red_2 * Red_3 * Red_4 * \frac{1}{2}Red_5\right)\right) + Red_3\left((S_h - 2F_t)W_t + (4-\pi)r^2\right)\right\} \Big/ Area$$

In this equation the following notations have been used:

S_w	Width of section
S_h	Height of section
F_t	Thickness of flange
W_t	Thickness of web
r	Flange to web radius
Area	Total cross-sectional area of column
Red_i	reduction factor due to temperature in cross section

After this weighted average of the reduction factor in the cross section of the column has been calculated the same methodology can be applied as before. To check the result of the weighted average reduction factor the temperatures as in the previous case can be entered throughout the cross section. The result is a Rayleigh buckling force of 1172 kN which is the same as previously calculated.

Rayleigh method for buckling force
Simply supported column

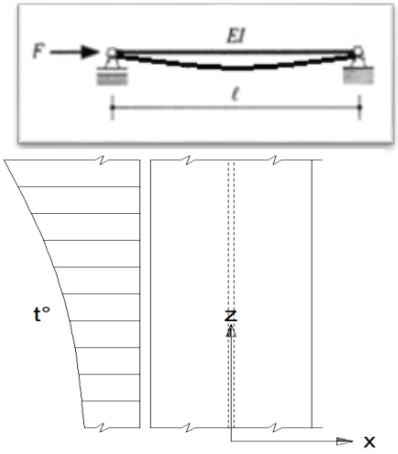

Dimensions		
Height of section	230	[mm]
Width of section	240	[mm]
Flange thickness	12	[mm]
Web thickness	7.5	[mm]
Radius	21	[mm]
Total cross-section area	7684	[mm^2]

Section information (weak axis)		
Izz	27690000	[mm^4]
E	210000	[Nmm^-2]

Insert known temperatures 1 → 5

		Width [mm]					Reduction factor for E				
	Height [mm]	0	60	120	180	240	1	2	3	4	5
1	0	224.238123	224.238123	224.238123	224.238123	224.238123	0.8758	0.8758	0.8758	0.8758	0.8758
2	500	235.045007	235.045007	235.045007	235.045007	235.045007	0.8650	0.8650	0.8650	0.8650	0.8650
3	1000	238.096399	238.096399	238.096399	238.096399	238.096399	0.8619	0.8619	0.8619	0.8619	0.8619
4	1500	239.730859	239.730859	239.730859	239.730859	239.730859	0.8603	0.8603	0.8603	0.8603	0.8603
5	2000	240.036646	240.036646	240.036646	240.036646	240.036646	0.8600	0.8600	0.8600	0.8600	0.8600
6	2500	235.893823	235.893823	235.893823	235.893823	235.893823	0.8641	0.8641	0.8641	0.8641	0.8641
7	3000	253.551416	253.551416	253.551416	253.551416	253.551416	0.8464	0.8464	0.8464	0.8464	0.8464
8	3500	304.378076	304.378076	304.378076	304.378076	304.378076	0.7956	0.7956	0.7956	0.7956	0.7956
9	4000	355.530298	355.530298	355.530298	355.530298	355.530298	0.7445	0.7445	0.7445	0.7445	0.7445
10	4500	422.741418	422.741418	422.741418	422.741418	422.741418	0.6773	0.6773	0.6773	0.6773	0.6773
11	5000	505.152612	505.152612	505.152612	505.152612	505.152612	0.5851	0.5851	0.5851	0.5851	0.5851
12	5500	618.265649	618.265649	618.265649	618.265649	618.265649	0.2771	0.2771	0.2771	0.2771	0.2771
13	6000	751.58389	751.58389	751.58389	751.58389	751.58389	0.1094	0.1094	0.1094	0.1094	0.1094
14	6400	785.84255	785.84255	785.84255	785.84255	785.84255	0.0957	0.0957	0.0957	0.0957	0.0957

Figure 7.6-1: Rayleigh method for buckling; reduction factors.

Avg. Reduction Factor In cross section	E mod. [Nmm^-2] in cross section	Delta z (mm)	Average red long	Product
0.8758	183909.9572			
0.8650	181640.5485	500	0.8704	435.1792
0.8619	180999.7562	500	0.8634	431.7146
0.8603	180656.5196	500	0.8611	430.5432
0.8600	180592.3043	500	0.8601	430.0581
0.8641	181462.2972	500	0.8620	431.0174
0.8464	177754.2026	500	0.8553	427.6387
0.7956	167080.6040	500	0.8210	410.5176
0.7445	156338.6374	500	0.7700	385.0229
0.6773	142224.3022	500	0.7109	355.4321
0.5851	122862.0593	500	0.6312	315.5790
0.2771	58195.5847	500	0.4311	215.5448
0.1094	22966.9532	500	0.1932	96.6221
0.0957	20089.2258	400	0.1025	41.0059

Total integral	4405.8756	
EvC^2	5.1239E+16	
u_f/C^2	43690666667	
F_R	1172778	N
F_R	1172.7780	kN

Figure 7.6-2: Excel file Rayleigh method for buckling; buckling load verification to figure 7-7.

The figures above show how the excel file has been built up. With the same section and the same temperature distribution as in chapter 10.5.5 the calculation is the same and the result will show the same value of 1172 kN. Having made this change to the excel file we can now include temperature distributions in both the cross section and the longitudinal direction of the column.

7.6.1. Results with temperatures obtained from CFD simulation

During the CFD simulation the temperatures in the column have been calculated and stored in an output file. After having organised the data and selected the time-step in which the highest temperatures appear we can create a table with the temperatures in the column in both the cross section and the longitudinal direction of the column. This set of data which consists of temperatures at specific points in the column can now be used to enter in the table of the excel sheet to calculate the buckling force according to Rayleigh. The formula used now takes into account the temperature differences both in the cross section of the column and the longitudinal direction of the column. In the figure below the temperatures which have been found in the column have been incorporated for every 500mm in elevation.

Rayleigh method for buckling force
Simply supported column

Dimensions		
Height of section	230	[mm]
Width of section	240	[mm]
Flange thickness	12	[mm]
Web thickness	7.5	[mm]
Radius	21	[mm]
Total cross-section area	7684	[mm^2]

Section information (weak axis)		
Izz	27690000	[mm^4]
E	210000	[Nmm^-2]

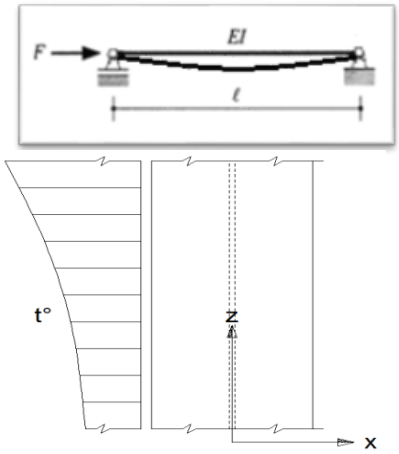

Insert known temperatures 1 → 5

		Width [mm]					Reduction factor for E				
	Height [mm]	0	60	120	180	240	1	2	3	4	5
1	0	224.24	195.56	171.19	164.98	168.45	0.8758	0.9044	0.9288	0.9350	0.9315
2	500	235.05	206.93	189.48	181.45	184.25	0.8650	0.8931	0.9105	0.9186	0.9157
3	1000	238.10	207.73	189.44	178.93	179.88	0.8619	0.8923	0.9106	0.9211	0.9201
4	1500	239.73	209.22	191.04	180.68	182.15	0.8603	0.8908	0.9090	0.9193	0.9179
5	2000	240.04	208.79	190.09	180.88	182.87	0.8600	0.8912	0.9099	0.9191	0.9171
6	2500	235.89	205.67	187.35	181.18	184.94	0.8641	0.8943	0.9126	0.9188	0.9151
7	3000	253.55	222.74	200.92	193.13	198.55	0.8464	0.8773	0.8991	0.9069	0.9015
8	3500	304.38	268.39	238.42	229.25	237.41	0.7956	0.8316	0.8616	0.8707	0.8626
9	4000	355.53	317.78	283.27	274.40	285.34	0.7445	0.7822	0.8167	0.8256	0.8147
10	4500	422.74	378.97	336.98	326.14	338.95	0.6773	0.7210	0.7630	0.7739	0.7611
11	5000	505.15	457.89	407.36	393.62	406.81	0.5851	0.6421	0.6926	0.7064	0.6932
12	5500	618.27	570.15	512.80	500.49	513.38	0.2771	0.3966	0.5629	0.5986	0.5612
13	6000	751.58	705.48	643.23	632.80	647.33	0.1094	0.1278	0.2322	0.2510	0.2248
14	6400	785.84	730.05	651.23	643.37	660.55	0.0957	0.1180	0.2178	0.2319	0.2010

Figure 7.6.1-1: Rayleigh method for buckling; reduction factors.

Avg. Reduction Factor In cross section	E mod. [Nmm^-2] in cross section	Delta z (mm)	Average red long	Product
0.9207	193345.3429			
0.9050	190045.3979	500	0.9128	456.4175
0.9054	190142.3982	500	0.9052	452.6045
0.9038	189790.5176	500	0.9046	452.3011
0.9041	189867.2724	500	0.9039	451.9736
0.9060	190270.1178	500	0.9051	452.5445
0.8917	187265.3963	500	0.8989	449.4470
0.8516	178835.4452	500	0.8717	435.8343
0.8050	169041.7811	500	0.8283	414.1396
0.7490	157281.7157	500	0.7770	388.4804
0.6757	141899.7717	500	0.7123	356.1684
0.5115	107407.2572	500	0.5936	296.7941
0.2039	42827.0055	500	0.3577	178.8503
0.1887	39629.7488	400	0.1963	78.5302

Total integral	4864.0856	
Ev/C^2	5.6568E+16	
u_f/C^2	43690666667	
F_R	1294747	N
F_R	1294.7466	kN

Figure 7.6.1-2: Excel file Rayleigh method for buckling; buckling load.

Having entered the data for the temperatures of the column the Rayleigh buckling load of the column will be calculated. For this fire situation and the column at hand the Rayleigh buckling load is 1295kN. The buckling load which has been calculated is higher than which had been found in the case where the temperature difference were only in the longitudinal direction of the column. Before this modification the buckling load was calculated to be 1172kN where now, with a more accurate representation of the temperatures in the column, the load was calculated at 1295kN. As a check we can calculate the Rayleigh buckling load when the column is subjected to the maximum temperature. Which is in fact the approach the Eurocode prescribes us to use. When the temperature field due to a fire situation is known in the column the highest temperature must be used. Using this methodology we get the following input and buckling load according to Rayleigh.

Rayleigh method for buckling force
Simply supported column

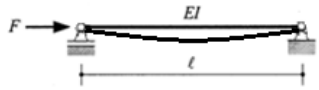

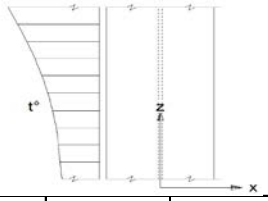

	Height (mm)	Temp (°C)	Reduction factor for E	Delta z (mm)	Average red	Product
1	0	785.84	0.0957			
2	500	785.84	0.0957	500	0.0957	47.8315
3	1000	785.84	0.0957	500	0.0957	47.8315
4	1500	785.84	0.0957	500	0.0957	47.8315
5	2000	785.84	0.0957	500	0.0957	47.8315
6	2500	785.84	0.0957	500	0.0957	47.8315
7	3000	785.84	0.0957	500	0.0957	47.8315
8	3500	785.84	0.0957	500	0.0957	47.8315
9	4000	785.84	0.0957	500	0.0957	47.8315
10	4500	785.84	0.0957	500	0.0957	47.8315
11	5000	785.84	0.0957	500	0.0957	47.8315
12	5500	785.84	0.0957	500	0.0957	47.8315
13	6000	785.84	0.0957	500	0.0957	47.8315
14	6400	785.84	0.0957	400	0.0957	38.2652

Section information (weak axis)		
Izz	27690000	mm^4
Esteel	210000	Nmm^-2

Total integral	612.2431
EvlC^2	7.1203E+15
u_f/C^2	43690666667

F_R	162969.9206	N
F_R	162.9699	kN

Figure 7.6.1-3: Rayleigh method for buckling using highest temperature.

Using the highest temperature which is encountered in the steel section the buckling load according to Rayleigh will be 163kN. Using the more accurate temperature profile we found a buckling load of 1295kN which is much higher than the one generated with a uniform temperature using the highest temperature found in the steel. Using a temperature profile in the calculation which closely resembles that which occurs in reality will allow for a higher buckling load than when only looking at the highest temperature or the temperature distribution in one direction.

8

Summary and conclusions

During this thesis the fire safety engineering approach has been used to investigate the influence of hydrocarbon pool fires on steel columns. Using a fire curve which closely resembles a natural fire curve the temperatures occurring in the steel have been investigated using a Computational Fluid Dynamics (CFD) model. The model consists of the compartment which has been discussed in chapter three. As can be seen in chapter four the model which has been introduced in the CFD software closely mimics the actual compartment, including windows, roof openings and a large overhead door in the wall. After the model had been entered the fire curve must be given as well. The fire curve which has been used is based on a pool fire with a three meter diameter and a height of 2.5cm. Using the mass burning rate and rate of heat release the maximum power emitted by the liquid can be calculated. After having run the CFD calculation which took about four days per scenario the results of the temperatures in the steel had been formulated. Having used a CFD calculation the results of this calculation were to be checked by a reference tool. Arcelor Mittal has created a software package called Ozone. Having entered the same compartment and fire curve as had been done in the CFD simulation the results can be compared to each other. The results and the comparison of the two simulations have been evaluated in chapter 6.4. Focussing on the load bearing capacity of the column chapter seven investigates the maximum stress which the cross section can endure in a fire situation. Please note that this chapter only checks the strength of the column at raised temperature and omits any phenomena of instability. As the temperatures have been calculated by CFD and are thus known we can distinguish two cases. The first case is the temperature profile in the cross section of the column at which the highest temperature appears. Secondly the case in which the highest temperature difference occurs in the cross section. Having formulated a series of excel sheets in which the buckling load with respect to temperature can be calculated according to Euler and Rayleigh the following conclusions can be made.

- From the results of the CFD model we can conclude that due to a fire on one side of a column a thermal difference will occur in the cross section of the column as well as over the height of the column.

- In the case where the fire area is perfectly and fully around a single column the thermal difference in the cross section will be minimal and only a thermal difference over the height of the column will be apparent.

- The Eurocode prescribes that in the case that a thermal difference occurs the highest temperature must be used during the buckling calculation. As the highest temperature which is found in the column is now being used in the entire column, in both cross section and height, this is a safe but very conservative calculation method in the case where deformation due to temperature is not taken into account. As stated in the recommendations more research on this effect should be completed to be able to formulate a conclusion about this effect.

- Using a temperature difference will yield a result which has a higher elastic critical buckling load than in the case where only the highest temperature is assumed to be on the entire section.

- The governing temperature case has been found to be the case in which the highest temperatures are apparent in the section.

- Based on the results the conclusion can be made that the buckling load as calculated by the Eurocode will increase when the temperature field in the column is more accurately described. This conclusion is based on this case study and assumptions only.

Due to the fact that the Rayleigh method used in this thesis is an upper-bound solution to the problem we can't conclude that this buckling load is the ultimate buckling resistance. Only when the lowest upper-bound of the problem has been investigated we can say with certainty that it is the ultimate buckling resistance of the structure.

9

Recommendations

As has been stated in the conclusions of this chapter, the method which has been described and incorporated in the excel sheets are an upper-bound solution. This means that we can say for certain that any load which is higher than the calculated buckling load will result in failure of the column. Any load which is lower than the calculated buckling load will result in a sort of grey area in which we are uncertain if the column will fail or remain intact. This is due to the fact that an upper-bound solution which is lower may be found when more accurately describing the behaviour of the column. When the behaviour of the column and all of its properties and effects have been taken into account the lowest upper-bound of the problem can be obtained. Only after this we can state that the lowest upper-bound and thus the lowest buckling force has been calculated. Having stated this there are some ways to improve the calculation which has been used in this thesis and will be described in this section of the recommendations.

- Using a calculation based on the Rayleigh buckling method the buckling shape of the section must be known. As a temperature difference in the cross section of a column is apparent the column has an initial curvature which can be taken into account to more accurately describe the deformation shape.

- Another major influence to the buckling load is the buckling length of the system. In this thesis a buckling length which is equal to the system length has been used. Whenever a clamped column is used or a building structure with more than one floor the buckling length of the system will change. The type of connections are also of influence to this. As a column is not hinged on both sides but schematized as rotational springs the buckling length will be less and influences the buckling load.

- Due to the fact that the temperature distribution in the column is not linear, stresses will occur in the material which have not been taken into account during this thesis. More research should be done so the influence of these stresses in the material can be introduced in the calculation. This will result in a more accurate approach and more realistic buckling load of the column.

- The temperature distribution which has been found during the Computation Fluid Dynamics (CFD) simulation is based on a HE240A column and a certain proposed fire. When using a different column or compartment with other dimensions or a different fire the temperature distribution will be different. This results in the fact that each case is different and the temperature distribution in the column must be predicted for each possible case.

- As a concluding remark the compartment which has been entered in the CFD calculation has not taken into account the fact that a possible wind may occur and flow through the compartment. This will either slow down or heat up the fire and should be investigated further to determine the effect of the wind on the temperatures in the compartment and the steel.

Bibliography

[1] NEN-EN 1991 part 1-2 +NB: “Actions on structures – Actions on structures exposed to fire”
[2] NEN-EN 1993 part 1-2 +NB: “Design of steel structures – Structural fire design”
[3] Ing. F.P.H. Jakobs, *Nauwkeurige berekening maakt brandwerende bekleding overbodig*, Bouwen met staal 149 (1999), p.52-56.
[4] Ir. H.A. Grüter en Ir. H.J Kuijer, S*taal voor krachtpatsers*, Bouwen met staal 210 (2009), p.54-57.
[5] J. Ingham MSc. *Forensic engineering of fire damaged structures*, Civil engineering 162 (2009), p.12-17.
[6] OGP Risk Assessment Data Directory, vulnerability of plant/structure. (2010)
[7] Publicatiereeks Gevaarlijke Stoffen 1, Deel 1B: Effecten van brand op constructies.(2003)
[8] BCSA and TATA, Steel Construction: Fire safety (2013)
[9] http://www.steelconstruction.info/Structural_fire_engineering
[10] British Steel Technical Swinden Laboratories. *The reinstatement of fire damaged steel and iron framed structures.* (1993)
[11] B.R. Kirby en D.E. Wainman, *The behaviour of structural steelwork in natural fires. (1997)*
[12] C. Crosti. *Structural analysis of steel structures under fire loading.* Acta Polytechnica Vol. 49 No.1 (2009)
[13] Z. Zhao. *Steel columns under fire – a neural network based strength model.*
[14] Zhi-Hua Wang en Kang-Hai Tan. *Temperature prediction for multi-dimensional domains in standard fire.*
[15] NEN-EN 1990: “Basis of structural design”
[16] Zhi-Hua Wang, *Geometric effects of radiative heat exchange in concave structure with application to heating of steel I-sections in fire.* (2010)
[17] Vikas Adarsh Narang. *Heat transfer analysis in steel structures.* (2005)
[18] M.B. Wong en J.I. Ghojel. *Sensitivity of heat transfer formulations for insulated structural steel components.* (2002)
[19] Zhi-Hua Wang en Kang-Hai Tan. *Radiative heat transfer for structural members exposed to fire: an analytical approach.* (2006)
[20] M. Munoz, J. Arnaldos, J. Casal en E. Planas. *Analysis of the geometric and radiative characteristics of hydrocarbon pool fires.* (2004)
[21] Cheng Qian en Kozo Saito. *Measurements of pool fire temperature using IR technique.* (…)
[22] Eulàlia Plans-Cuchi en Joachim Casal. *Flame temperature distribution in a pool-fire.* (1998)
[23] S. Sudheer en S.V. Prabhu. *Measurement of the flame emissivity of gasoline pool fires.* (2010)
[24] Kevin B. McGrattan. *Thermal radiation from large poolfires.* (2000)
[25] J.P. Spinti, J.N. Thornock, E.G. Eddings, P.J. Smith, A.F. Sarofim. *Heat transfer to objects in pool fires.*(2008)
[26] I.W. Bugess, A.O. Olawale, R.J. Plank. *Failure of steel columns in fire.*(1991)
[27] J.A. Milke. *Analytical methods for determining fire resistance of steel members.* (2002)
[28] D. Somaini, M. Knobloch, M. Fontana. *Simplified analytical model for global buckling of steel columns in fire.* (2010)
[29] Wee-Siang Toh, Kang-Hai Tan, Tat-Ching Fung. *Rankine approach for steel columns in fire: numerical studies.* (2002)
[30] Y. Yao, K.H. Tan. *Extended rankine approach for bi-axially loaded steel columns under natural fire.* (2008)
[31] Arcelor. *Fire resistance of steel structures.* (2006)
[32] R. Becker. *Structural behavior of simple steel structures with non-uniform longitudinal temperature distributions under fire conditions.* (2001)
[33] S.E. Quiel, M.E.M. Garlock, M.M.S. Dwaikat, V.K.R. Kodur. *Predicting the demand and plastic capacity of axially loaded steel beam-columns with thermal gradients.* (2013)

[34] A.O. Olawale. *Collapse behaviour of steel columns in fire.* (1988)
[35] A.F. Hamerlinck. Bouwen met staal publicatie *Brand*. (2010)
[36] A.J. Tromp en R.J.M. van Mierlo. *Fire safety engineering handboek voor de bouw*. Efectis Nederland BV (2013)
[37] www.brandveiligmetstaal.nl
[38] J.W. Welleman, A. Dolfing, J.W. Hartman. *Basisboek toegepaste mechanica* (2001)
[39] H.K. Versteeg, W. Malalasekera. *An Introduction to Computational Fluid Dynamics The Finite Volume Method.* (2007)
[40] ANSYS Inc., *ASYS CFX-solver theory guide. (2012)*
[41] A. Hamins, A. Maranghides, G. Mulholland. *The global combustion behaviour of 1 MW to 3MW hydrocarbon spray fires burning in an open environment.* NIST (2003)

Appendix A: Compartment model.

Appendix B: Rayleigh method, thermal difference in two directions.

Rayleigh method for buckling force

Simply supported column

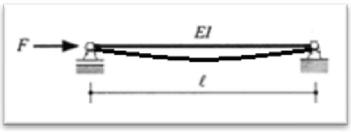

Dimensions		
Height of section	230	[mm]
Width of section	240	[mm]
Flange thickness	12	[mm]
Web thickness	7,5	[mm]
Radius	21	[mm]
Total cross-section area	7684	[mm^2]

Section information (weak axis)		
Izz	27690000	[mm^4]
E	210000	[Nmm^-2]

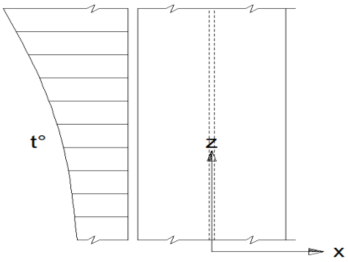

Insert known temperatures

1 → 5

		Width [mm]					Reduction factor for E				
	Height [mm]	0	60	120	180	240	1	2	3	4	5
1	0	224,24	195,56	171,19	164,98	168,45	0,8758	0,9044	0,9288	0,9350	0,9315
2	500	235,05	206,93	189,48	181,45	184,25	0,8650	0,8931	0,9105	0,9186	0,9157
3	1000	238,10	207,73	189,44	178,93	179,88	0,8619	0,8923	0,9106	0,9211	0,9201
4	1500	239,73	209,22	191,04	180,68	182,15	0,8603	0,8908	0,9090	0,9193	0,9179
5	2000	240,04	208,79	190,09	180,88	182,87	0,8600	0,8912	0,9099	0,9191	0,9171
6	2500	235,89	205,67	187,35	181,18	184,94	0,8641	0,8943	0,9126	0,9188	0,9151
7	3000	253,55	222,74	200,92	193,13	198,55	0,8464	0,8773	0,8991	0,9069	0,9015
8	3500	304,38	268,39	238,42	229,25	237,41	0,7956	0,8316	0,8616	0,8707	0,8626
9	4000	355,53	317,78	283,27	274,40	285,34	0,7445	0,7822	0,8167	0,8256	0,8147
10	4500	422,74	378,97	336,98	326,14	338,95	0,6773	0,7210	0,7630	0,7739	0,7611
11	5000	505,15	457,89	407,36	393,62	406,81	0,5851	0,6421	0,6926	0,7064	0,6932
12	5500	618,27	570,15	512,80	500,49	513,38	0,2771	0,3966	0,5629	0,5986	0,5612
13	6000	751,58	705,48	643,23	632,80	647,33	0,1094	0,1278	0,2322	0,2510	0,2248
14	6400	785,84	730,05	651,23	643,37	660,55	0,0957	0,1180	0,2178	0,2319	0,2010
15	6400	785,84	730,05	651,23	643,37	660,55	0,0957	0,1180	0,2178	0,2319	0,2010
16	6400	785,84	730,05	651,23	643,37	660,55	0,0957	0,1180	0,2178	0,2319	0,2010
17	6400	785,84	730,05	651,23	643,37	660,55	0,0957	0,1180	0,2178	0,2319	0,2010
18	6400	785,84	730,05	651,23	643,37	660,55	0,0957	0,1180	0,2178	0,2319	0,2010
19	6400	785,84	730,05	651,23	643,37	660,55	0,0957	0,1180	0,2178	0,2319	0,2010
20	6400	785,84	730,05	651,23	643,37	660,55	0,0957	0,1180	0,2178	0,2319	0,2010
21	6400	785,84	730,05	651,23	643,37	660,55	0,0957	0,1180	0,2178	0,2319	0,2010
22	6400	785,84	730,05	651,23	643,37	660,55	0,0957	0,1180	0,2178	0,2319	0,2010
23	6400	785,84	730,05	651,23	643,37	660,55	0,0957	0,1180	0,2178	0,2319	0,2010
24	6400	785,84	730,05	651,23	643,37	660,55	0,0957	0,1180	0,2178	0,2319	0,2010
25	6400	785,84	730,05	651,23	643,37	660,55	0,0957	0,1180	0,2178	0,2319	0,2010
26	6400	785,84	730,05	651,23	643,37	660,55	0,0957	0,1180	0,2178	0,2319	0,2010
27	6400	785,84	730,05	651,23	643,37	660,55	0,0957	0,1180	0,2178	0,2319	0,2010
28	6400	785,84	730,05	651,23	643,37	660,55	0,0957	0,1180	0,2178	0,2319	0,2010
29	6400	785,84	730,05	651,23	643,37	660,55	0,0957	0,1180	0,2178	0,2319	0,2010
30	6400	785,84	730,05	651,23	643,37	660,55	0,0957	0,1180	0,2178	0,2319	0,2010

Avg. Red. Factor In cross section	E mod. [Nmm^-2] in cross section	Delta z (mm)	Average red f	Product
0,9207	193345,3429			
0,9050	190045,3979	500	0,9128	456,4175
0,9054	190142,3982	500	0,9052	452,6045
0,9038	189790,5176	500	0,9046	452,3011
0,9041	189867,2724	500	0,9039	451,9736
0,9060	190270,1178	500	0,9051	452,5445
0,8917	187265,3963	500	0,8989	449,4470
0,8516	178835,4452	500	0,8717	435,8343
0,8050	169041,7811	500	0,8283	414,1396
0,7490	157281,7157	500	0,7770	388,4804
0,6757	141899,7717	500	0,7123	356,1684
0,5115	107407,2572	500	0,5936	296,7941
0,2039	42827,0055	500	0,3577	178,8503
0,1887	39629,7488	400	0,1963	78,5302
0,1887	39629,7488	0	0,1887	0,0000
0,1887	39629,7488	0	0,1887	0,0000
0,1887	39629,7488	0	0,1887	0,0000
0,1887	39629,7488	0	0,1887	0,0000
0,1887	39629,7488	0	0,1887	0,0000
0,1887	39629,7488	0	0,1887	0,0000
0,1887	39629,7488	0	0,1887	0,0000
0,1887	39629,7488	0	0,1887	0,0000
0,1887	39629,7488	0	0,1887	0,0000
0,1887	39629,7488	0	0,1887	0,0000
0,1887	39629,7488	0	0,1887	0,0000
0,1887	39629,7488	0	0,1887	0,0000
0,1887	39629,7488	0	0,1887	0,0000
0,1887	39629,7488	0	0,1887	0,0000
0,1887	39629,7488	0	0,1887	0,0000
0,1887	39629,7488	0	0,1887	0,0000

Total int	4864,0856
Ev/C^2	5,6568E+16

u_f/C^2	4E+10

F_R	1294747	N
F_R	**1294,7466**	kN

Appendix C: Rayleigh method, thermal diff. in longitudinal direction.

Rayleigh method for buckling force

Simply supported column

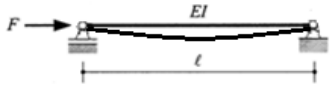

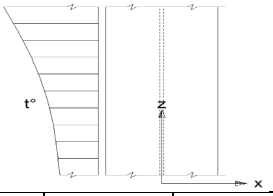

	Height (mm)	Temp (℃)	Reduction factor for E	Delta z (mm)	Average red	Product
1	0	785,84	0,0957			
2	500	785,84	0,0957	500	0,0957	47,8315
3	1000	785,84	0,0957	500	0,0957	47,8315
4	1500	785,84	0,0957	500	0,0957	47,8315
5	2000	785,84	0,0957	500	0,0957	47,8315
6	2500	785,84	0,0957	500	0,0957	47,8315
7	3000	785,84	0,0957	500	0,0957	47,8315
8	3500	785,84	0,0957	500	0,0957	47,8315
9	4000	785,84	0,0957	500	0,0957	47,8315
10	4500	785,84	0,0957	500	0,0957	47,8315
11	5000	785,84	0,0957	500	0,0957	47,8315
12	5500	785,84	0,0957	500	0,0957	47,8315
13	6000	785,84	0,0957	500	0,0957	47,8315
14	6400	785,84	0,0957	400	0,0957	38,2652
15	6400	785,84	0,0957	0	0,0957	0,0000
16	6400	785,84	0,0957	0	0,0957	0,0000
17	6400	785,84	0,0957	0	0,0957	0,0000
18	6400	785,84	0,0957	0	0,0957	0,0000
19	6400	785,84	0,0957	0	0,0957	0,0000
20	6400	785,84	0,0957	0	0,0957	0,0000
21	6400	785,84	0,0957	0	0,0957	0,0000
22	6400	785,84	0,0957	0	0,0957	0,0000
23	6400	785,84	0,0957	0	0,0957	0,0000
24	6400	785,84	0,0957	0	0,0957	0,0000
25	6400	785,84	0,0957	0	0,0957	0,0000
26	6400	785,84	0,0957	0	0,0957	0,0000
27	6400	785,84	0,0957	0	0,0957	0,0000
28	6400	785,84	0,0957	0	0,0957	0,0000
29	6400	785,84	0,0957	0	0,0957	0,0000
30	6400	785,84	0,0957	0	0,0957	0,0000

Section information (weak axis)		
Izz	27690000	mm^4
Esteel	210000	Nmm^-2

Total integral	612,2431
Ev/C^2	7,1203E+15

u_f/C^2	43690666667

F_R	162969,9206	N
F_R	**162,9699**	kN

Appendix D: Euler buckling with thermal difference in cross section.

Euler buckling calculation with thermal gradient in the cross section

Dimensions

Height of section	230	[mm]
Width of section	240	[mm]
Flange width	12	[mm]
Web width	7,5	[mm]

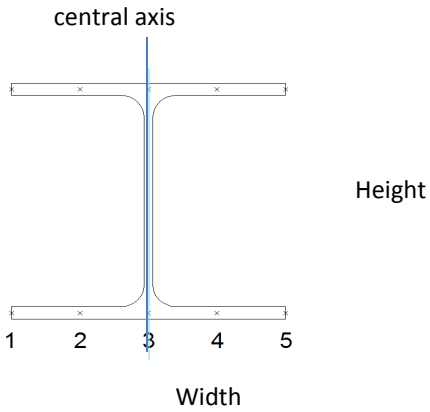

E*A*dist. 38064675600
EA total 287857710
Neutral axis x direction
E*A*dist/EA 132,2343445 mm from left
12,23434453 mm from central axis

	x (mm)	T (C°)	E (N/mm^2)	respect to NA	EI (Nmm^2)
1	-120	785	20160	-132,2343445	14212265669
2	-60	730	24780	-72,23434453	3880268997
3	0	651	45822	-12,23434453	1780615210
4	60	643	48846	47,76565547	17079487042
5	120	660	42420	107,7656555	

EI A1	4,43432E+11	[Nmm^2]
EI A2	10928387999	[Nmm^2]
Total EI	8,97792E+11	[Nmm^2]

Buckling length	6400	[mm]
Buckling force	216329,3129	[N]
Buckling force	216,33	[kN]

Appendix E: Calculation to excel sheets in appendix B,C,D.

Calculation for Euler formula using a bending stiffness of the column which changes over the cross section

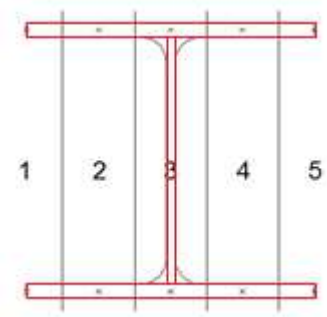

Calculation of Euler buckling with a non-uniform EI

$$F_{Euler} = \frac{\pi^2 EI}{l_{buc}^2}$$

$$I = \int_A x^2 \, dA$$

$$\mathrm{EI} = \int_A E(T_x)\, x^2 \, dA$$

$$"EI" = \int_{Aweb} E(T_3)\, x^2 \, dA + 2 \int_{Aflange} E(T_x)\, x^2 \, dA$$

Integral for web of section calculated in which 3.75 is half the thickness of the web

$$E(T_3) \int_{-103}^{103} \int_{-3.75}^{3.75} x^2 \; dx \, dy = 206 E(T_3) * \left[\frac{1}{3} x^3\right]_{-3.75}^{3.75}$$

$$"EI"_{web} = 7242.1875 E(T_3)$$

Intermezzo Linear interpolation

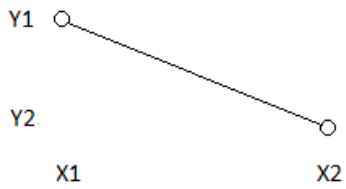

$$\frac{Y_2 - Y_1}{X_2 - X_1}(x - X_1) + Y_1$$

Y1 and Y2 are Young's moduli while X1 and X2 are distances

End of intermezzo

As five known temperatures are apparent in the cross section we have four domains with changing EI

$$\begin{pmatrix} x_1 < x < x_2 \\ x_2 < x < x_3 \\ x_3 < x < x_4 \\ x_4 < x < x_5 \end{pmatrix}$$

Formula for EI_{flange}

$$"EI"_{flange} = \int_{Aflange} E(T_x)\, x^2\, dA$$

Solving the integral in y direction first yield the thickness of the flange which is twelve mm and the summation of areas in which i =1 to 4.

$$"EI"_{flange} = 12 \sum_{i=1}^{4} \int_{x_i}^{x_{i+1}} \left(\frac{y_{i+1} - y_i}{x_{i+1} - x_i} (x - x_i) + y_i \right) x^2\, dx$$

$$"EI"_{flange} = 12 \sum_{i=1}^{4} \left(\frac{y_{i+1} - y_i}{x_{i+1} - x_i} \int_{x_i}^{x_{i+1}} (x^3 - x_i x^2)\, dx + y_i \int_{x_i}^{x_{i+1}} (x^2)\, dx \right)$$

$$"EI"_{flange} = 12 \sum_{i=1}^{4} \left(\frac{y_{i+1} - y_i}{x_{i+1} - x_i} \left[\frac{1}{4} x^4 - \frac{1}{3} x_i x^3 \right]_{x_i}^{x_{i+1}} + y_i \left[\frac{1}{3} x^3 \right]_{x_i}^{x_{i+1}} \right)$$

$$"EI"_{flange} = 12 \sum_{i=1}^{4} \left(\frac{y_{i+1} - y_i}{x_{i+1} - x_i} \left(\frac{1}{4} x_{i+1}^4 - \frac{1}{3} x_i * x_{i+1}^3 - \frac{1}{4} x_i^4 + \frac{1}{3} x_i^4 \right) + y_i \left(\frac{1}{3} x_{i+1}^3 - \frac{1}{3} x_i^3 \right) \right)$$

The total solution to the problem now is:

$$"EI" = 2"EI"_{flange} + "EI"_{web}$$

Using Eulers formula for buckling we can now calculate the buckling force of this column with a thermal gradient.

$$F_{Euler,thermalgrad.} = \frac{\pi^2 "EI"}{l_{buc}^2}$$

Calculation of Rayleigh buckling force for a column with a thermal difference over the height of the column.

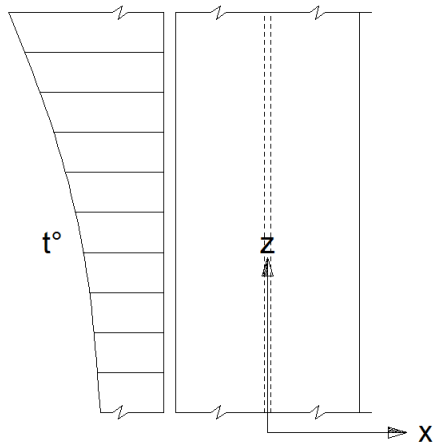

Buckling shape of the column and its derivatives: parabolic

$$w(z) = Cz(l - z)$$

$$\frac{dw}{dz} = C(l - 2z)$$

$$\frac{d^2w}{dz^2} = -2C$$

$$\left(\frac{dw}{dz}\right)^2 = C^2(l^2 - 4lz + 4z^2)$$

$$\left(\frac{d^2w}{dz^2}\right)^2 = 4C^2$$

The deformation energy produced by buckling is:

$$\Delta E_v = \int_0^l \frac{1}{2} E(Z) I \left(\frac{d^2w}{dz^2}\right)^2 dz$$

$$\Delta E_v = \int_0^l \frac{1}{2} E(Z) I 4C^2 \, dz = \frac{1}{2} I 4C^2 \int_0^l E(Z) \, dz$$

The integral solving E(z) consists of 13 parts as we have 14 points at which the temperature is known.

$$E(z) \begin{cases} z_1 < z < z_2 \\ z_2 < z < z_3 \\ z_3 < z < z_4 \\ \vdots \quad \vdots \quad \vdots \\ \\ z_{13} < z < z_{14} \end{cases}$$

$$\Delta E_v = 2IC^2 \sum_{i=1}^{13} \int_{z_i}^{z_{i+1}} E(z) \, dz$$

Solving the integral we must make use of linear interpolation in between the known temperature points.

Intermezzo Linear interpolation

$$E(z) = \frac{Y_2 - Y_1}{Z_2 - Z_1}(z - Z_1) + Y_1$$

Y1 and Y2 are Young's moduli while Z1 and Z2 are distances

End of intermezzo

Using this in the integral we obtain the following equation and simplification:

$$\int_{Z_1}^{Z_2} \left(\frac{Y_2 - Y_1}{Z_2 - Z_1}(z - Z_1) + Y_1\right) dz$$

$$\frac{Y_2 - Y_1}{Z_2 - Z_1}\left[\frac{1}{2}z^2 - Z_1 z\right]_{Z_1}^{Z_2} + [Y_1 z]_{Z_1}^{Z_2}$$

$$\frac{Y_2 - Y_1}{Z_2 - Z_1}\left(\frac{1}{2}Z_2^2 - Z_2 z - \frac{1}{2}Z_1^2 + Z_1^2\right) + Y_1(Z_2 - Z_1)$$

$$\frac{Y_2 - Y_1}{Z_2 - Z_1}\frac{1}{2}(Z_2^2 + Z_1^2 - Z_2 Z_1) + Y_1(Z_2 - Z_1)$$

$$\frac{Y_2 - Y_1}{Z_2 - Z_1}\frac{1}{2}(Z_2 - Z_1)^2 + Y_1(Z_2 - Z_1)$$

$$(Y_2 - Y_1)\frac{1}{2}(Z_2 - Z_1) + Y_1(Z_2 - Z_1)$$

$$(Z_2 - Z_1)\left(\frac{1}{2}Y_2 - \frac{1}{2}Y_1\right)$$

Incorporating this integral in the equation for the deformation energy we obtain:

$$\Delta E_v = 2IC^2 \sum_{i=1}^{13} \int_{z_i}^{z_{i+1}} E(z)\, dz$$

$$\Delta E_v = 2IC^2 \sum_{i=1}^{13} (z_{i+1} - z_i)\frac{1}{2}(E_{i+1} + E_i)$$

Take note that E_{i+1} and E_i both consist of the product of the Young's modulus of steel and a reduction factor. Thus the Young's modulus of steel can be moved outside the summation sign to create an equation which is more easily entered in Microsoft excel for example.

$$\Delta E_v = 2E_{steel} I C^2 \sum_{i=1}^{13} (z_{i+1} - z_i) \frac{1}{2} (red_{i+1} + red_i)$$

The amount of work produced by the force is determined with the following formula

$$u_f = \int_0^l \frac{1}{2} \left(\frac{dw}{dz}\right)^2 dz = \int_0^l \frac{1}{2} C^2 (l^2 - 4lz + 4z^2)\, dz$$

$$A = F u_f = F \frac{1}{2} C^2 \left(l^3 - 2l^3 + \frac{4}{3} l^3\right) = F \frac{1}{6} C^2 l^3$$

Using the formulas for the deformation energy and the amount of work produced by the force the Rayleigh buckling force can be determined.

$$F_R = \frac{\Delta E_v}{u_f} = \frac{2E_{steel} I \sum_{i=1}^{13} (z_{i+1} - z_i) \frac{1}{2} (red_{i+1} + red_i)}{\frac{1}{6} l^3}$$

Appendix F: Calculation for critical steel temperature in columns.

Calculation for critical steel temperature columns.

based on calculation "brand" bouwen met staal

Floor area carried by column	24	[m2]
Amount of floors	1	[-]
Permanent load	5	[kN/m2]

Variable load is not in fire situation due to accidental load case

Calculation value bottom column 120000 [N]

Steel section information (from e.g. "tabellenboek")

Area of cross section	7680	[mm2]		**check steel section**
Steel quality	235	[N/mm2]	>	stress = force / area
Iz	27690000	[mm4]		15,625 OK

$i_z = \sqrt{(I/A)}$ 60,04556

c According to EN 1993-1-1	164	[mm]	
t According to EN 1993-1-1	7,5	[mm]	
Height of column	6400	[mm]	
buckling length factor	1	[-]	0,5 / 0,7 / 1,0

Section Class in fire situation

$\varepsilon = 0{,}85\sqrt{(235/f_y)}$ 0,85

If any of these 3 values comply, this method is fit for use

c/t ≤ 33ε	class 1	21,86667	≤	28,05	OK
c/t ≤ 38ε	class 2	21,86667	≤	32,3	OK
c/t ≤ 42ε	class 3	21,86667	≤	35,7	OK

$Lambda1 = 93{,}9\sqrt{(235/f_y)}$ 93,9

	lambda = Lfi/i	106,5857	
non dim slen	lambda.rel = lambda / lambda1	1,135098	relative slenderness

option 1

Plastic degree of utilization

mu,pl = Efi,d / A*fy 0,066489

look up value in GREEN box in table 4.7-4.9 of bouwen met staal "Brand" according to the degree of utilization and rel slenderness

	plastic degree of utilization low	**high**	
rel slenderness	0,06	0,07	
1,12	718	693	[℃]
1,16	706	689	[℃]

	0,06	**0,07**	
1,135098	716,1882	692,3961	[℃]

Critical steel temperature

700,7486 [℃]

option 2

use table 4.2 to find critical temperature by matching loads

k,y,theta	0,23	
k,E,theta	0,13	

$lambda.rel.theta = lambda.rel\ \sqrt{(k_{(y,\theta)}/k_{(E,\theta)})}$ 1,509822 [-]

$\alpha = 0{,}65\sqrt{(235/f_y)}$ 0,65 [-]

$\varphi_\theta = 0{,}5(1+\alpha[\![lambda]\!]_{rel\theta\wedge} + [\![lambda\wedge 2]\!]_{rel\theta\wedge})$

2,130473 [-]

$X_{fi} = 1/(\varphi_\theta + \sqrt{([\![\varphi\wedge 2]\!]_{\theta\wedge} - [\![lambda\ rel\wedge 2]\!]_{\theta\wedge})})$ 0,27521 [-]

Nfi,t,rd = Xfi * A* k,y,theta * fy **114240,8** [N]

This sheet is based on the calculation conducted in "brand"
it takes into account the reduced material properties
of steel due to a EC standard fire curve.

Appendix G: Buckling according to Eurocode (room temperature).

Buckling load according to eurocode.

Ambient temperature

Section information

Area	7680	[mm2]	
Length	6400	[mm]	
Buckling length factor			
	1	[-]	
iz	60	[mm]	iz is weak axis -> governing buckling case
steel quality	235	[N/mm2]	

Applied load on column

Ned 120 kN

Unity check:

$N\_ed/N\_(b, Rd) \leq 1$ 0,14284487 **check?!** OK

section class 1, 2, 3

$lambda1 = Pi * \sqrt{(E/f\_y)} = 93{,}9\varepsilon = 93{,}9\sqrt{(235/f\_y)}$

Lambda1 = 93,9

$(lambda)^{-} = \sqrt{((Af\_y)/N\_cr)} = l\_cr/i * 1/[\![lambda]\!]\_1$

lambda dash 1,13596024 wanneer < 0,2 is knik te verwaarlozen

non dim slen

read alpha from table according to cross section

alpha 0,49

$\varphi = 0{,}5[1 + \alpha((lambda)^{-} - 0{,}2) + (lambda)^{-}\text{^}2]$

phi 1,37451309

$X = 1/(\varphi + \sqrt{(\varphi\text{^}2 - (lambda)^{-}\text{^}2)})$

X = 0,46546552

Nb,Rd = X*A*fy / gamma m1

Nb,Rd = 840072,172 [N]

840,072172 [kN]

gamma m1 = 1 for buildings

Tabel 6.2 — Keuzetabel voor de knikkrommen voor een doorsnede

Doorsnede		Begrenzingen		Knik om de as	Knikkromme S 235 S 275 S 355 S 420	Knikkromme S 460
Gewalste profielen	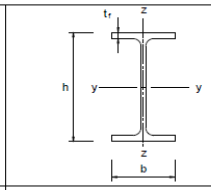	$h/b > 1{,}2$	$t_f \leq 40$ mm	y – y	a	a_0
				z – z	b	a_0
			$40 \text{ mm} < t_f \leq 100$ mm	y – y	b	a
				z – z	c	a
		$h/b \leq 1{,}2$	$t_f \leq 100$ mm	y – y	b	a
				z – z	c	a
			$t_f > 100$ mm	y – y	d	c
				z – z	d	c
Gelaste profielen	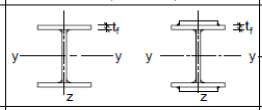		$t_f \leq 40$ mm	y – y	b	b
				z – z	c	c
			$t_f > 40$ mm	y – y	c	c
				z – z	d	d
Buisprofielen		Warmvervaardigd		Elke as	a	a_0
		Koudgevormd en gelast		Elke as	c	c
Gelaste kokerprofielen	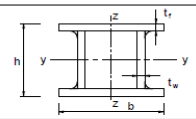	Algemeen (behalve in het hieronder gegeven geval)		Elke as	b	b
		Dikke lassen: $a > 0{,}5t_f$ $b/t_f < 30$ $h/t_w < 30$		Elke as	c	c
U-, T- en massieve profielen	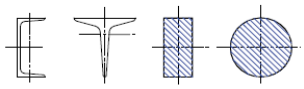			Elke as	c	c
L-profielen				Elke as	b	b

buckling cu	a0	a	b	c	d
alpha	0,13	0,21	0,34	0,49	0,76

Appendix H: Reduction factors for steel according to Eurocode.

Reduction factor Ky,Θ for the reduction of the yield strength and KE,Θ for the reduction in Young's modulus according to table 3,1 of NEN-EN 1993-1-2 as a function of the steel temperature

Θa	Ky,Θ	KE,Θ
20	1,000	1,000
30	1,000	1,000
40	1,000	1,000
50	1,000	1,000
60	1,000	1,000
70	1,000	1,000
80	1,000	1,000
90	1,000	1,000
100	1,000	1,000
110	1,000	0,990
120	1,000	0,980
130	1,000	0,970
140	1,000	0,960
150	1,000	0,950
160	1,000	0,940
170	1,000	0,930
180	1,000	0,920
190	1,000	0,910
200	1,000	0,900
210	1,000	0,890
220	1,000	0,880
230	1,000	0,870
240	1,000	0,860
250	1,000	0,850
260	1,000	0,840
270	1,000	0,830
280	1,000	0,820
290	1,000	0,810

Θa	Ky,Θ	KE,Θ
300	1,000	0,800
310	1,000	0,790
320	1,000	0,780
330	1,000	0,770
340	1,000	0,760
350	1,000	0,750
360	1,000	0,740
370	1,000	0,730
380	1,000	0,720
390	1,000	0,710
400	1,000	0,700
410	0,978	0,690
420	0,956	0,680
430	0,934	0,670
440	0,912	0,660
450	0,890	0,650
460	0,868	0,640
470	0,846	0,630
480	0,824	0,620
490	0,802	0,610
500	0,780	0,600
510	0,749	0,571
520	0,718	0,542
530	0,687	0,513
540	0,656	0,484
550	0,625	0,455
560	0,594	0,426
570	0,563	0,397
580	0,532	0,368
590	0,501	0,339

Θa	Ky,Θ	KE,Θ
600	0,470	0,310
610	0,446	0,292
620	0,422	0,274
630	0,938	0,256
640	0,374	0,238
650	0,350	0,220
660	0,326	0,202
670	0,302	0,184
680	0,278	0,166
690	0,254	0,148
700	0,230	0,130
710	0,218	0,126
720	0,206	0,122
730	0,194	0,118
740	0,182	0,114
750	0,170	0,110
760	0,158	0,106
770	0,146	0,102
780	0,134	0,098
790	0,122	0,094
800	0,110	0,090
810	0,105	0,088
820	0,100	0,086
830	0,095	0,083
840	0,090	0,081
850	0,085	0,079
860	0,080	0,077
870	0,075	0,074
880	0,070	0,072
890	0,065	0,070

Θa	Ky,Θ	KE,Θ
900	0,060	0,068
910	0,058	0,065
920	0,056	0,063
930	0,054	0,061
940	0,052	0,059
950	0,050	0,056
960	0,048	0,054
970	0,046	0,052
980	0,044	0,050
990	0,042	0,047
1000	0,040	0,045
1010	0,038	0,043
1020	0,036	0,041
1030	0,034	0,038
1040	0,032	0,036
1050	0,030	0,034
1060	0,028	0,032
1070	0,026	0,029
1080	0,024	0,027
1090	0,022	0,025
1100	0,020	0,023
1110	0,018	0,020
1120	0,016	0,018
1130	0,014	0,016
1140	0,012	0,014
1150	0,010	0,011
1160	0,008	0,009
1170	0,006	0,007
1180	0,004	0,005
1190	0,002	0,002
1200	0,000	0,000

Appendix I: Calculating critical steel temperature in fire situation.

Buckling at raised temperatures

based on "brand, bouwen met staal"

steel temperature known

section info

length	6400	[mm]
area	7680	[mm2]
yield strength	235	[N/mm2]
iz	60	[mm]
buckling factor	1	[-]

Applied load	**120**	[N]

$Lambda1=93{,}9\sqrt{(235/f\_y)}$ 93,9 [-]

lambda = Lfi/i	106,6667	[-]
lambda.rel = lambda / lambda1	1,13596	[-]

Table 4.2 per steel temperature

k,y,theta	0,134	[-]	785	degrees
k,E,theta	0,098	[-]		

$lambda.rel.theta=lambda.rel\sqrt{(k\_(y,\theta)/k\_(E,\theta))}$ 1,328319 [-]

$\alpha=0{,}65\sqrt{(235/f\_y)}$ 0,65 [-]

$\varphi\_\theta=0{,}5(1+\alpha[\![lambda]\!]\_rel\theta\text{^}+[\![lambda\text{^}2]\!]\_rel\theta\text{^}\ )$ 1,81392 [-]

$X\_fi=\ 1/(\varphi\_\theta+\sqrt{([\![\varphi\text{^}2]\!]\_\theta\text{^}-[\![lambda\ rel\text{^}2]\!]\_\theta\text{^}\ )})$ 0,327957 [-]

Nfi,t,rd = Xfi * A* k,y,theta * fy **79,31412** [kN]

Using table 4.2 in "brand" use the data and temperature to obtain the load applied on the structure.
the temperature at which this occurs is the critical steel temperature

Appendix J: Fire resistance according to ArcelorMittal

Fire resistance time in minutes calculated via method used in Arcelor based on Eurocode method.

section classes 1,2,3

[1] **section information (from e.g. "tabellenboek")**

a	7680	[mm2]
iz	60	[mm]
steel qual.	235	[N/mm2]
length	6400	[mm]
correction factor for buckling length		
=	1	[0,5 / 0,7 / 1,0]
lfi	6400	[mm]

loads definition

only permanent loads will be used as fire is an accidental load case

storeys	1	[-]
perm load	5	[kN/m2]
area	24	[m2]

permanent load on column in fire situation

=	120	[kN]
	120000	[N]

$[\![f']\!]_{(y,\theta,lambda\ rel)} = N_{(b,fi,Rd)}/A$ **CHECK**

= 15,625 [N/mm2] ≤ 235 OK

If check is NOT OK, load too high

$lambda1 = 93{,}9\sqrt{(235/f_y)}$

= 93,9

non dim slen

$lambda20° = lambda/lambdaE20 = lfi/(i*lambda1)$

= 1,13596

[2] **Look up the green values and the range of temperature and note the values in the table below.**

		temperature low	temperature high	
		700	800	[℃]
lambda20°	1,1	16	9	[N/mm2]
	1,2	14	8	[N/mm2]

	700	800	[℃]
1,14	15,2808	8,640398	[N/mm2]

Critical steel temperature

694,8165 [℃]

[3] **Look up the section factor of the section used in "section factor" sheet**

110 [1/m]

[4] **In "fire resistance time" sheet find the values of critical temperature and section factor to read the resistance time in minutes.**

17 [min]

Table 4.1 : Critical compression stress $f'_{y,\theta,\bar{\lambda}}$ for S235 steel

	Temperature θ_a					
	400°C	500°C	600°C	700°C	800°C	900°C
$\bar{\lambda}(20°C)$	$f'_{y,\theta,\bar{\lambda}}$ [N/mm²]					
0.0	235	183	110	54	26	14
0.1	218	171	102	50	24	13
0.2	202	159	94	46	22	13
0.3	187	147	87	42	21	12
0.4	171	136	80	38	19	11
0.5	156	124	72	34	18	10
0.6	140	113	65	30	16	10
0.7	126	102	58	26	15	9
0.8	112	91	51	23	13	8
0.9	99	81	45	20	12	7
1.0	88	73	40	18	11	7
1.1	78	65	35	16	9	6
1.2	70	58	31	14	8	6
1.3	62	52	28	12	8	5
1.4	56	47	25	11	7	5
1.5	50	42	22	10	6	4
1.6	45	38	20	9	6	4
1.7	41	35	18	8	5	4
1.8	37	31	17	7	5	3
1.9	34	29	15	7	4	3
2.0	31	26	14	6	4	3

Table 4.2 : Critical compression stress $f'_{y,\theta,\bar{\lambda}}$ for S355 steel

	Temperature θ_a					
	400°C	500°C	600°C	700°C	800°C	900°C
$\bar{\lambda}(20°C)$	$f'_{y,\theta,\bar{\lambda}}$ [N/mm²]					
0.0	355	277	167	82	39	21
0.1	334	261	157	76	37	20
0.2	313	246	147	71	35	19
0.3	293	231	137	66	33	18
0.4	272	215	126	60	31	17
0.5	250	199	116	54	28	16
0.6	227	182	105	49	26	15
0.7	204	165	94	43	24	14
0.8	182	148	83	38	21	13
0.9	161	132	73	33	19	12
1.0	143	118	65	29	17	11
1.1	126	105	57	25	15	10
1.2	112	93	51	22	14	9
1.3	100	83	45	19	12	8
1.4	89	75	40	17	11	8
1.5	80	67	36	15	10	7
1.6	72	61	32	14	9	6
1.7	65	55	29	13	8	6
1.8	59	50	26	11	7	5
1.9	54	46	24	10	7	5
2.0	49	42	22	9	6	4

Table 4.3 : Critical compression stress $f'_{y,\theta,\bar{\lambda}}$ for S460 steel

	Temperature θ_a					
	400°C	500°C	600°C	700°C	800°C	900°C
$\bar{\lambda}(20°C)$	$f'_{y,\theta,\bar{\lambda}}$ [N/mm²]					
0.0	460	359	216	106	51	28
0.1	435	341	204	100	48	26
0.2	412	323	193	93	46	25
0.3	388	305	181	87	43	24
0.4	362	286	169	80	41	23
0.5	335	266	155	73	38	22
0.6	305	245	141	66	35	21
0.7	276	222	127	58	32	19
0.8	246	200	112	51	29	18
0.9	218	179	99	44	26	16
1.0	193	159	87	39	23	15
1.1	170	142	77	34	21	14
1.2	151	126	68	30	19	12
1.3	134	112	60	26	17	11
1.4	119	100	54	23	15	10
1.5	107	90	48	21	13	9
1.6	96	81	43	18	12	8
1.7	87	73	39	17	11	8
1.8	79	67	35	15	10	7
1.9	72	61	32	14	9	6
2.0	66	56	29	12	8	6

Section factors

$[A_m/V]_{sh}$ $[m^{-1}]$

IPE		
IPE 80 A	285	350
IPE 80	243	297
IPE A 100	257	314
IPE 100	222	270
IPE A 120	244	296
IPE 120	207	251
IPE A 140	234	283
IPE 140	194	233
IPE A 160	221	266
IPE 160	180	217
IPE A 180	204	247
IPE 180	169	203
IPE O 180	151	182
IPE A 200	189	228
IPE 200	158	190
IPE O 200	142	171
IPE A 220	174	208
IPE 220	149	178
IPE O 220	134	161
IPE A 240	160	193
IPE 240	138	166
IPE O 240	125	150
IPE A 270	154	185
IPE 270	132	158
IPE O 270	114	137
IPE A 300	144	173
IPE 300	125	150
IPE O 300	109	131
IPE A 330	134	160
IPE 330	118	141
IPE O 330	103	123
IPE A 360	124	149
IPE 360	110	131
IPE O 360	96	114
IPE A 400	120	142
IPE 400	104	123
IPE O 400	93	110
IPE A 450	114	134
IPE 450	99	117
IPE O 450	85	99
IPE A 500	106	124
IPE 500	94	109
IPE O 500	80	94
IPE A 550	100	116
IPE 550	87	102
IPE O 550	77	88
IPE A 600	93	107
IPE 600	82	95
IPE O 600	66	77
750 x 137	91	104
750 x 147	85	98
750 x 173	73	84
750 x 196	65	75

HP		
HP 200 x 43	101	135
HP 200 x 53	81	109
HP 220 x 57	79	107
HP 260 x 75	72	97
HP 260 x 87	63	85
HP 305 x 79	82	109
HP 305 x 88	73	98
HP 305 x 95	68	91
HP 305 x 110	59	79
HP 305 x 126	52	70
HP 305 x 149	45	60
HP 305 x 180	38	50
HP 305 x 186	37	50
HP 305 x 223	32	42
HP 320 x 88	73	97
HP 320 x 103	63	85
HP 320 x 117	56	75
HP 320 x 147	46	61
HP 320 x 184	38	50
HP 360 x 84	88	119
HP 360 x 109	69	93
HP 360 x 133	58	77
HP 360 x 152	50	68
HP 360 x 174	45	60
HP 360 x 180	43	59
HP 400 x 122	63	86
HP 400 x 140	55	75
HP 400 x 158	50	67
HP 400 x 176	45	60
HP 400 x 194	41	56
HP 400 x 213	38	51
HP 400 x 231	35	48

HD		
HD 260 x 54,1	97	131
HD 260 x 68,2	79	105
HD 260 x 93,0	59	79
HD 260 x 114	50	66
HD 260 x 142	41	54
HD 260 x 172	35	46
HD 320 x 74,2	86	114
HD 320 x 97,6	67	88
HD 320 x 127	52	69
HD 320 x 158	43	57
HD 320 x 198	35	46
HD 320 x 245	30	39
HD 320 x 300	25	32
HD 360 x 134	57	77
HD 360 x 147	52	70
HD 360 x 162	48	64
HD 360 x 179	44	59
HD 360 x 196	41	54
HD 400 x 187	42	58
HD 400 x 216	38	50
HD 400 x 237	34	47
HD 400 x 262	32	42
HD 400 x 287	29	39
HD 400 x 314	27	36
HD 400 x 347	25	33
HD 400 x 382	23	31
HD 400 x 421	21	28
HD 400 x 463	20	26
HD 400 x 509	18	24
HD 400 x 551	17	23
HD 400 x 592	16	21
HD 400 x 634	15	20
HD 400 x 677	14	19
HD 400 x 744	14	18
HD 400 x 818	13	16
HD 400 x 900	12	15
HD 400 x 990	11	14
HD 400 x 1086	10	14

HE		
HE 100 AA	163	221
HE 100 A	124	167
HE 100 B	104	139
HE 100 M	59	77
HE 120 AA	164	222
HE 120 A	123	167
HE 120 B	95	127
HE 120 M	55	72
HE 140 AA	155	210
HE 140 A	116	157
HE 140 B	88	117
HE 140 M	52	68
HE 160 AA	135	183
HE 160 A	108	145
HE 160 B	79	106
HE 160 M	49	64
HE 180 AA	127	171
HE 180 A	104	140
HE 180 B	75	99
HE 180 M	47	61
HE 200 AA	117	158
HE 200 A	97	131
HE 200 B	69	92
HE 200 M	44	59
HE 220 AA	110	149
HE 220 A	89	121
HE 220 B	65	87
HE 220 M	42	56
HE 240 AA	103	139
HE 240 A	82	110
HE 240 B	61	82
HE 240 M	35	47
HE 260 AA	97	131
HE 260 A	79	105
HE 260 B	59	79
HE 260 M	35	46
HE 280 AA	94	125
HE 280 A	76	102
HE 280 B	58	77
HE 280 M	34	45
HE 300 AA	87	118
HE 300 A	70	95
HE 300 B	54	72
HE 300 M	30	39
HE 320 AA	86	114
HE 320 A	67	88
HE 320 B	52	69
HE 320 M	30	39
HE 340 AA	85	111
HE 340 A	65	85
HE 340 B	51	68
HE 340 M	31	39
HE 360 AA	83	108
HE 360 A	63	82
HE 360 B	50	66
HE 360 M	31	40
HE 400 AA	81	104
HE 400 A	61	78
HE 400 B	50	64
HE 400 M	32	41
HE 450 AA	82	103
HE 450 A	59	75
HE 450 B	50	62
HE 450 M	34	42
HE 500 AA	82	102
HE 500 A	59	72
HE 500 B	49	60
HE 500 M	35	43
HE 550 AA	79	97
HE 550 A	59	71
HE 550 B	50	60
HE 550 M	37	45
HE 600 AA	79	95
HE 600 A	59	71
HE 600 B	50	60
HE 600 M	38	46
HE 600 x 337	33	40
HE 600 x 399	29	34
HE 650 AA	79	95
HE 650 A	59	70
HE 650 B	50	59
HE 650 M	40	47
HE 650 x 343	34	41
HE 650 x 407	30	35
HE 700 AA	77	92
HE 700 A	58	68
HE 700 B	50	59
HE 700 M	41	48
HE 700 x 352	35	41
HE 700 x 418	31	36
HE 800 AA	76	88
HE 800 A	59	68
HE 800 B	51	59
HE 800 M	43	50
HE 800 x 373	37	43
HE 800 x 444	32	37
HE 900 AA	73	84
HE 900 A	59	67
HE 900 B	51	59
HE 900 M	45	51
HE 900 x 391	39	44
HE 900 x 466	33	38
HE 1000 AA	71	81
HE 1000 x 249	64	73
HE 1000 A	59	67
HE 1000 B	51	59
HE 1000 M	47	53
HE 1000 x 393	42	48
HE 1000 x 415	40	45
HE 1000 x 438	38	43
HE 1000 x 494	34	39
HE 1000 x 584	30	33
HL 920 x 345	47	56
HL 920 x 368	44	52
HL 920 x 390	41	50
HL 920 x 420	39	46
HL 920 x 449	37	43
HL 920 x 491	33	40
HL 920 x 537	32	37
HL 920 x 588	29	33
HL 920 x 656	26	31
HL 920 x 725	23	28
HL 920 x 787	23	26
HL 920 x 970	18	22
HL 1000 AA	57	66
HL 1000 A	52	61
HL 1000 B	46	53
HL 1000 M	41	49
HL 1000 x 443	39	45
HL 1000 x 483	36	41
HL 1000 x 539	32	38
HL 1000 x 554	32	37
HL 1000 x 591	30	35
HL 1000 x 642	28	32
HL 1000 x 748	24	28
HL 1000 x 883	21	24
HL 1100 A	53	61
HL 1100 B	47	54
HL 1100 M	42	50
HL 1100 R	38	43

UPN		
UPN 80	186	227
UPN 100	185	222
UPN 120	174	206
UPN 140	167	196
UPN 160	160	188
UPN 180	154	179
UPN 200	148	171
UPN 220	139	160
UPN 240	134	154
UPN 260	126	145
UPN 280	123	141
UPN 300	119	136
UPN 320	98	111
UPN 350	103	116
UPN 380	107	120
UPN 400	99	111

UPE		
UPE 80	209	258
UPE 100	204	248
UPE 120	195	233
UPE 140	187	223
UPE 160	180	212
UPE 180	173	203
UPE 200	165	193
UPE 220	155	180
UPE 240	148	171
UPE 270	142	163
UPE 300	124	141
UPE 330	113	128
UPE 360	107	121
UPE 400	100	112

Section factors for unprotected steel members - European sections

Fire resistance time

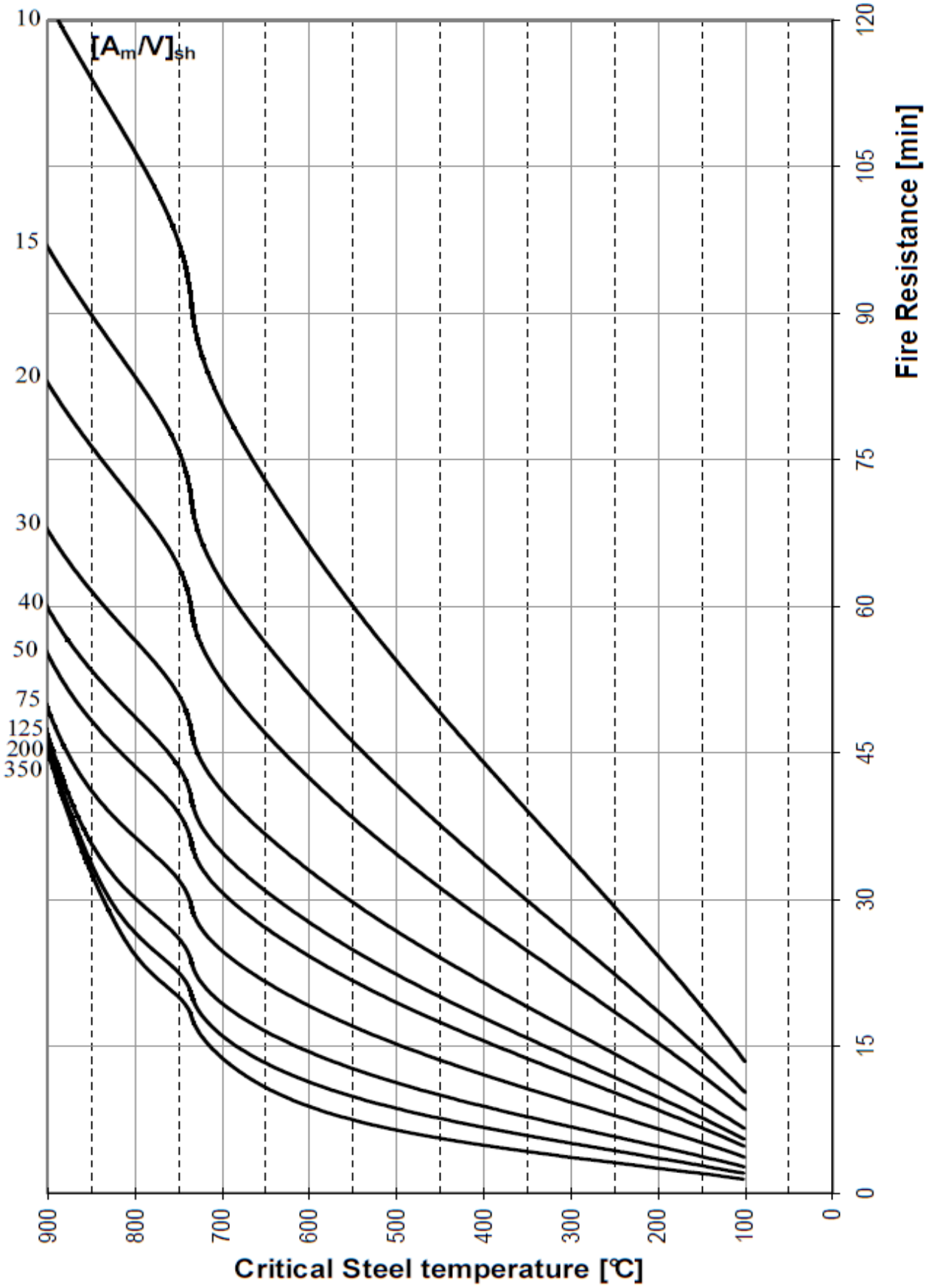

Faculty of Civil Engineering and Geosciences

Stevinweg 1
2628 CN Delft
The Netherlands